NKS-487
ISBN 978-87-7893-583-0

Source Term and Timing Uncertainty in Severe accidents NKS-STATUS Phase 3 report

Sergey Galushin[1],
Govatsa Acharya[2], Dmitry Grischenko[2], Pavel Kudinov[2]
Sara Ojalehto[3], Tuomo Sevón[3], Ilona Lindholm[3]
Patrick Isaksson[4]
Naeem Ul-Syed[5]

[1] Vysus Sweden AB
[2] KTH Royal Institute of Technology
[3] VTT Technical Research Centre of Finland Ltd
[4] SSM Swedish Radiation Safety Authority
[5] DSA Norwegian Radiation and Nuclear Safety Authority

June 2024

Abstract

The overall goal of the project is to generate a body of knowledge regarding the uncertainty in the magnitude of fission products release in the case of a potential severe accident in Nordic nuclear power plants. The work aims to provide insights into the effect of various types of uncertainty on the source term predictions. The results of the work will be useful both for probabilistic and deterministic safety assessments as well as for emergency response applications.
The third phase of the project focused on the assessment of the source term uncertainty in Nordic BWR-type reactors, in cases of containment bypass, containment failure, and filtered release scenarios.
In the case of containment bypass scenarios, the results showed that structures, systems, and components outside containment can reduce conservatism in source term analysis. Further refinement of the level of detail in modeling release paths and system effects could enhance the accuracy of the source term analysis results.
Analysis of release pathways for fission products in the case of containment failure, especially through failed containment hatch doors can lead to significant changes in the source term. Critical concerns include basemat melt-through and non-coolable debris beds.
The analysis of the effect of the independent spray system on the source term released to the environment in filtered containment venting scenarios showed significant reduction in the Cs release compared to that in the unmitigated scenarios. The analysis includes quantification of uncertainties related to the MELCOR code's epistemic modeling parameters and options, and their effects on the timing and magnitude of the source term. Furthermore, for the Finnish BWR the Morris method and SNAP/DAKOTA analyses highlighted the relative influence of parameters, with some unexpected influential parameters likely due to numerical noise. Containment spraying effectively reduced Cs and I releases, although it did not affect FCV opening times.
The analysis of the effectiveness of pool scrubbing in the Multi-Venturi Scrubbing System and the refined modelling of the MVSS showed how the efficiency of pool scrubbing changes during different stages of severe accident progression. It also showed the impact of MVSS structures on the behavior of fission products in the scrubber and the source term released to the environment.

Key words

Severe accident, uncertainty quantification, MELCOR, Nordic BWR, fission products, source term

NKS-487
ISBN 978-87-7893-583-0
Electronic report, June 2024

NKS Secretariat
P.O. Box 49
DK - 4000 Roskilde, Denmark
Phone +45 4677 4041
www.nks.org
e-mail nks@nks.org

Source Term and Timing Uncertainty in Severe accidents

Final Report from the NKS-R STATUS activity
(Contract: AFT/NKS-R(23)133/2)

Sergey Galushin[1]

Govatsa Acharya[2], Dmitry Grischenko[2], Pavel Kudinov[2]

Sara Ojalehto[3], Tuomo Sevón[3], Ilona Lindholm[3]

Patrick Isaksson[4]

Naeem Ul-Syed[5]

[1] Vysus Sweden AB

[2] KTH Royal Institute of Technology

[3] VTT Technical Research Centre of Finland Ltd

[4] SSM Swedish Radiation Safety Authority

[5] DSA Norwegian Radiation and Nuclear Safety Authority

NKS conveys its gratitude to all organizations and persons who by means of financial support or contributions in kind have made the work presented in this report possible.

Table of contents

1. Introduction

Analyzing and estimating risks is an integral part of both the industrial use and the public debate on nuclear power. At the same time, global climate change is increasing the demand for low-carbon sources of electricity, and the nuclear industry strives to maintain and expand its share of global energy production. With these observations in mind, it is reasonable to expect that the need for technological advances and reduction of uncertainties in both financial and radiological risks related to nuclear power will be as big as ever in the coming decades.

An important part of the risk profile of nuclear power relates to so-called severe accidents – i.e., events leading to a partly or fully damaged (melted) reactor core. State-of-the-art assessments of radiological risks related to such events rely on estimations of two fundamental quantities: their frequency and their consequence. As simple as these notions may seem, their quantification depends heavily on input data as well as on scope and complexity of the mathematical modelling used.

In so-called level 2 probabilistic safety assessments (L2 PSA), the main frequency estimate of interest is the large release frequency (LRF), or sometimes the large early release frequency (LERF). Assessing these frequencies based on summation over a large number of possible event sequences implies, among other things, that radioactive releases (the source term) need to be calculated for a set of representative scenario classes and compared to a predefined threshold to classify them as large or not large. These assessments are typically performed with integral plant response codes, such as ASTEC, MAAP or MELCOR, and are in themselves subject to uncertainty, both regarding the accident scenarios (aleatory uncertainty) and in the modelling of phenomena (epistemic uncertainty). Aleatory uncertainty arises from the natural variability of stochastic processes and cannot be reduced beyond this level, while epistemic uncertainty relates to our knowledge of systems, processes or parameters and can therefore be reduced by gathering more knowledge.

Typically, the source term evaluation is performed for a limited set of accident scenarios, using point-estimate values of epistemic uncertain parameters in the code used. Furthermore, such analyses typically do not consider the effect of epistemic uncertainty on interactions between physical phenomena or processes and transient accident scenarios, i.e., when different samples on the epistemic uncertainty range can significantly affect the course of the accident progression.

For some accident sequences, the standard practice, for the sake of conservatism, is to define the source term as everything escaping the containment. This creates a situation where a potentially very diverse family of realistic scenarios is represented by a set of assumed sequences that may contribute substantially to the LRF in a typical PSA L2. In this case, the uncertainty lies in the level of applied conservatism.

In both cases described above, source term uncertainty presents a challenge for any attempt to develop, use or increase the level of detail in L2 PSA results and merits targeted research solely on the basis of this.

Within the field of nuclear emergency preparedness towards severe accidents, the main goal is ultimately to be able to perform relevant and efficient actions to protect the public. The International Atomic Energy Agency (IAEA) states on the one hand that decisions on these actions should be based on observations of plant conditions, and on the other hand that decisions or protective actions should not be delayed by attempts to perform detailed source term estimates [1,2]. It is acknowledged that performing source term assessments with integral plant response codes is sufficiently complicated outside of accident conditions, which

creates a need for simpler and faster tools for assessment of plant condition and source term estimation. One such tool is the Rapid Source Term Prediction (RASTEP) methodology, developed by Vysus Group. This method relies on a database of pre-calculated source term scenarios together with a probabilistic Bayesian Belief Network (BBN) model. The tool has the ability to take observed plant conditions and rescale results from L1-L2 PSA using conditional probabilities, logical relations and expert judgements. The output is a complete list of scenarios ranked by likelihoods, which is continuously updated with any new observations. In this way, current plant conditions can always be mapped to a representative class of scenarios. A problem arises if a RASTEP model (or any approach based on pre-calculated source terms) is used with overly conservative or uncertain data. Within emergency preparedness planning, source term uncertainties therefore also come with an operational aspect, directly impacting decisions taken in a stressful situation.

Within this project, the analysis of severe accident progression and fission products release to the environment are performed using MELCOR. MELCOR is a fully integrated, engineering-level computer code that models the progression of severe accidents in light water reactor nuclear power plants. A broad spectrum of severe accident phenomena in both boiling and pressurized water reactors is treated in MELCOR in a unified framework. These include thermal-hydraulic response in the reactor coolant system, reactor cavity, containment, and confinement buildings; core heat-up, degradation, and relocation; core-concrete attack; hydrogen production, transport, and combustion; fission product release and transport behavior. Current uses of MELCOR include estimation of severe accident source terms and their sensitivities and uncertainties in a variety of applications [6,7].

It is our hope that this project will be able to shine some light on all of the above-mentioned aspects of the source term uncertainty, limited to Nordic Boiling Water Reactors (BWR).

2. Project scope and goals

The overall goal of the project is to generate a body of knowledge regarding the uncertainty in the magnitude of fission products release in the event of a potential severe accident in Nordic nuclear power plants. The work aims to provide insights into the effect of various types of uncertainty on the source term predictions. The results will be useful for both probabilistic and deterministic safety assessments, as well as for emergency response applications.

Within the first phase of the project (see [23]) the participating organizations performed the analysis of the safety design of Swedish and Finnish Nordic BWRs and respective MELCOR modelling, review of the PSA L2 for a typical Nordic BWR design and identification of risk significant accident sequences, as well as the state-of-the-art review of the modelling of severe accident phenomena and identification of possible sources of uncertainty in severe accident progression and the source term.

In the second phase of the project (see [50]) the participating organizations focused on evaluating methods and tools to perform sensitivity and uncertainty analyses. Using these methods and tools, they identified the main contributors to the uncertainty in the source term released to the environment and quantified the source term uncertainty due to the most influential MELCOR code modeling parameters. In these analyses, the uncertain modeling parameters involved the modeling of core degradation and relocation, fission product release from fuel, debris behavior in the core region and vessel lower head, vessel lower head failure, fission product behavior in the RCS and the containment, as well as modeling of the filter trapping, containment sprays, and pool scrubbing.

The main goal of the third phase of the project and this report is to perform:

- Analysis of containment bypass sequences, with the focus on the sequences involving failed isolation of main steam valves and release paths through the turbine system and condenser.
- Sensitivity and uncertainty analysis including the effect of release path in case of containment failure due to ex-vessel phenomena.
- Analysis of the effect of mitigative actions in filtered containment venting scenarios.
- Development and implementation of a more refined modelling of the filtered containment venting system using the MELCOR pool scrubbing model (SPARC-90 code).

The third phase of the NKS-STATUS project is expected to provide important insights into the effect of the MELCOR code modelling uncertainties on the accident progression and radioactive release to the environment in the accident scenarios that lead to filtered venting of the containment and filtered release to the environment, as well as scenarios where containment failure occurs. Additionally, the project aims to provide the insights on the effect of potential mitigative actions on the source term released to the environment, and the impact of limiting factors, such as structures, systems and components (SSC) located outside the containment, on the source term release to the environment in the accident scenarios where containment barrier is bypassed (containment bypass sequences) or fails (sequences where containment failure due to energetic phenomena in the containment can occur).

3. Background on Nordic Boiling Water Reactors

Designed by ASEA/ABB Atom, a total of 10 BWRs have been commissioned in Sweden and Finland since the first unit, Oskarshamn 1, was brought online in 1972. Two of the original design families, BWR69 and BWR75, are in operation today, distributed as four units in Sweden and two units in Finland, all with planned lifetimes extending to around 2040.

Over time, these reactors have evolved in partly different directions. The configurations of the sister reactors Forsmark 1/2 as well as Olkiluoto 1/2 are still more or less identical within the sites, while the differences between the sites are more marked.

3.1. Safety design

The Nordic Boiling Water Reactor (NBWR) will hereby be used as a common name for ~3300 MW_{th} BWRs designed by ASEA/ABB Atom. A summary of main technical data for the currently operational NBWRs is given in [3].

Table 3-1. Main technical data for operating NBWRs, some numbers rounded.

	O3/F3 (BWR75)	**F1/2 (BWR69)**	**OL1/2 (BWR69)**
Thermal power [MW]	3900/3300	3000/3250	2500
Reactor operating pressure [MPa]	7.0	7.0	7.0
Number of fuel elements [-]	700	676	500
Number of control rods [-]	169	161	121
Gas volume in containment [m^3]	8300/8500	6800	7600
Capacity of system [kg/s]:			
Containment drywell spray	300	360	250
Containment wetwell spray	400	N/A	120
Containment design pressure [MPa]	0.6	0.5	0.5
Containment operating pressure [MPa]	<0.1	<0.1	<0.1
Filtered containment venting pressure setpoint [MPa]	0.5	0.57	0.2/0.5-0.6*
Unfiltered containment venting pressure setpoint [MPa]	0.65		
Containment rupture pressure [MPa]	~1	~1	~1

*For wetwell venting in OL1/2, the drywell pressure needs to exceed the defined overpressure that depends on drywell gas temperature (total pressure 0.5-0.6 MPa). The drywell venting takes place if the water level in the wetwell is too high to allow venting from there, and the drywell pressure is higher than 0.2 MPa.

The safety design of the NBWRs is described further in the following.

The reactor pressure vessel (RPV) consists of carbon steel clad by stainless steel on the inside. The reactor containment is of the pressure suppression (PS) type with vertical blowdown pipes, and its outer cylindrical shell is made of pre-stressed concrete. It is sealed at the top by a large steel cupola which sits at the bottom of the reactor service pool. The containment also functions as a radiological shield to the environment. During normal operation, the

containment gas volume is filled with nitrogen to prevent ignition of hydrogen if generated during a severe accident.

Details on the NBWR safety systems relevant for severe accident progression (and source term) are provided below:

- Hydraulic control rod insertion: The hydraulic actuating power shut-off system gives full insertion of all control rods within a few seconds after initiation. Should this system fail, an electromechanic system inserts the rods within a few minutes. If this also fails, boric acid can be added to the reactor vessel via a dedicated injection system.
- Pressure control and relief system: This system has several operating modes and can operate with battery backup only:
    - TA Function: The spring-operated part of the overpressure protection system will open valves stepwise, starting at slightly above 7 MPa to release steam and protect the RPV from catastrophic failure. After a properly controlled pressure transient, the system will continue to control the pressure to around 7 MPa.
    - TB Function (ADS): Activation of TB initiates steam discharge into the wetwell (WW) on setpoint 1 m below top of active fuel (TAF). The pressure is reduced to a level sufficient for water injection by the emergency core cooling system (ECCS) or the independent core cooling system. The TB function is at the same time leading to coolant being lost from the primary system quite rapidly, which leads to core uncover.
- Emergency core cooling system (ECCS): This is an AC power driven, low-pressure coolant injection system comprised of four independent trains, which can pump water to the reactor from the suppression pool. The system has activation setpoints on water level 2 m above TAF and low reactor pressure. Actual water injection will not occur unless the pressure difference between WW and downcomer (DC) is less than 1.25 MPa and the injection capacity is, in general, dependent on this pressure difference.
- Independent core cooling system: This is, in the Swedish configuration, an AC power driven injection system comprised of one independent train with one or several separate water sources as well as a dedicated diesel generator. In the Finnish configuration, this is a separate steam turbine driven injection system, taking suction from water storage tanks in the system for distribution of demineralized water.
- Auxiliary feedwater system (AFW): This is an AC power driven high-pressure coolant injection system comprised of four independent trains, which provides water to the reactor from the wetwell or from a separate storage tank into the downcomer. The system activation logics includes several different setpoints. Water injection is more or less independent of reactor pressure.
- Drywell flooding system: Flooding of drywell from the wetwell is initiated to provide cooling of melt fragmentation and debris in case of melt release from the reactor pressure vessel. The system is typically actuated on downcomer water level 2 m below the TAF for more than 10 minutes, or 30 minutes after containment isolation, depending on plant.
- Non-filtered containment venting system: This is a pressure relief directly to the ambient atmosphere designed for LOCA events with failing PS function. It is

activated by the opening of a rupture disc at around 0.65 MPa containment pressure. The line is automatically closed by a shut-off valve 20 minutes after containment isolation signal. It should be noted that this containment isolation signal is triggered individually by any of the typical conditions that are indicative of a serious event e.g. low reactor water level, high containment temperature, high containment pressure or triggered TB function.

- Filtered containment venting system: In the Swedish configuration, this is achieved from the upper drywell to the atmosphere via a multi-venturi scrubbing system situated in a separate building, equipped with a dedicated stack. Venting is activated by a rupture disc opening around 0.55 MPa containment pressure. In parallel with this rupture disc, two valves for manual depressurization are also installed for cases where additional capacity is required, e.g. when manual operation of the filtered venting is an option due to for instance favorable weather conditions.

  In the Finnish configuration, filtered venting can be done both from the wetwell and drywell to the atmosphere via a SAM-scrubber placed inside the reactor building. Wetwell venting is possible if the water level is below 14.5 m. The drywell pressure needs to exceed the defined overpressure that depends on drywell gas temperature. At a drywell temperature of 293 K, the threshold overpressure is 0.5 MPa.
  The drywell venting through a rupture disk takes place if the water level in the wetwell has been higher than 14.5 m for longer than a specified time (which precludes possibility of venting from wetwell) and the drywell pressure is higher than 0.2 MPa.

- Suppression pool: The suppression pool, located in the wetwell, is an inherently passive system designed to limit the containment pressure by use of the so-called PS function; Steam leaking or blown out from the primary system to the drywell will be pushed through blowdown pipes ending in the wetwell pool where the steam is condensed. Vacuum valves in large pipes between wetwell and lower drywell ensure that the wetwell pressure will not be higher than that of the drywell.
- Residual heat removal and containment spray system (RHR and CSS): This is an AC power driven system, comprised of four independent trains with heat exchangers, all recirculating water from the suppression pool. All four loops are connected to feed spray nozzles located in the containment. The safety functions of the system are to reduce the containment pressure by condensing steam in case of a LOCA, to remove heat from the suppression pool through a series of heat exchangers and to provide scrubbing of airborne fission products from the containment atmosphere in case of core damage.
- Independent containment heat removal and spray system: This is an EOP/SAMG spray system in the upper drywell (UDW) that takes water from an independent external water source. It can be used to reduce pressure in the containment as well as to provide scrubbing of airborne fission products. Water level control is provided in order to not damage the containment.

3.2. MELCOR models

3.2.1. Swedish MELCOR modelling of NBWR

The MELCOR model of NBWR used in this project is the further development of the input deck originally developed for the analysis of accidents in power uprated plants [4], mainly

maintained by KTH. In this model, the core is represented by five non-uniform radial rings and eight axial levels. The 6th ring represents the downcomer region (Figure 3-1).

The reactor pressure vessel (Figure 3-2) and the containment (Figure 3-3) are represented by 27 control volumes (CV), connected with 45 flow paths (FL) and 73 heat structures (HS). The vessel is represented by 6 rings and 19 axial levels, with the first 10 axial levels representing the lower plenum; the 11th axial level represents the core support plate; levels 12 and 19 represent the core inlet and outlet regions and structures; and levels 13-18 represent the active core region. Lower head penetrations for 66 instrumentation guide tubes (IGTs) are distributed between rings 1-5 proportionally to the cross-sectional area of these rings. Containment leakage is modelled from the drywell directly to the environment.

The containment is subdivided into control volumes for upper and lower drywell, wetwell, blowdown pipes and overflow pipes from lower drywell to wetwell.

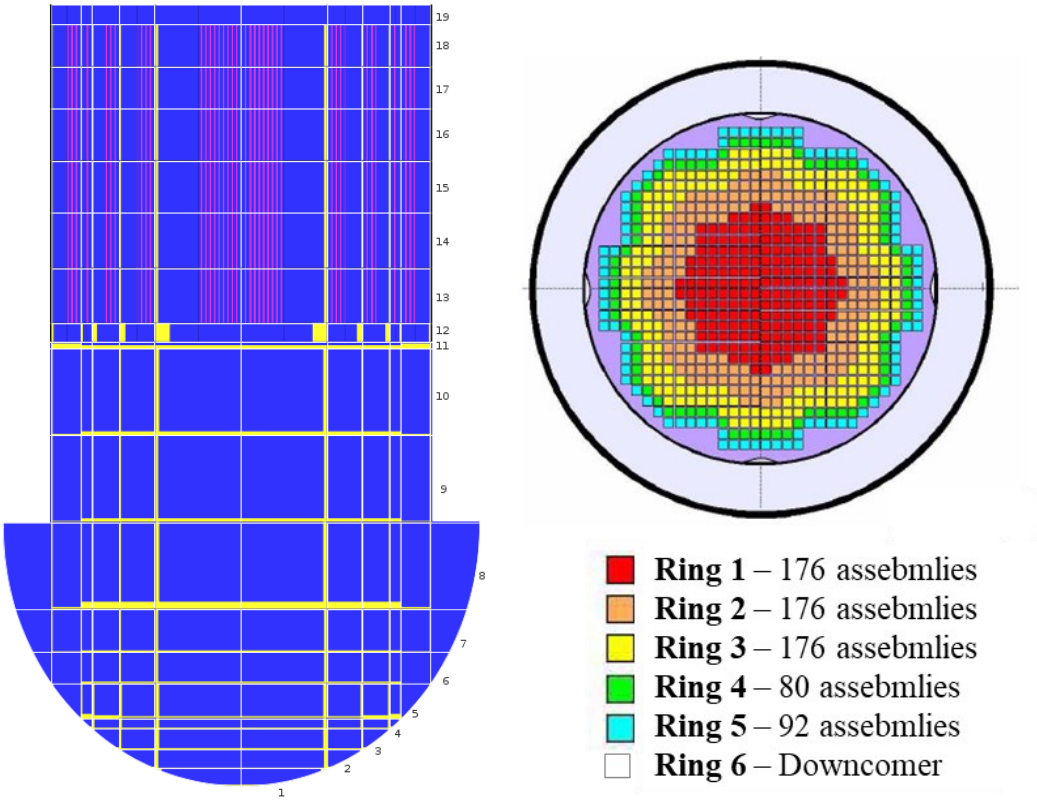

Figure 3-1. Swedish NBWR model COR nodalization.

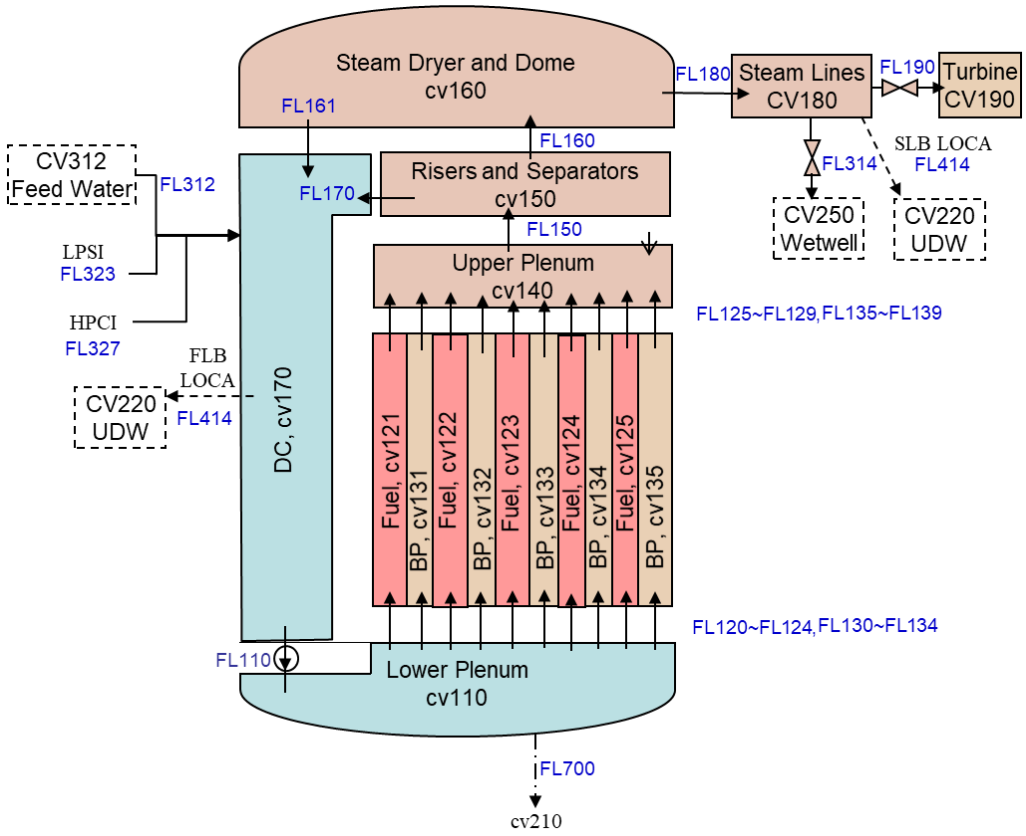

Figure 3-2. Swedish NBWR model CVH nodalization of the core.

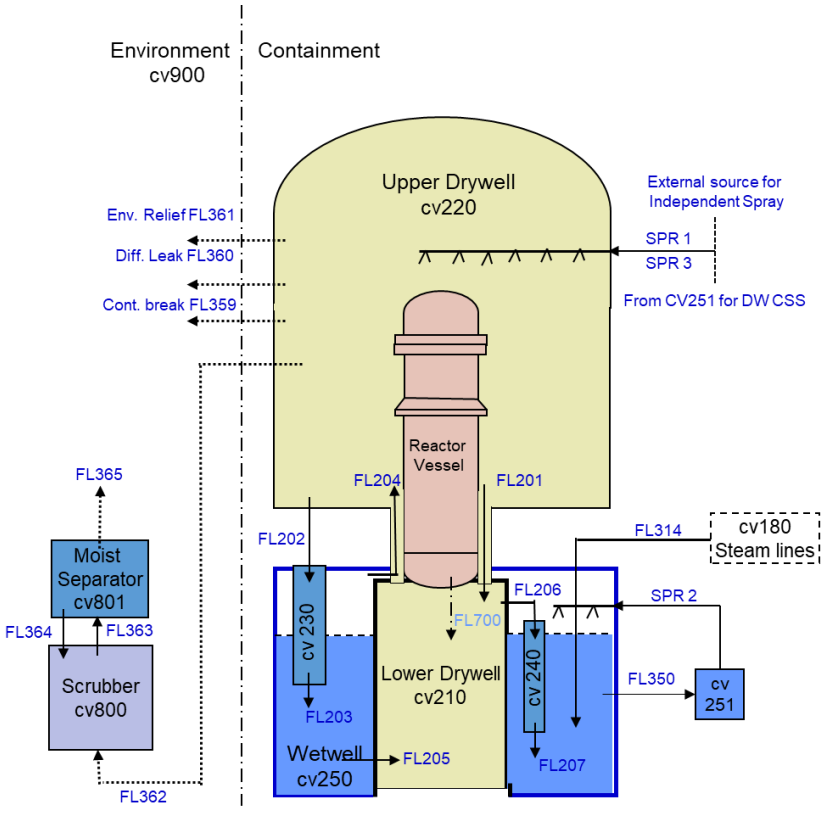

Figure 3-3. Swedish NBWR model containment nodalization.

The following safety systems are implemented in the model:

- Hydraulic control rod insertion
  - The effect of this system is modeled in MELCOR by fission power decrease (during 3.5 s) according to a tabular function at time zero.
- Pressure control and relief system
  - Both TA and TB valves as well as pipelines are implemented as a single flow path (FL314) from the steamlines to the wetwell, controlled by a set of control and tabular functions. SPARC pool scrubbing model is activated at the pool discharge end of the 314-pipes.
- Emergency core cooling system
  - All 4 trains are modeled by a single flow path (FL323) to the downcomer, with the number of trains and flow managed by a set of control functions. Flow rate vs. back pressure is controlled by a tabular function. The wetwell is used as water source for the system in the model and the injection is stopped on high suppression pool temperature.
- Auxiliary feedwater system.
  - All 4 trains are modeled by a single flow path (FL171) to the downcomer, with the number of trains and flow managed by a set of control functions. It is assumed that the system injects water with constant flow rate of 26 kg/s regardless of the pressure difference between DW and WW. The wetwell is used as water source for the system in the model and the injection is stopped on high suppression pool temperature.
- Drywell flooding system.
  - The system is implemented as a single flow path (FL205) from the wetwell to the lower drywell; the valves are controlled by a set of control functions. Together with the drywell flooding system an overflow pipe is modelled connecting the lower drywell and the wetwell to prevent lower drywell overfilling.
- Drywell blowdown pipes
  - A total of 24 drywell blowdown pipes are modelled from the drywell floor to the suppression pool. The diameter of the pipes is about 60 cm. The SPARC pool scrubbing model is activated at wetwell discharge at the end of the blowdown pipe. The blowdown pipes are purposed for the LOCA situations, when rapid and large steam release is able to clear the water in the pipes, and steam is driven into the suppression pool for condensation.
- Vacuum breakers
  - Vacuum breakers are modelled as a single flow path (FL204) that connects wetwell gas space with upper drywell to prevent wetwell pressure exceeding the drywell pressure.
- Non-filtered containment venting system.
  - Implemented as a single flow path (FL361) from the upper drywell to the environment, the rupture disk and shut-off valves are modelled as a set of control functions.

- Filtered containment venting system.
    - Implemented by a set of flow paths and control volumes (c.f. Figure 3-3). The rupture disk and valves are controlled by a set of control functions. The actual filtering of substances containing radionuclides is modelled by simple filter factors based on system requirements.
- Residual heat removal and containment spray system.
    - Currently modelled as two sprays (SPR2 in the wetwell and SPR3 in the drywell). The wetwell spray (SPR2) represents up to 4 trains of the containment spray system with 100 kg/s per train, with a possibility to reroute up to 3 spray trains to the upper drywell. Control volume CV251 represents the heat exchangers in the residual heat removal system and used as a water (and temperature) source by the containment spray system and enthalpy source for the residual heat removal system.
- Independent containment spray system
    - Implemented as a single train system with flow path (SPR1) ending in the upper drywell. The capacity is 100 kg/s assuming a constant water source temperature at 293.15 K.

The MELCOR model does not include the newly implemented independent core cooling system. As the aim is to study source terms of severe accidents, i.e. cases where all core cooling fails, this is judged to be acceptable.

The MELCOR model is not built to treat cases with failing hydraulic control rod insertion, as sequences with failing reactor shutdown also require the electromechanical insertion and the boron injection to fail, thereby rendering this core damage mode a very small contributor in the PSA.

Note that steam lines, condenser and turbine plant are not modelled, as is also the case for the reactor building and its ventilation system. This implies that containment rupture or bypass cases will be conservative in terms of the source term, as any retention and delay in the turbine system or building structures will not be taken into account.

In the last few years, KTH has developed and demonstrated a systematic approach to quantification of uncertainty in severe accident scenarios and phenomena based on the Risk Oriented Accident Analysis Methodology framework (ROAAM+). The approach combines the most recent development in the areas of sensitivity analysis, uncertainty quantification and surrogate modeling approaches. In the previous ROAAM+ work the focus was on the quantification of uncertainty in containment failure probability. The next step in the ROAAM+ development is application to quantification of uncertainty in the source term.

3.2.2. Finnish MELCOR modelling of NBWR

VTT's MELCOR model of Olkiluoto 1&2 was developed for code version 1.8.2 in 1994. The model has been updated several times when new code versions have been taken into use. The latest update was made in 2017 by Magnus Strandberg who converted the model to MELCOR 2.1 with funding from the SAFIR2018 research program [5]. Systematic checking of the input deck or comparisons to current plant configuration have not been made for at least 19 years. The model is somewhat outdated because it does not follow current best modelling practices, and plant modifications are not included in the model.

The core nodalization is presented in Figure 3-4 (left). The core is modelled with five uniform radial rings; the sixth ring represents the downcomer region. The first three axial levels represent the lower plenum; the fourth axial level represents the core support plate; levels 5–14 represent the active core region; and level 15 represents the core outlet region.

The reactor thermal-hydraulic nodalization is presented in Figure 3-4 (right). There are 7 control volumes and 10 flow paths, plus one flow path from the core to the bypass that is opened upon failure of the channel boxes. The steam lines are not modelled as a separate volume. Instead, the steam to the safety relief valves is taken directly from the downcomer volume. The instrument guide tube penetrations in the lower head were added to the model during the current project.

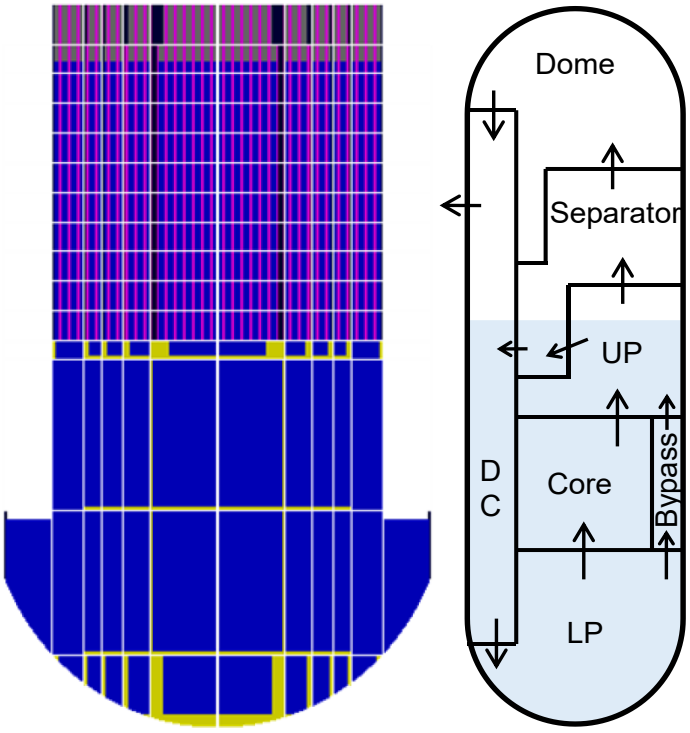

Figure 3-4. Finnish NBWR core model COR (left) and CVH (right) nodalization.

The containment is modelled with four control volumes, see Figure 3-5. The biological shield volume represents the space between the RPV and the concrete wall around it. The RPV lower head is interfaced with the biological shield volume. In addition, the model has six volumes representing rooms in the reactor building and a time-independent volume representing the environment. The control volumes of the reactor building represent major potential leakage routes from the containment to the reactor building and were purposed for hydrogen spreading and combustion analyses. The reactor building model is not purposed to model the entire complex RB configuration. Containment leakage is modelled from the drywell to the reactor building.

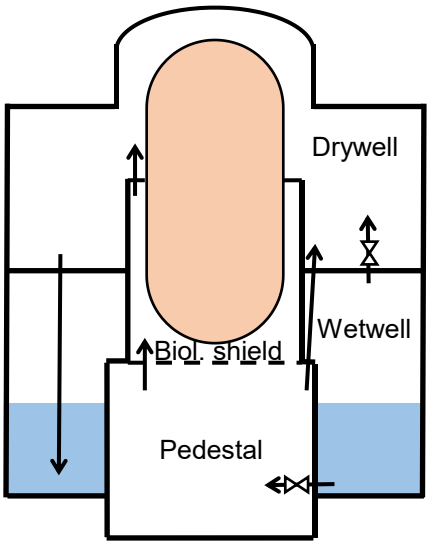

Figure 3-5. Finnish NBWR model containment nodalization.

The following systems are implemented in the Finnish NBWR MELCOR model:

- Hydraulic control rod insertion
  - Reactor scram is assumed to take place at time zero.
- Containment isolation
  - Closure of the main steam isolation valves (system 311) is activated by I-isolation or at a predefined time.
- Reactor main recirculation,
  - Modelled as a coast-down curve during the first 9.1 s of the calculation
- Pressure control and relief system
  - Relief valves controlled by downcomer pressure are modelled to discharge from the RPV downcomer to the suppression pool in the wetwell as four different groups: Group 1 opens when the downcomer pressure exceeds 8 MPa and closes when the pressure decreases below 7.4 MPa. The second group opens at 7.4 MPa and close at 7.1 MPa, the third group of valves opens at 8.5 MPa and closes at 7.6 MPa and the fourth group is open at pressure higher than 7.0 MPa and otherwise closed. The vertical discharge lines are submerged 4.5 meters in the suppression pool. SPARC pool scrubbing model is activated at the pool discharge end of the 314-pipes.
  - Automatic depressurization system of the reactor (314-ADS)

    Automatic depressurization is initiated on any of the following three signals:

    1) automatic TB signal

    2) manual TB signal

    3) on L4 signal lasting for the delay of 906 s.

    The automatic TB signal is generated if L4 signal is obtained and drywell pressure simultaneously exceeds 95 kPa and the drywell pressure increases faster than 130 Pa/s. The valve opening generates a delay of 15 s. The ADS blowdown takes place from the downcomer to the suppression pool at water

submergence of 4.5 m. SPARC model is activated at the pool discharge end of the 314 pipes by input parameter.

- Emergency core cooling system
  - The system 323 injects water to the Upper Plenum (UP node) and takes suction from the suppression pool. The injection starts when L4 signal is obtained (downcomer water level goes below 28.25 m (0.5 meters above TAF)) and the 323 pumps run until the water level in the downcomer reaches 32.25 m (= 4.5 meters above TAF). There are four (4) pumps with each having the capacity ranging from a maximum of 115 kg/s to zero at respective downcomer counter pressure range from 0.1 MPa to 1.0 MPa. The initiation of 323 injection to core spray requires also that suppression pool heat removal recirculation mode (system 322) is first locked-off.
- Auxiliary feedwater system
  - System 327 injects coolant to downcomer (50%) and to upper plenum via core spray spargers (50%). The system incorporates four (4) piston-driven pumps that produce constant water flow rate of 25 kg/s per pump independently of counter-pressure up to the pressure 2.0 MPa. The signals L2 and L3 are received when the collapsed water level in the downcomer becomes less than 2.9 m and less than 1.8 m above the top of active fuel (TAF), respectively (i.e. DC water height is less than 30.65 m and 29.55 m). Two 327 pumps start to inject water to downcomer when L2 signal is reached and a 10-s pump delay has elapsed. The DC injection continues until the collapsed water height in the DC reaches 4.0 meters above TAF. The 327 injection with two pumps through core spray spargers initiates from L3 signal with a 10-s pump delay and continues until the DC collapsed level reaches 4.5 meters above TAF.
- Failure of reactor lower head
  - A flow path from the reactor lower plenum to the pedestal is opened when MELCOR calculates lower head failure. The flow area is determined by MELCOR.
- Vacuum breaker between wetwell and drywell
  - Vacuum breakers are modelled as valves between the wetwell and the drywell near the ceiling of the wetwell. The vacuum breakers are purposed to relief wetwell pressure in situations where non-condensable gases accumulate in the wetwell thus diminishing steam suppression in the wetwell pool. The valves open when the pressure in 10 kPa higher in the wetwell than in the drywell. After pressure balancing to the level 1000 Pa the valves are fully closed.
- Drywell-wetwell leak
  - A small leakage between the wetwell and drywell is modelled, the leak area is assumed to increase with drywell pressure being at least 0.01 m2 at drywell pressure higher than 0.5 MPa.
- Drywell blowdown pipes
  - A total of 16 drywell blowdown pipes are modelled from the drywell floor to the suppression pool with a submergence depth of 6.5 m. The diameter of the pipes is about 60 cm. The SPARC pool scrubbing model is activated at wetwell discharge at the end of the blowdown pipe. The 316 pipes are purposed for the LOCA

situations, when rapid and large steam release is able to clear the water in the pipes, and steam is driven into the suppression pool for condensation.

- Containment heat removal and spray system
  - Drywell spray starts on I-isolation signal or by manual activation of the operator. The 322 system is also used for wetwell pool cooling in recirculation mode. A heat exchanger aligned in the 322 recirculation loop removes 172 kJ/K/kg from the pool water with flow capacity of 45 kg/s. The cut-off pool temperature for recirculation cooling is 291 K. Manual starting of spray requires that the water level in the drywell is lower than 2.5 m. The drywell spray flow rate is 60 kg/s.
  - The 322 spray can also be aligned to sprinkle wetwell airspace. The flow rate is then 30 kg/s. The initiation signal is I-isolation or manual start.
- Drywell flooding.
  - Assumed within 30 minutes in a station blackout situation.
- Filtered containment venting system
  - Wetwell venting is possible if the water level is below 14.5 m. The vent line elevation in the wetwell is 17.5 m. The drywell pressure needs to exceed the defined overpressure (to ambient pressure) that depends on drywell gas temperature in the following way: at a drywell temperature of 293 K, the threshold overpressure is 0.5 MPa and at 453 K the threshold is 0.4 MPa. The actual filtering of substances containing radionuclides is modelled by simple filter factors based on system requirements.
  - The drywell venting through a rupture disk takes place if the water level in the wetwell has been higher than 14.5 m for longer than a specified time (which precludes possibility of venting from wetwell) and the drywell pressure is higher than 0.2 MPa.
- Reactor building blow-off panel
  - opening at a pressure difference of 2.5 kPa to the environment.

4. Methods and Tools for Uncertainty Analysis with MELCOR code

4.1. Methods used for sensitivity and uncertainty analysis

4.1.1. Sensitivity analysis

The sources of uncertainty in analysis of severe accident progression are numerous and it is impractical to address all of them quantitatively. Experience in performing uncertainty studies of severe accident phenomena (e.g. [15,16,17,18]) suggests that the effects of uncertainties from some sources are larger and more dominant than the effects of uncertainties from other sources. In an integral sense, then, the aggregate uncertainty in main figures of merit (FOMs) can be estimated by selecting the dominant sources of uncertainty and treating them in detail. The dominant sources of uncertainty should be identified by sensitivity analysis.

A review of global sensitivity analysis methods (see [12] for more details) presents a brief summary on a great variety of different sensitivity analysis methods. Figure 4-1 provides a synthesis of SA methods presented in the paper.

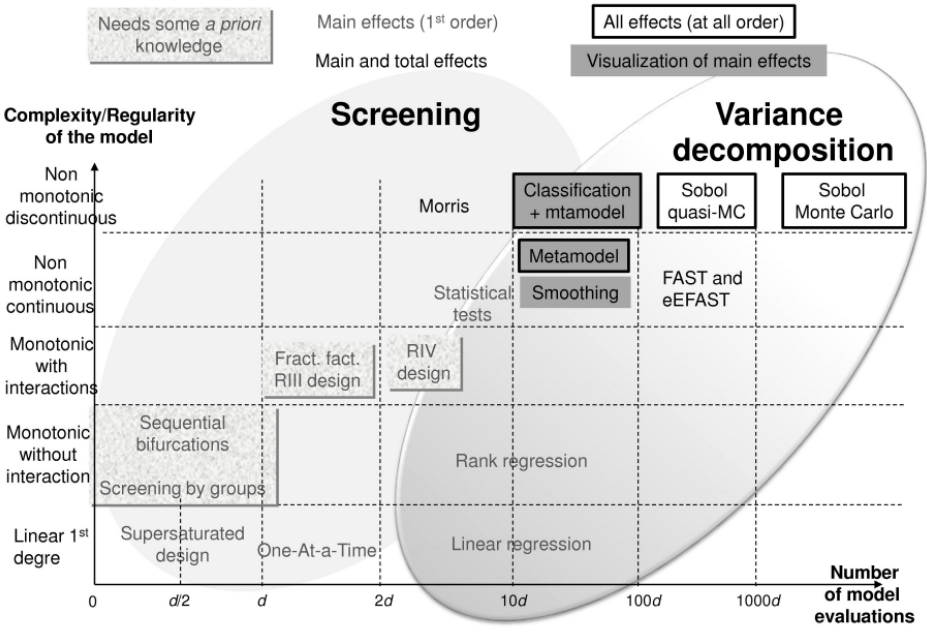

Figure 4-1. SA methods graphical synthesis [12].

Based on the review, the Morris method has been selected as an appropriate tool to perform sensitivity analysis. The Morris method is a screening method that can be applied to models with non-monotonic and discontinuous behavior. Furthermore, based on [8,12] the Morris method should give reasonable results given relatively low computational effort (from approximately *2d* to *10d* model evaluations, where *d* is the number of uncertain parameters).

4.1.1.1. Morris method for sensitivity analysis

The Morris method [9] is a global sensitivity analysis method. The Morris method performs analysis of the model outputs along different trajectories in the input space where parameters are varied "one-factor-at-a-time" (OAT) and the effect of changing every parameter is evaluated through elementary effects - $d_i(x^j)$ calculated by:

$$d_i(x^j) = \frac{[f(x^{i+1}) - f(x^i)]}{\Delta} \quad (1)$$

where $f(x)$ – is the model function, x^j – j-th input vector, Δ - variation step, which is linked to the number of levels (p) as follows:

$$\Delta = \frac{p}{2(p-1)} \tag{2}$$

The number of levels - p and number of elementary effects – r, are defined by a user. The large values of p will require large number of r to be calculated to have reasonable coverage on input domain. Based on [8] the recommended choice for the number of elementary effects is $r = 10$ (or at least $r \geq 4$), and the number of levels should be equal to $p = 4$.

When r – elementary effects are calculated for each input parameter, two sensitivity measures are used:

$$\mu_i = \sum_{i=1}^{r} \frac{|d_i|}{r}; \sigma_i = \sqrt{\sum_{i=1}^{r} (d_i - \mu)^2 / r} \tag{3}$$

where the values of μ_i, substantially different from zero, indicate significant overall influence of i^{th} input; and large values of σ_i indicate possible interactions with other input parameters and non-linear behaviour of the output with respect to the input.

The number of model evaluations to be performed is calculated by

$$N = r * (k + 1) \tag{4}$$

where k is the number of input factors and r is the number of elementary effects.

The Morris method for SA is available in the Dakota package [10]. A pyDakota coupling interface for Morris SA has been developed and implemented in pyMELCOR simulation platform (see section 4.1.3). It performs processing of the user input and generation of the sampling set, as well as processing of the results and generation of sensitivity analysis results.

4.1.1.2. One-way ANOVA

One-way ANOVA can be used to perform analysis of variance in the data set produced by Morris method for SA. The levels p and variation step Δ divide the space of the model input parameters into the subsets where each parameter has an unique fixed value. The variance within each subset can be analyzed whether the subsets means are equal (null hypothesis).

The F-statistic can be used to judge the effect/importance of the parameter in question, i.e., as F-value is defined as variation between sample means vs. variation within the samples, large F>>1 values can indicate that the parameter has significant effect on the results.

4.1.2. Uncertainty analysis

Uncertainty quantification (UQ) is the process of determining the effect of input uncertainties on model responses. These input uncertainties may be characterized as either aleatory uncertainties, which are irreducible variabilities inherent in nature, or epistemic uncertainties, which are reducible uncertainties resulting from a lack of knowledge. Since sufficient data is generally available for aleatory uncertainties, probabilistic methods are commonly used for computing response distribution statistics based on input probability distribution specifications. Conversely, for epistemic uncertainties, data is generally sparse, making the use of probability theory questionable and often leading to non-probabilistic methods based on e.g., interval specifications (Dempster-Shafer evidence theory) [10].

The objective of evidence theory is to model the effects of epistemic uncertainties. Epistemic uncertainty refers to the situation where one does not know enough to specify a probability distribution on a variable. Sometimes epistemic uncertainty is referred to as subjective, reducible, or lack of knowledge uncertainty. In Dempster-Shafer theory of evidence, the uncertain input variables are modelled as sets of intervals. The user assigns a basic probability assignment (BPA) to each interval, indicating how likely it is that the uncertain input falls within the interval. The intervals may be overlapping, contiguous, or have gaps. The intervals and their associated BPAs are then propagated through the simulation to obtain cumulative distribution functions on belief and plausibility. Belief is the lower bound on a probability estimate that is consistent with the evidence, and plausibility is the upper bound on a probability estimate that is consistent with the evidence [10,14].

Alternatively, ROAAM+ methods can be employed, which make use of the second order probabilities [13]. The ROAAM+ framework for Nordic BWR employs the concept of second-order probability in quantification of the conditional containment failure probability. The need for the second-order probabilities comes from the realization of the nature of epistemic uncertainties in prediction of failure probability (i.e., partial probabilistic knowledge). Epistemic uncertain parameters in ROAAM+ framework is separated into two groups, depending on the degree of knowledge:

- Model deterministic parameters – complete probabilistic knowledge (i.e., range and probability distribution).
- Model intangible parameters – incomplete or no probabilistic knowledge, one can only speculate regarding the possible range.

Based on ROAAM+ formulation, since probabilities are designed to handle uncertainty, it would be logical to consider representing uncertain probabilities with probabilities. Thus, in order to assess the importance of the missing information about the distributions of intangible parameters the distributions itself are considered as uncertain (i.e., parameters that characterize distributions, as in hierarchical Bayesian models).

4.1.2.1. Sampling-based uncertainty propagation

An analysis outcome of a model will have an uncertainty structure that derives from the uncertainty structure of the model input parameters. For uncertainty propagation through a model, it is important that the sampling set of model input parameters provides an adequate coverage of the space of these parameters. Adequate coverage of the uncertainty space of model input parameters depends on various factors, such as the number of samples, selected probability distributions as well as the choice of sampling approach.

4.1.2.2. Number of samples

Wilks' non-parametric method for setting tolerance limits is one of the common choices to determine tolerance limits with some confidence level for input parameters with unknown distributions in computational applications in the nuclear industry. The advantage of Wilks' method is the required sample size is independent of the number of input parameters and all input parameters can be sampled simultaneously.

Table 4-1 provides the minimum sample size N required to obtain various tolerance/confidence upper bounds (one sided) and intervals (two-sided) for ranks from 1 to 10. It shows that larger sample sizes N are required to increase the tolerance and the confidence. In addition, higher rank order statistics require an increase in the number of samples [19].

Table 4-1. Minimum sample size required for tolerance/confidence Wilks tolerance limits and bounds. Results are shown for four common tolerance/confidence combinations for ranks from 1 to 10 [19].

r	95%/95%		95%/99%		99%/95%		99%/99%	
	Bound	**Interval**	**Bound**	**Interval**	**Bound**	**Interval**	**Bound**	**Interval**
1	59	93	90	130	299	473	459	662
2	93	153	130	198	473	773	662	1001
3	124	208	165	259	628	1049	838	1307
4	153	260	198	316	773	1312	1001	1596
5	181	311	229	371	913	1568	1157	1874
6	208	361	259	425	1049	1818	1307	2144
7	234	410	288	478	1182	2064	1453	2409
8	260	458	316	529	1312	2306	1596	2669
9	286	506	344	580	1441	2546	1736	2925
10	311	554	371	631	1568	2784	1874	3179

Higher rank Wilks' estimates correspond to using more centrally located order statistics to estimate the desired tolerance limit. These estimates require larger sample sizes but estimate the same tolerance with approximately equal confidence [19].

4.1.2.3. Random and LHS Sampling

Random sampling is a part of the sampling technique in which each sample has an equal probability of being chosen.

A sample chosen randomly is meant to be an unbiased representation of the total population. Latin hypercube sampling (LHS) is a statistical method for generating a near-random sample of parameter values from a multidimensional distribution. When sampling a function of N variables, the range of each variable is divided into M equally probable intervals. M sample points are then placed to satisfy the Latin hypercube requirements; this forces the number of divisions, M, to be equal for each variable. This sampling scheme does not require more samples for more dimensions (variables); this independence is one of the main advantages of this sampling scheme. Another advantage is that random samples can be taken one at a time, remembering which samples were taken so far.

Both random and LHS sampling techniques are available in the Dakota[1] package [10]. A pyDakota interface for random and LHS sampling in Dakota has been developed. It performs user input processing (parameters, ranges and distributions) and generation of the sampling set. Currently, the interface supports truncated normal, truncated lognormal, uniform, loguniform, triangular, exponential, beta, gamma and Weibull distributions, as well as discrete real and integer sets with predefined probabilities. Furthermore, the sampling accounts for correlations among the variables, which can be defined by a user-supplied correlation matrix.

[1] Dakota is an open-source Multilevel Parallel Object-Oriented Framework for Design Optimization, Parameter Estimation, Uncertainty Quantification, and Sensitivity Analysis developed by SNL.

4.1.2.4. Importance sampling

Importance sampling is a method that allows one to estimate statistical quantities such as failure probabilities in a way that is more efficient than Monte Carlo sampling. The core idea in importance sampling is that one generates samples that are preferentially placed in important regions of the space (e.g. in or near the failure region or user-defined region of interest), then appropriately weights the samples to obtain an unbiased estimate of the failure probability [10].

Importance sampling technique can be applied when performing post-processing of the uncertainty analysis results, to assess the effect of missing information regarding probability distributions of intangible parameters (see section 4.1.2).

4.1.3. MELCOR simulation platform

A simulation platform (pyMELCOR) has been developed in Python to perform sensitivity and uncertainty analysis with MELCOR code.

Based on the user input, the pyDakota interface generates an input file for sensitivity/uncertainty analysis using Dakota [10]. The simulation driver (pyMELCOR) generates a set of MELCOR input decks and performs parallel execution of the MELCOR code. In case of code convergence issues and crashes, pyMELCOR performs adaptive refinement of the maximum time step and restarting in case of crashed simulations. The plot data (FOMs and other MELCOR code plot variables defined by the user) is extracted using the pyPTF extraction script, written in Python based on the MELCOR plot file format described in [11]. The extracted data is stored in the MELCOR database of solutions, while FOMs are analyzed in the Dakota package [10].

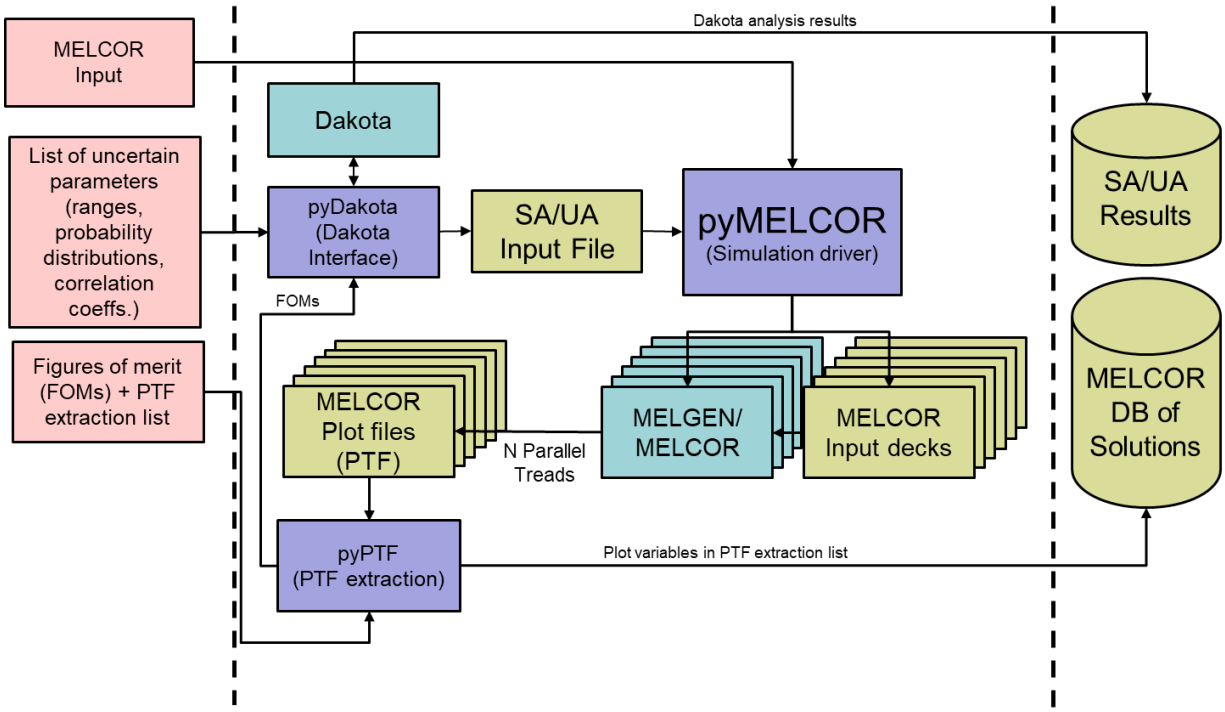

Figure 4-2. pyMELCOR simulation platform.

4.2. Methods used for sensitivity and uncertainty analysis by VTT

VTT's method of choice for both the sensitivity and uncertainty analyses was Dakota SNAP plug-in, which was used to sample the model parameters and to post-process majority of the results.

SNAP (Symbolic Nuclear Analysis Package) is an analysis tool developed by ISL (Information Systems Laboratories), and it consists of multiple integrated analysis code applications such as MELCOR, CONTAIN, and TRACE. It enables the creation and editing of model inputs, as well as setting up job streams and running the models and the other codes. SNAP also provides a robust visualization of the models [37].

Dakota (Design Analysis Kit for Optimization and Terascale Applications) toolkit has been developed by Sandia National Laboratories (SNL) for optimization and uncertainty quantification [38]. The SNAP plug-in for Dakota enables the addition of the uncertainty step in the job stream in SNAP. The main tasks of the uncertainty step are parameter sampling according to the user-input data (sampling method, target probability and confidence levels, bounds of the parameter values, probability distributions) of which Dakota calculates the adequate number of samples using the Wilks method mentioned in chapter 4.1.2.2, and post-processing of the results into a report form.

Using Dakota with SNAP is not necessarily straightforward. One well-known issue with the plug-in is that if even one of the generated MELCOR input files fails during the MELGEN step, no Dakota uncertainty report is generated at the end of the simulation run. Crashes during the MELCOR step might not prevent Dakota from generating the report, but they may produce incomplete results, which will affect the final results of the sensitivity and uncertainty studies. Moreover, even though the SNAP plug-in for Dakota uses the actual Dakota code, the features within SNAP are rather limited. For example, there seems not to be an intuitive way to use other sensitivity analysis methods such as the Morris method.

To combat these issues, Python directed job streams were set up in SNAP. With Python, it is possible to extend the definition of the failed cases to cover the crashed cases as well and to utilize SNAP's "replacement samples" feature, which allows the resampling and rerunning of the failed cases. To use other sensitivity methods, it should be possible to run Dakota with Python. However, that was unsuccessful, so SALib Python library was used instead to perform the Morris sensitivity analysis.

For SNAPs default sensitivity analysis method, Dakota calculates multiple correlation coefficients that can be used in assessing the sensitivity of the model against the input parameters. The first one is called simple correlation coefficient in Dakota, but it is also known as Pearson correlation coefficient. It measures the linear correlation between two datasets, in this case between the parameter and the FOM. Pearson correlation between variables x and y can be calculated with [38].

$$Corr(x,y) = \frac{\sum_i (x_i - \bar{x})(y_i - \bar{y})}{\sqrt{\sum_i (x_i - \bar{x})^2 \sum_i (y_i - \bar{y})^2}} \quad (5)$$

The second coefficient is called partial correlation coefficient. In addition to the linear correlation between two variables, it also considers the effect of the other parameters. Both coefficients also have a rank form. The rank form of Pearson correlation coefficient is called simple rank correlation coefficient in Dakota and Spearman correlation coefficient elsewhere.

The difference between the original correlation and rank correlation is that instead of actual values, rank correlation coefficients are calculated from the ranks of the datasets. This way, the effect of possible outliers in datasets can be minimized.

5. Results

5.1. Analysis of containment bypass scenarios in Nordic BWR

5.1.1. Release pathways in case of containment bypass scenarios in Nordic BWR

Boiling Water Reactors are single-cycle systems where the water in the primary system is converted into steam in the reactor vessel. The steam from the reactor pressure vessel travels through the main steam lines to the turbine building, where it spins the turbine. To achieve better efficiency, the turbine is subdivided into a high-pressure turbine and low-pressure turbine, both sitting on the same shaft connected to the generator. The high-pressure turbine steam exhaust is typically passed through a set of moisture separators and steam reheaters before it enters the low-pressure turbine. The steam from the low-pressure turbine is then directed to the condenser, condensed, and finally reused by the main feedwater system, forming a closed loop.

Furthermore, during normal operation, part of the steam produced by the reactor is used by other systems, such as the turbine gland sealing system, to prevent leakages of high-pressure steam along the turbine shaft or the ingress of non-condensable gases at the low-pressure turbine exhaust due to the vacuum in the condenser.

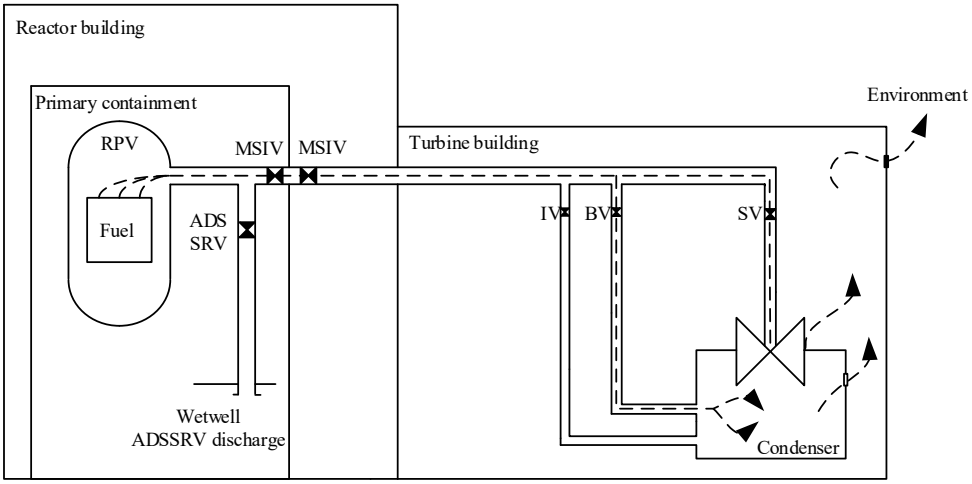

Figure 5-1. Release pathways in case of failed isolation of main steam lines.

The main steam lines are equipped with main steam isolation valves (MSIVs), with one MSIV located just inside the containment and one MSIV just outside the containment. In case of an accident, the MSIVs should close and isolate the containment from the environment. Outside the containment, the main steam lines are equipped with turbine stop valves (SVs) and turbine bypass valves (BVs). Furthermore, according [44], some reactors designs are equipped with a drainage line with drainage isolation valves (IVs), connected to the main steam lines. MSIVs close automatically in response to containment isolation, isolation of main feedwater lines or isolation of main steam-lines signals.

In case of an initiating event that results in a turbine trip, the reactor power will be decreased (partial SCRAM), the turbine will be isolated by the turbine stop valves (SVs), and the steam will be diverted to the main condenser by opening the turbine bypass valves (BVs). Loss of condenser vacuum (due to loss of cooling water) will trigger a turbine trip, reactor shutdown (SCRAM), and isolation of the main condenser by closing the BVs and MSIVs. The steam will then be diverted to the condensation pool via the safety relief valves (SRVs). Failure to isolate the condenser may result in high pressure in the condenser, leading to the opening of the rupture disks and steam release to the turbine building.

In the case of a severe accident, unisolated main steam lines can lead to a large early release to the environment. According to analyses performed in [40-43], containment bypass sequences, including accident sequences with open MSIVs, are one of the largest contributors to the unacceptable release[2] frequency in Nordic BWRs.

Release path to the environment

Possible release paths to the environment in case of leakage from the MSIVs are discussed in [44] and depicted in Figure 5-1.

Some modifications in Figure 5-1 include rupture disks in the condenser, which can be relevant in case of failed isolation of the main steam lines, and failed isolation of the BV valves. These failures can lead to the pressures in the condenser above the opening pressure of the rupture disks in the condenser/LP turbine exhaust (at ~0.3-0.5 Bar overpressure).

The analysis performed in [44] suggests with all valves in the main steam lines and in the steam system in closed position, all leakages through the MSIVs would be along the main steam lines, through the turbine SVs and control valves, through the high-pressure turbine, into the turbine steam seals (which are no longer sealed because of the lost steam) and into the turbine building (the turbine stop and control valves are not as tight sealing as the MSIVs, so any leakage past the MSIVs would be expected to leak past the turbine stop valves and control valves) [44].

An alternative path could be through the turbine bypass valves (BVs), if the valves fail to close or leaking, to the condenser. Without AC power, the vacuum in the condenser will be lost and pressure will increase to normal atmospheric pressure [44]. Leakage from the condenser would be through the LP turbine seals [44], or, alternatively, through the rupture disks if the leakage rate from the MSIVs, BVs exceed the leakage rate through the LP turbine seals, which may lead to condenser pressure increase and opening of the condenser rupture disks.

In all cases, the fission products will be released to the turbine building. BWR turbine buildings have a large volume and are completely enclosed, which promotes deposition of fission products.

5.1.2. MELCOR modelling

Due to limited information available regarding the design and operation procedures for Nordic BWRs, the analysis conducted within the scope of this project will be limited to a sensitivity analysis, using the information available for other BWR reactors designs, e.g. as presented in [45] for Browns Ferry NPP Units 1,2,3 (GE BWR4 – Mark I reactor design).

The existing version of the MELCOR model of Nordic BWR was updated to include additional volumes and heat structures representing the high-pressure turbine, turbine casing and turbine building, as illustrated in Figure 5-2.

[2] Releases over 0.1 % of the inventory of the cesium isotopes Cs-134 and Cs-137 in a core of 1800 MW_{Th}, excluding noble gases, which corresponds to a release of 160 TBq of Cs-134 and of 103 TBq of Cs-137 [48].

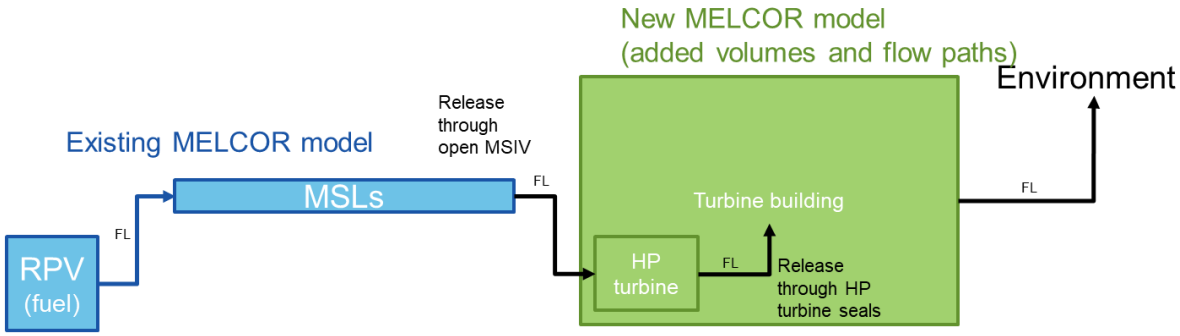

Figure 5-2. Modelling of the high-pressure turbine and the turbine building in the MELCOR model of Nordic BWR.

Some of the modelling parameters were assumed due to the lack of available information, as discussed in the text below.

Modelling of the seal leakage flow path (HP turbine to Turbine building):

- Turbine rotor diameter – 0.5 m (assumed).
- Radial clearance between the rotor and casing – 1 mm (assumed).
- Number of fins in the seal – 10, 50, 100 and 150 (assumed, treated as uncertain parameters, see section 5.1.3).
- Flow geometry and form loss coefficients were adjusted based on the calculations performed in 5.1.2.1, using the process variables from MELCOR code simulations of the Nordic BWR at steady state conditions.

Modelling of the high-pressure turbine and turbine building:

- HP turbine free volume, Turbine building free volume –Browns Ferry BWR data was used [45].
- Geometries of the heat structures representing the HP turbine casing and turbine building were assumed (assumed).
- No credit taken for the HP turbine internal parts (turbine blades) and other equipment in the turbine building.
- Release from turbine building (0.126 m^2 – assumed).
- No credit taken for the turbine building ventilation and filtering system.

5.1.2.1. Steam seals leakage

Estimation of leakage rates through steam seals is very important for correct prediction of the reactor coolant system response, fission products transport along the release pathways from the reactor coolant system to the environment in the MELCOR code.

Various approaches exist for estimating leakage rates through steam seals. For more precise results, particularly for complex seal designs, detailed empirical data or computational fluid dynamics (CFD) simulations may be necessary to obtain accurate estimates. However, these approaches require in-depth knowledge of the system design and operational data.

Alternatively, several analytical models for estimating leakage rates through labyrinth seals are available [46,47]. Since most of these approaches require relatively detailed data regarding labyrinth seal design, the Martin's model was selected for this project:

$$\dot{m} = A_f \sqrt{\rho_i P_i \frac{1 - (P_e/P_i)^2}{N - \ln(P_e/P_i)}} \quad (6)$$

where A_f – flow area (m^2), ρ_i – steam density at operating conditions (on the turbine side) (kg/m^3), P_e, P_i – external and internal pressure (Pa) and N – number of fins in the labyrinth seal.

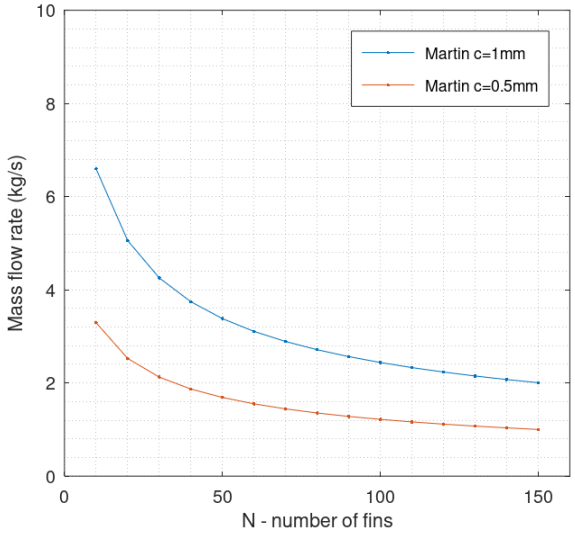

Figure 5-3. Mass flow rate through the labyrinth seal as a function of N – number of fins in the seal.

Mass flow rate though the labyrinth seal as a function of number of fins at steady state conditions (as predicted by MELCOR) in the steam lines and turbine inlet was calculated using the Martin´s model. This calculation was performed for two turbine rotor – turbine casing clearance values, as illustrated in Figure 5-3.

The form loss coefficients in the turbine seals' leakage flow path in the updated MELCOR model of Nordic BWR were adjusted to match the mass flow rate calculated by the Martin´s model at 10, 50, 10 and 150 fins, and 0.5mm and 1mm clearance.

5.1.3. Accident scenarios

The source term analysis was performed using the MELCOR code for four accident scenarios, summarized in Table 5-1.

All considered scenarios originally belong to the RC3 release category - Containment bypass due to unisolated RPV (failure to close main steam or main feedwater isolation valves) [23].

It the default scenario – Case DEF, the accident is initiated by a guillotine break in the steam lines outside the containment with failed isolation of the MSIVs. No credit taken for the components and structures outside the containment. This type of scenario leads to a large early release to the environment, and typically assumed as a representative source term in the L2 PSA for Nordic BWR for all accident sequences with failed isolation of MSIVs, regardless the type of initiating event.

Case 1,2 and 3 (Table 5-1) employ refined MELCOR modelling discussed in section 5.1.2, The accident is initiated by a transient, with all active safety systems being unavailable (SBO). Furthermore, it is assumed that the turbine BV and IV valves are closed, while the turbine SV valves remain open. The valves in the steam reheating system are closed, meaning that there is no steam flow passed the high-pressure turbine. The reactor coolant system

depressurization and flooding of the lower drywell are initiated according to the standard logic (see section 3). Containment pressure relief through MVSS is initiated:

- Case 1 - automatically when the pressure in the containment exceeds 5.5 Bar(a);
- Case 2 - manually by operators when the pressure in the containment exceeds 2.5 Bar(a);
- Case 3 - manually by operators when pressure in the containment exceed 2.5 Bar(a), and the independent spray system is activated after the failure of the RPV lower head.

The radial clearance between the rotor and casing of the high-pressure turbine was assumed to be equal c = 1 mm.

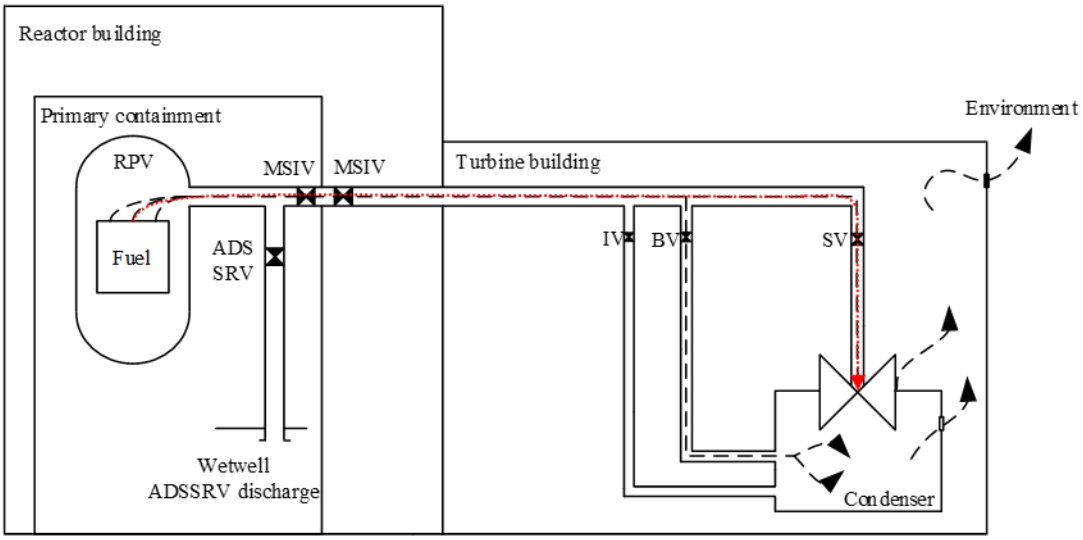

Figure 5-4. Containment bypass release path considered in the analysis (in red).

Table 5-1. Accident scenarios considered in the analysis of the containment bypass scenarios.

Description	**N fins in the seal**	**Case ID**
Case DEF: Unmitigated SL-LOCA outside the containment with failed isolation of MSLs (representative scenario for all containment bypass release categories in the PSA L2 for Nordic BWR).	N/A	DEF
Case 1: Unmitigated (automatic opening of the MVSS scrubber)	10	C1C1
	50	C1C2
	100	C1C3
	150	C1C4
Case 2: Mitigated 1 (manual opening of the MVSS filter at 2.5 Bar overpressure)	10	C2C1
	50	C2C2
	100	C2C3
	150	C2C4
Case 3: Mitigated 2 (manual opening of the MVSS filter at 2.5 Bar overpressure and spray in the containment with the independent spray system)	10	C3C1
	50	C3C2
	100	C3C3
	150	C3C4

5.1.4. Results

The results of the analysis are summarized in Table 5-2 and Figures 5-5 - 5-8.

Figure 5-5 and Figure 5-6 show the fraction of the core inventory of Cs released to the environment in the accident scenarios considered in the analysis (Table 5-1). The default scenario (DEF) leads to a large early release (over 10% of the core inventory of Cs) with over 80% of the core inventory of Cs released to the environment.

Table 5-2. Analysis of containment bypass scenarios – results summary.

Case ID		**Cs release over acceptable release threshold [h]**	**Cs release after 6 h hours [-]**	**Cs release after 12 hours [-]**	**Cs release after 24 hours [-]**	**Cs release after 72 hours [-]**
Case DEF	DEF	0.15	8.15E-01	8.17E-01	8.18E-01	8.19E-01
Case 1	C1C1	1.42	3.32E-03	4.71E-03	5.13E-03	5.29E-03
	C1C2	2.75	1.26E-03	3.03E-03	3.58E-03	3.84E-03
	C1C3	5.96	4.71E-04	1.52E-03	1.92E-03	2.20E-03
	C1C4	28.81	6.97E-05	1.96E-04	3.63E-04	5.91E-04
Case 2	C2C1	1.44	2.11E-03	3.92E-03	5.22E-03	5.43E-03
	C2C2	2.46	7.56E-04	2.22E-03	2.87E-03	3.30E-03
	C2C3	5.64	5.72E-04	1.73E-03	2.22E-03	2.54E-03
	C2C4	21.00	7.57E-05	4.06E-04	5.08E-04	7.47E-04
Case 3	C3C1	1.44	2.59E-03	5.84E-03	7.18E-03	7.56E-03
	C3C2	2.46	5.90E-04	2.57E-03	4.20E-03	4.96E-03
	C3C3	11.78	9.69E-05	4.84E-04	1.39E-03	1.69E-03
	C3C4	16.72	4.43E-05	4.13E-04	6.99E-04	9.77E-04

The total release of Cs to the environment in Case1-3 is below the large early release threshold, however above the acceptable release[2] threshold.

Overall, the results for Case1-3 show that the magnitude of Cs release to the environment depends on the mass flow rate through the steam seals (depends on the number of fins), which can change the release size by over one order of magnitude.

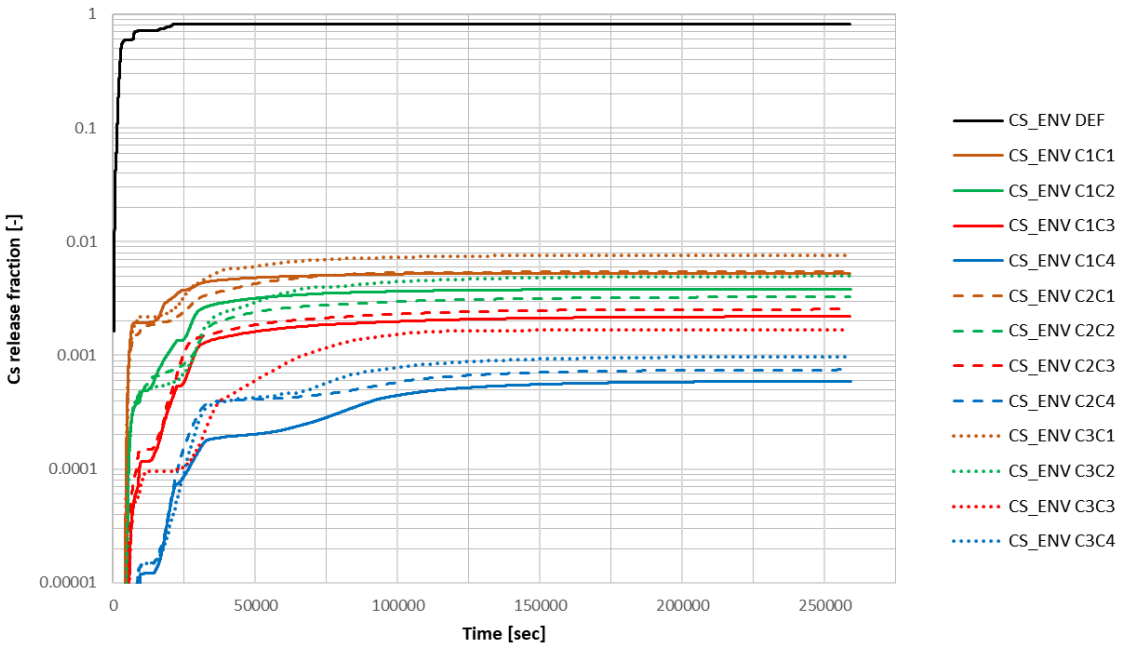

Figure 5-5. Fraction of the core inventory of Cs released to the environment.

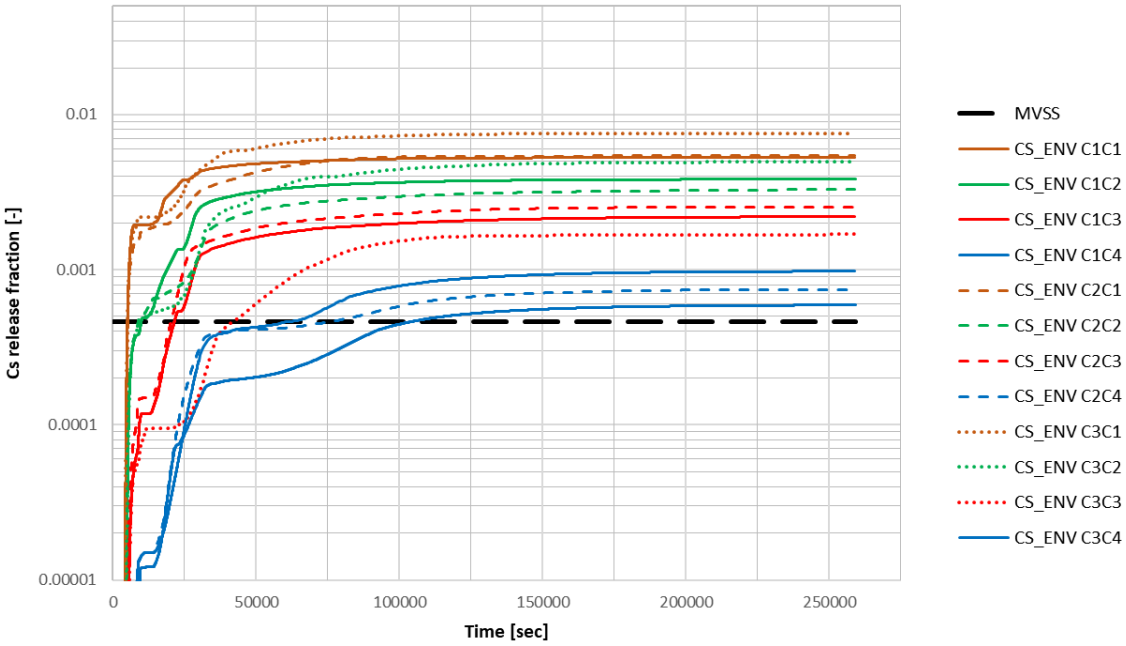

Figure 5-6. Fraction of the core inventory of Cs released to the environment in Case 1 – 3; acceptable release[2] threshold (MVSS).

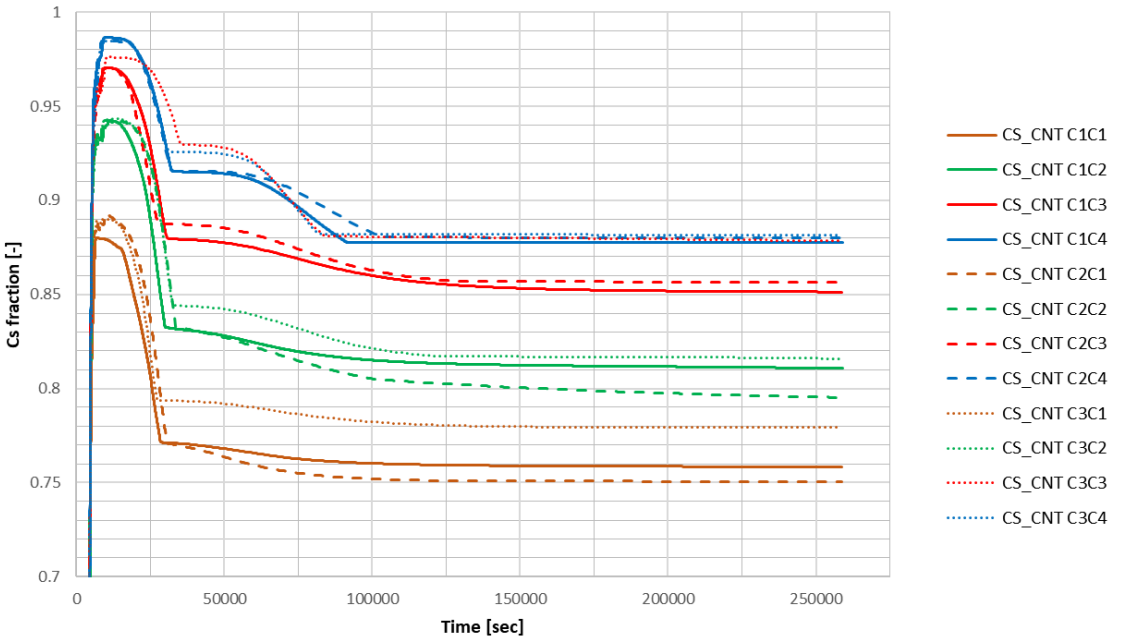

Figure 5-7. Fraction of the core inventory of Cs deposited in the containment and MVSS (deposited on HSs, pool and airborne).

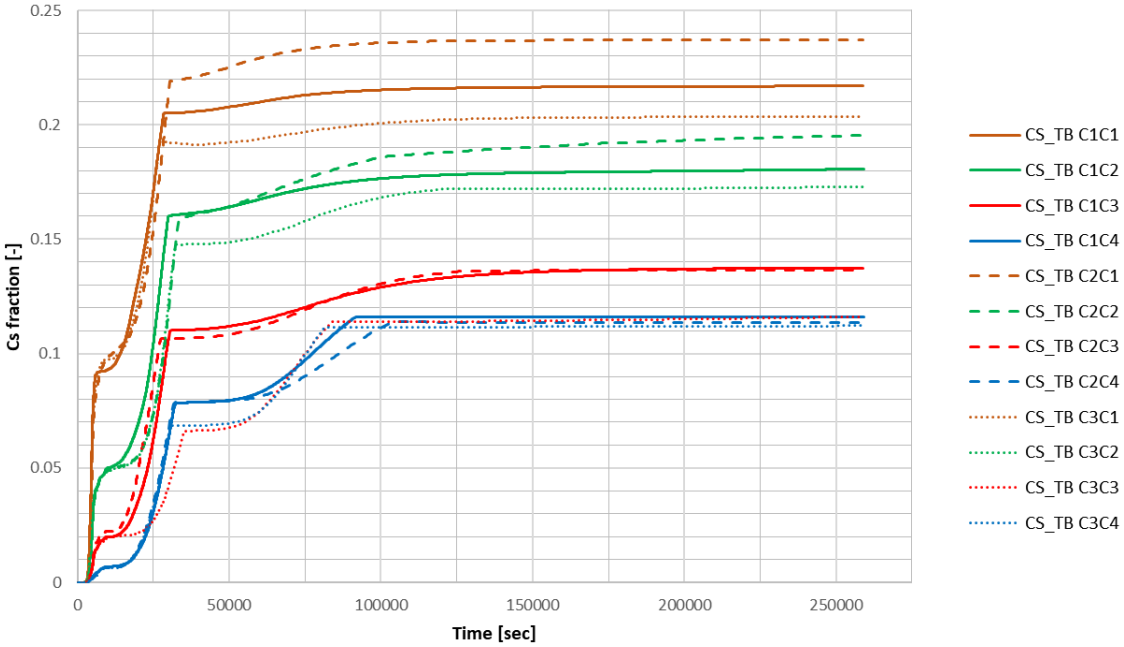

Figure 5-8. Fraction of the core inventory of Cs deposited in the turbine building (deposited on HSs, pool and airborne).

The deposition of fission products inside the turbine building is significantly affected by extensive steam condensation during the early phases of severe accident progression. In all accident scenarios considered in the analysis, a substantial amount of steam is released from the reactor coolant system through the turbine seals into the turbine building during the early stages of accident progression. When the core is completely uncovered and starts to heat up, degrade, and release volatile fission products, such as Cs, into the reactor coolant system and via the main steam lines, high-pressure turbine, and turbine seals into the turbine building, the steam flow from the core is significantly lower than during the earlier phases. This results in sub-atmospheric conditions in the turbine building, causing air ingress from the environment, which essentially limits the release of volatile fission products from the turbine building into

the environment, and provide additional time to deposit the fission products inside the turbine building.

Another important observation from the analysis is that the differences between accident scenarios considered in Case 1-3 are not as significant compared to the uncertainty in the flow rate from the high-pressure turbine to the turbine building (number of fins in the steam seals and flow path geometry).

5.1.5. Discussion and Conclusions

The analysis show that the SSC located outside the containment can significantly reduce conservatism in the source terms in the case of a containment bypass (RC3 release category [23]). The results indicate that further reducing the uncertainty in the release path geometry, the effect of components and structures (such as turbine internals and turbine building internals), and systems (such as the turbine building ventilation system) may lead to even greater reduction of the conservativism in the analysis.

Finally, the analysis was performed using the best estimate/recommended values of the MELCOR code's uncertain parameters, which can affect accident progression and the environmental source term. Therefore, it is recommended that future analyses be complemented by sensitivity analysis and uncertainty quantification.

5.2. Analysis of the effect of mitigative actions in filtered containment venting scenarios in Nordic BWR

The uncertainty analysis performed within the second phase of the NKS-STATUS project [49] showed that the magnitude of the source term released to the environment in unmitigated filtered containment venting scenarios initiated by a LB-LOCA may lead to exceedance of the acceptable release[2] threshold for some MELCOR modelling parameters combinations, such as the mode of debris ejection from the vessel (IDEJ) and decontamination factor for radioactive vapors (MVSSDFV), for further details refer to [23,49,50].

This, however, contradicts the grouping of accident scenarios into release categories (RC) in the L2 PSA for Nordic BWR, where these accident sequences belong to the RC7 - acceptable release category [23].

This issue can be addressed either by revising the PSA modeling of the MVSS in the PSA L2 or by considering additional mitigative safety functions in the analysis.

One of the mitigative safety functions that can limit fission products release to the environment in these scenarios is the independent containment spray system, which is typically activated after RPV failure, to scrub the containment atmosphere, reduce pressure in the containment, and flood the containment to ensure debris coolability. The purpose of this paper is to evaluate the effect of the independent spray system on the containment pressure response and the source term released to the environment in accident scenarios initiated by a LB-LOCA that leads to filtered containment venting to the environment.

5.2.1. Uncertain modelling parameters

Table 5-3 summarize MELCOR code uncertain modelling parameters considered in uncertainty analysis of filtered containment venting scenarios.

Table 5-3. MELCOR code modelling parameters considered in uncertainty analysis.

Parameter ID	Parameter description and proposed distribution	Accident scenario
STICK [-]	Particle sticking probability. Scaled beta (2.5, 1.0), scaled on [0.5, 1.0] [31]	All
FCELRA [-]	Radiative exchange factors. Truncated normal (0.1, 0.035) truncated on [0.020, 0.30] [27]	All
SC71521 [m]	Initial bubble diameter correlation coefficient in SPARC-90 model. Triangular M = 7.E-3, range [5.E-3, 8.E-3] [EJ]3	LOCA-IDEJ0 LOCA-IDEJ0-SPR
SC1020 [-]	Multiplication factor for time constant for radial solid and molten debris relocation. Scaled beta (1.33, 1.67) scaled on range [1.0, 4.0] [29]	LOCA-IDEJ0 LOCA-IDEJ0-SPR
CORNSBLD [K]	NS failure temperature threshold. Uniform [1520-1700] [30]	All
VFALL [m/s]	Velocity of falling debris. Scaled beta (0.85, 1.14), scaled on range [0.01, 1.0] [29]	All
TZRSSINC [K]	Solidus temperatures for ZR/SS and ZR/INC eutectic pairs. Scaled beta (2.0, 1.0), scaled on range [1210, 1700] [EJ]	All

[3] EJ – expert judgement.

Parameter ID	Parameter description and proposed distribution	Accident scenario
SC715010 [-]	Scaling factor for SPARC-90 model vent exit condensation decontamination factor. Triangular M = 2, range [1.0, 3.0] [EJ]	All
CHI [-]	Aerosol dynamic shape factor. Scaled beta (1.0, 1.5) scaled on [1.0, 5.0] [31]	All
MVSSDFV [-]	MVSS decontamination factor for radioactive vapors. Lognormal (4.6, 0.916) truncated on [10,1000], 0.99 – correlation with MVSSDFA [EJ]	All
SC71568[-]	Multiplicative constant in a temperature correction correlation in the SPARC-90 model. Triangular M = -0.00232, [-2.6691e-03, -1.9728e-03] [EJ]	All
TPFAIL [K]	Penetration failure temperature. Scaled beta (2.0, 2.0) scaled on [1273, 1600] [EJ]	All
HFRZZR [W/m2K]	Refreezing heat transfer coefficient for Zr. Lognormal (8.9227, 0.55962) truncate on [2000, 22000] [27]	All
SC7170CSM [kg/kgH2O]	Saturation solubility at high and low temperature reference for CsM. Triangular M = 0.67, range [0.5695, 0.7705] [EJ]	LOCA-IDEJ0 LOCA-IDEJ0-SPR
SC71555 [-]	SPARC-90 model multiplication constants in the DF factor correlations for and large Stokes numbers. Triangular M = 1.13893, range [0.9681, 1.3098] [EJ]	All
RHONOM [kg/m3]	Aerosol density. Triangular M = 2000, range [870,4500] [26]	All
SC7111CS2 [K]	Characteristic energy of interaction between the molecules divided by the Boltzmann constant for CsI/CsM. Triangular M = 97, range [82.450,111.550] [EJ]	LOCA-IDEJ0 LOCA-IDEJ0-SPR
SC7170CS [kg/kgH2O]	Saturation solubility at low/high temperature reference for Cs. Triangular M = 3.95, range [3.3575, 4.5425] [EJ]	LOCA-IDEJ1 LOCA-IDEJ1-SPR
SC7111CS1 [Å]	Characteristic diameter of the molecule for Cs. Triangular M = 3.617, range [3.0745,4.1595] [EJ]	LOCA-IDEJ1 LOCA-IDEJ1-SPR
TURBDS m2/s3]	Turbulence dissipation rate. Uniform [7.5E-4, 1.25E-3] [28][EJ]	LOCA-IDEJ1 LOCA-IDEJ1-SPR
SC7111I1 [Å]	Characteristic diameter of the molecule for I. Triangular M = 4.982, range [4.2347, 5.7293] [EJ]	LOCA-IDEJ1 LOCA-IDEJ1-SPR
GAMMA [-]	Aerosol agglomeration shape factor. Scaled beta (1.0,1.5) scaled on range [1.0, 5.0] [31]	All
MVSSDFA [-]	MVSS decontamination factor for radioactive aerosols. Truncated normal (500, 250) truncated on [100,1000], 0.99 – correlation with MVSSDFV [EJ][54]	All
PDPor [-]	Particulate debris porosity. Truncated normal (0.38, 0.1) truncated on [0.25, 0.50] [27][EJ]	All
HFRZSS [W/m2K]	Refreezing heat transfer coefficient for SS. Lognormal (7.824, 0.40547), truncated on [1000, 5000] [27]	All

Parameter ID	Parameter description and proposed distribution	Accident scenario
DIAMO [m]	Initial spray droplet diameter. Triangular M = 1.E-3, range [1.E-4, 2.E-3].	LOCA-IDEJ0-SPR LOCA-IDEJ1-SPR

Furthermore, the MELCOR code has two options for core debris ejection from the vessel, determined by a solid debris ejection switch (IDEJ). In the default option (ON, IDEJ = 0), the masses of each material available for ejection are the total debris and molten pool material masses, regardless of whether or how much they are molten [6,7]. In the second option (OFF, IDEJ = 1), the masses of steel, Zircaloy, and UO2 available for ejection are simply the masses of these materials that are molten; the masses of steel oxide and control poison materials available for ejection are the masses of each of these materials multiplied by the steel melt fraction, based on an assumption of proportional mixing; the mass of ZrO_2 available for ejection is the ZrO_2 mass multiplied by the Zircaloy melt fraction. Additionally, the mass of solid UO_2 available for ejection is the Zircaloy melt fraction times the mass of UO_2 that could be relocated with the Zircaloy as calculated in the candling model using the secondary material transport model [6,7]. Furthermore, the MELCOR code puts additional constraints on the mass that can be ejected at vessel failure: (i) to initiate melt ejection, the mass of molten materials should be greater than SC1610(2) (5000 kg – default value), or a melt fraction should be larger than SC1610(1) (0.1 – default value). Here, the values of sensitivity coefficients SC1610(1,2) were set to zero, so any amount of melt available for ejection would be ejected. In the event of a gross failure of the vessel lower head (e.g. due to creep-rupture), it is assumed that all debris in the bottom axial level of the corresponding ring, regardless its state, is discharged linearly over a 1-second time step without taking into account the failure opening diameter [6,7].

The results of the sensitivity and uncertainty analyses performed in [24,25,49,50] showed that the mode of debris ejection from the vessel (IDEJ) has a dominant effect on the code predictions of the debris ejection from the vessel and magnitude of the Cs and I2 source terms released to the environment in case of an accident initiated by a LOCA. As it is not feasible to treat this parameter probabilistically due to a lack of knowledge, it will be considered as a phenomenological splinter[4]. Consequently, the uncertainty analyses will be conducted for the accident scenarios considered in the analysis and two IDEJ parameter combinations, resulting in 2 sets of calculations per single accident scenario.

5.2.2. Accident scenarios

Two accident scenarios were considered in the analysis:

i. an accident initiated by a Loss of Coolant Accident (LOCA) that leads to filtered containment venting, with all active safety systems unavailable, such as Emergency Core Cooling Systems (High and Low pressure ECCS) or containment sprays;
ii. an accident initiated by a Loss of Coolant Accident (LOCA) that leads to filtered containment venting, with all active safety systems unavailable, such as Emergency Core Cooling Systems (High and Low pressure ECCS), however with activation of the independent containment spray system.

[4]In ROAAM formulation a splinter scenario is a phenomenological scenario where relevant epistemic uncertainties are *beyond the reach of any reasonably verifiable quantification*.

The independent spray system is activated one hour after the initiating event and before RPV lower head failure to limit pressure and temperature in the containment. It is deactivated when the water level in the drywell reaches a predetermined setpoint, due avoid excessive reduction of the gas space in the containment that can lead to containment overpressure due to FCI phenomena at RPV lower head failure. After RPV lower failure and melt/debris ejection into the cavity, the system is activated again until the water level in the containment reaches the level where the RPV lower head hemisphere is covered by water. In both accident scenarios, the lower drywell is flooded with water from the condensation pool, to prevent failure of cable penetrations and ensure ex-vessel debris coolability. Containment filtered venting via MVSS is initiated automatically when the pressure in the drywell exceeds 0.55 MPa (absolute) [23].

To conduct uncertainty analysis, a set of MELCOR code modelling parameters, along with their respective ranges, which can influence severe accident progression and the source term released to the environment was identified. This identification was based on a literature review conducted in [23]. Subsequently, a screening analysis was performed to eliminate MELCOR code modeling parameters with a negligible effect on the predictions of severe accident progression and source terms. Additional details on parameter selection and the screening analysis can be found in [23].

Typically, the sources of uncertainty in a Level 2 PSA are numerous and it is impractical to address all of them quantitatively. Experience in performing uncertainty studies for limited aspects of severe accident phenomena suggests that the effects of uncertainties from some sources are larger and more dominant than the effects of uncertainties from other sources. In an integral sense, then, the aggregate uncertainty in Level 2 PSA results can be estimated by selecting the dominant sources of uncertainty and treating them in detail. To identify the dominant sources of uncertainty, the Morris method for sensitivity analysis was employed. The detailed results of the sensitivity analysis are presented and discussed in [49]. The most influential parameters identified by the Morris method are summarized in Table 5-3 and will be utilized in the uncertainty analysis presented in this paper. Furthermore, it should be noted that the sensitivity analysis was performed for unmitigated scenarios, without consideration of the independent spray system. The uncertainty analysis of the LOCA-SPR scenario will be based on the same set of the MELCOR modelling parameters as for the LOCA scenario, however including the spray water droplet diameter (DIAMO) as shown in Table 5-3.

For every accident scenario, the MELCOR code simulations are performed for two options of the mode of debris ejection from the vessel – IDEJ0 and IDEJ1. In total 4 sets of calculations are considered in the analysis:

- LOCA-IDEJ0 – Accident initiated by a LOCA that leads to filtered containment venting via MVSS with IDEJ0.
- LOCA-IDEJ1 – Accident initiated by a LOCA that leads to filtered containment venting via MVSS with IDEJ1.
- LOCA-IDEJ0-SPR – Accident initiated by a LOCA that leads to filtered containment venting via MVSS with IDEJ0, and activation of the independent spray system.
- LOCA-IDEJ1-SPR – Accident initiated by a LOCA that leads to filtered containment venting via MVSS with IDEJ1, and activation of the independent spray system.

For the uncertainty analysis, a sample size of 100 MELCOR code calculations was chosen for each accident scenario and IDEJ parameter combination (in total - 400 MELCOR code runs). This sample size is expected to yield adequate results based on the 95% tolerance/confidence levels for upper bounds and lower bounds (two sided), as discussed in section 4.1.2.

5.2.3. Results

The results of MELCOR code simulations are summarized in Table 5-4 and Figure 5-9, which illustrate the time of automatic activation of the MVSS (via rupture disk, when pressure in the containment > 5.5 Bar), and the time delay between vessel lower head failure and MVSS activation; and in Figure 5-10, which illustrates the fraction of the core inventory of Cs released to the environment after 4, 8, 12, 24, 48 and 72 hours after initiating event.

Table 5-4. Summary of uncertainty analysis results (mean/median values and [range])

Scenario\FOM	**MVSS Time (h)**	**Vessel lower head failure (h)**	**Cs release fraction[5] (-)**	**I release fraction[5] (-)**
LOCA-IDEJ1	6.55/6.39 [1.75, 18.39]	2.39/1.92 [1.18, 7.20]	1.83E-3/1.26E-3 [2.27E-4, 1.65E-2]	2.49E-3/1.61E-3 [2.8E-4, 2.16E-2]
LOCA-IDEJ0	3.79/3.70 [1.78, 8.02]	2.45/1.98 [1.08, 7.64]	2.56E-4/1.67E-4 [5.03E-5, 1.82E-3]	2.67E-4/1.51E-4 [4.78E-5, 2.49E-3]
LOCA-IDEJ1-SPR	7.52/6.58 [4.10, 18.22]	2.01/1.90 [1.06, 3.92]	4.07E-5/3.69E-5 [1.49E-5, 1.11E-4]	4.39E-5/3.92E-5 [1.86E-5, 1.06E-5]
LOCA-IDEJ0-SPR	13.58/17.05 [1.57, 20.83]	2.11/2.02 [1.40, 6.10]	2.93E-5/2.55E-5 [1.22E-5, 8.78E-5]	3.34E-5/2.99E-5 [1.60E-5, 9.04E-5]

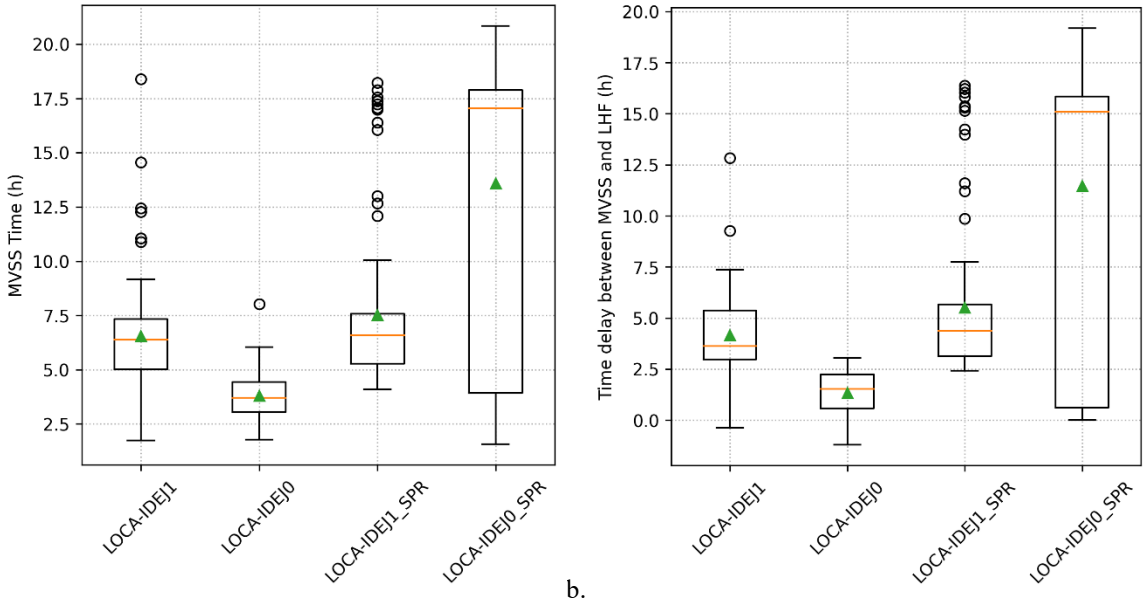

a. b.

Figure 5-9. (a) MVSS activation time [h] after IE; (b) Time delay between MVSS activation and vessel lower head failure [h].

The results indicate that the effect of the containment spray system has a relatively low impact on the timing of MVSS activation in LOCA-IDEJ1 (LOCA-IDEJ-SPR) scenarios. This can be explained by the effect of the mode of debris ejection from the vessel (IDEJ) on debris ejection rate and activation conditions of the independent spray system. Typically, when the modelling option IDEJ=1 is used, debris ejection from the vessel is protracted in time and typically starts with dripping mode directly after the failure of vessel lower head penetrations, followed by massive debris ejection from the vessel due to global failure of the vessel lower head wall due to creep-rupture, which typically occurs after ~1-1.5 h after initial failure of the lower head penetrations [17,18]. The activation of the independent spray system is triggered

[5] Fraction of the initial core inventory released to the environment.

manually by operators, when there are clear indicators that the corium and debris are ex-vessel, to maintain an adequate gas space in the containment and avoid containment over-pressurization due to FCI phenomena in the water-filled drywell after RPV failure. Both these factors contribute to the late activation of the spray system, and, thus, relatively low impact of this system on the pressure response of the containment during the first hours after the vessel lower head failure and timing of activation of the MVSS in LOCA-IDEJ1(SPR) scenarios.

On the contrary, when the IDEJ=0 option is used, debris ejection from the vessel occurs gradually over time directly after the initial failure of the vessel lower head penetrations. This triggers the activation of the independent spray system relatively early in the sequence. Consequently, it can reduce pressure in the containment by condensation of steam and delay the activation of the MVSS by ~12 hours when compared to the MVSS-IDEJ0 scenario (vs. MVSS-IDEJ0-SPR).

The fraction of the core inventory of Cs released to the environment after 4 h, 8 h, 12 h, 24 h, 46 h and 72 h after the initiating event, illustrated in Figure 5-10a-f, show that in the case of LOCA-IDEJ1 the acceptable release threshold is exceeded already after 8 hours in a few cases and12 hours after initiating event in over 50% of simulated cases. After 72 hours, the fraction of Cs released to the environment increases to 90% of simulated cases in the LOCA-IDEJ1 scenario and 16% in the LOCA-IDEJ0 scenario.

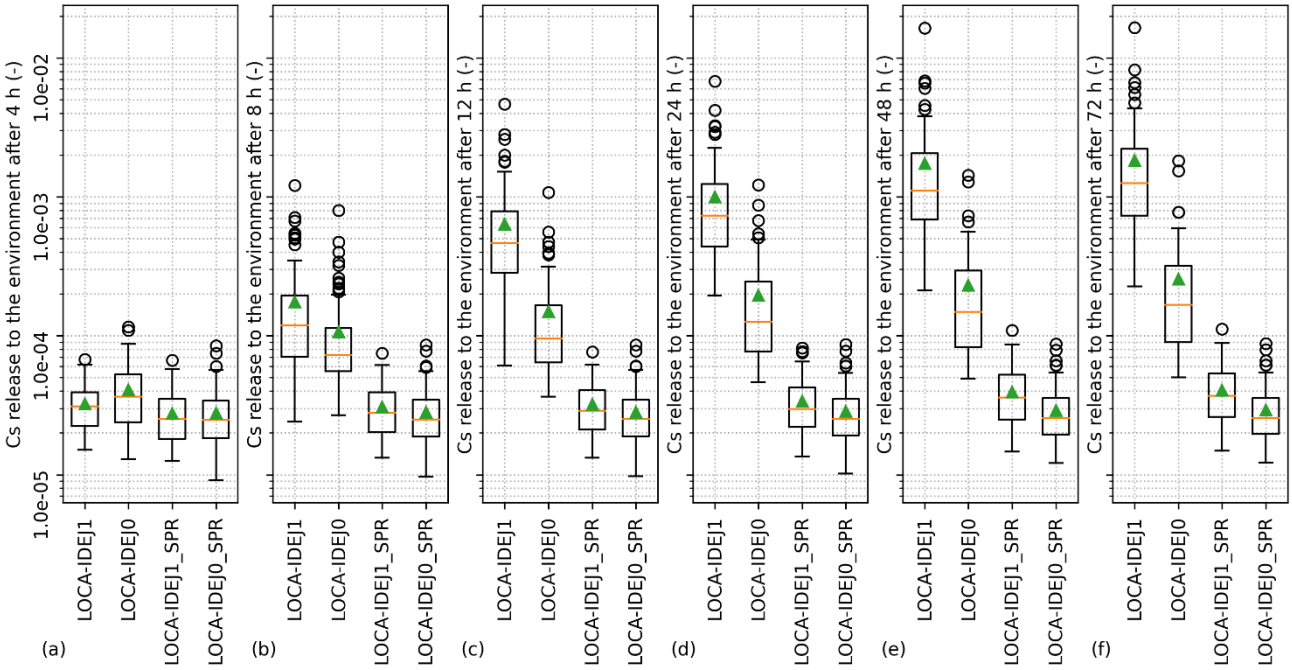

Figure 5-10. Fraction of the core inventory of Cs [-] released to the environment after (a) 4 hours; (b) 8 hours; (c) 12 hours; (d) 24 hours; (e) 48 hours; (f) 72 hours after initiating event.

Based on the simulation results, spraying inside the containment with the independent spray system can significantly reduce the fraction of Cs released to the environment below the acceptable release threshold in all simulations performed for LOCA-IDEJ1-SPR and LOCA-IDEJ-SPR scenarios, regardless uncertainty in the MELCOR code modelling parameters considered in the analysis.

The analysis performed in [48] suggest that elevated temperatures inside the RPV and the drywell in the accident scenarios initiated by a LOCA, especially in the case of IDEJ=1, is the main driving factor for remobilization of Cs deposited on the heat structures inside the reactor pressure vessel and the containment, resulting in a larger release of Cs released from the

containment to the MVSS and to the environment. Figure 5-11 illustrate the speciation of Cs released to the environment in different accident scenarios considered in this analysis, which clearly show that Cs is majorly released in form cesium hydroxide (MELCOR RN Class 2 [6,7]).

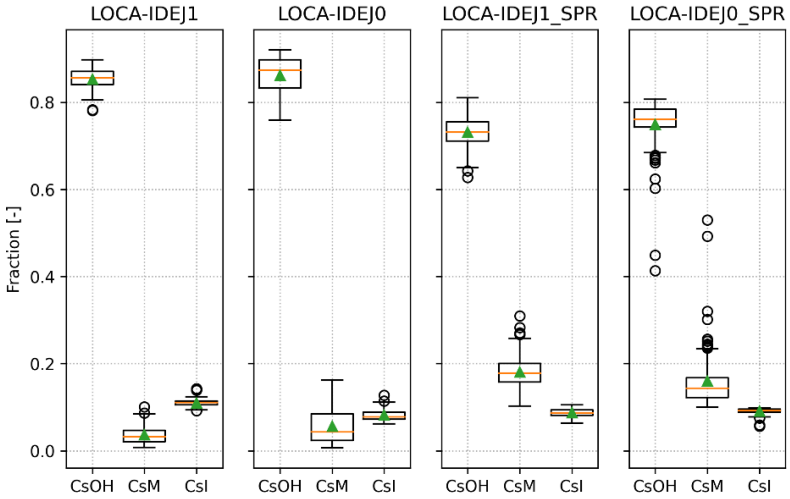

Figure 5-11. Speciation of Cs released to the environment [-]

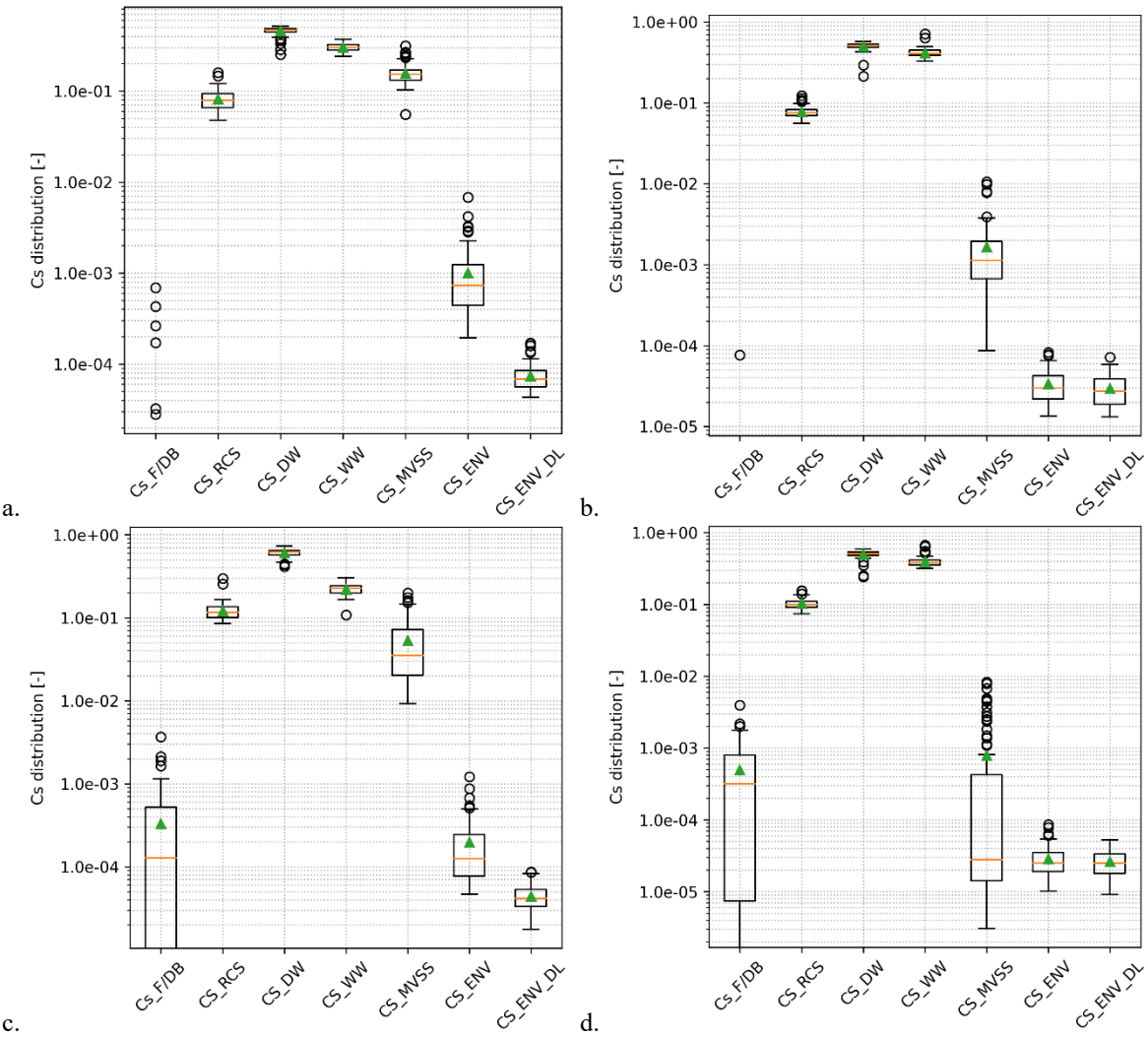

Figure 5-12. Fractional distribution of Cs between different control volumes groups after 24 hours after initiating event; (a) LOCA-IDEJ1, (b) LOCA-IDEJ1-SPR, (c) LOCA-IDEJ0, (b) LOCA-IDEJ0-SPR.

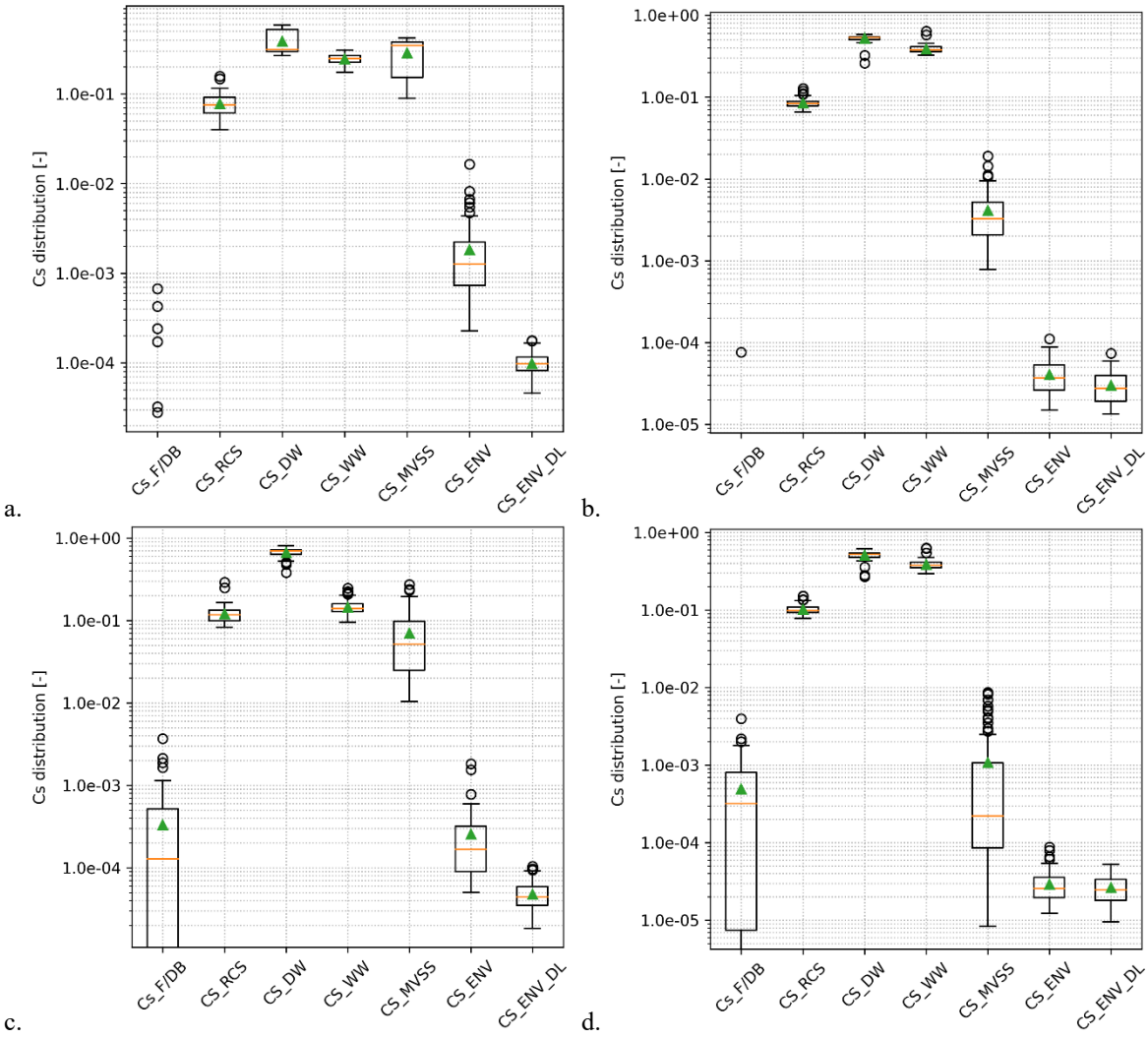

Figure 5-13. Fractional distribution of Cs between different control volumes groups after 72 hours after initiating event; (a) LOCA-IDEJ1, (b) LOCA-IDEJ1-SPR, (c) LOCA-IDEJ0, (b) LOCA-IDEJ0-SPR.

When it comes to the filtering efficiency of the MVSS, it depends on the state of Cs being released from the containment into the MVSS (vapor or aerosol) and, for aerosols, aerosols size, since the scrubbing efficiency of the self-priming venturi greatly depends on aerosols size. Smaller aerosol particles are trapped less efficiently in the venturi scrubber by the processes of impaction, interception and diffusion with water droplets.

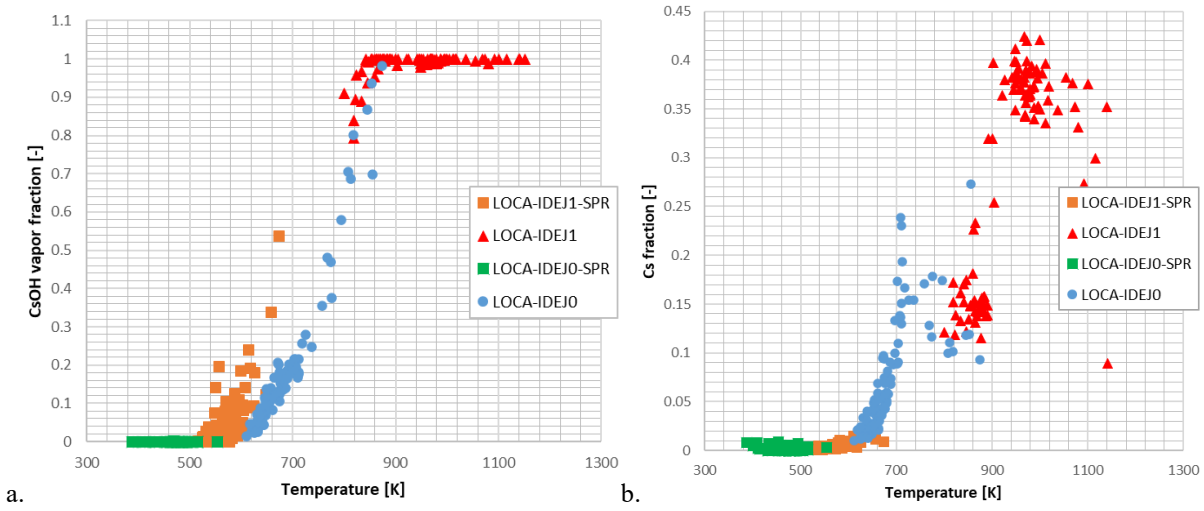

a. b.

Figure 5-14. Mass averaged temperature in the drywell [K] vs. (a) Vapor fraction of CsOH (RN2) released from the containment to the MVSS [-]; (b) Fraction of the core inventory of Cs deposited in the MVSS [-]

Figure 5-14a illustrate the mass fraction of CsOH vapor (vs. the total mass of CsOH) released from the containment to the MVSS as a function the temperature in the drywell averaged against the mass of CsOH released from the containment to the MVSS (as illustrated in Eq (7)).

$$T_{DW_M} = \sum T_{DW_i} \frac{\Delta m_{i_{CsOH_{DW \rightarrow MVSS}}}}{m_{CsOH_{DW \rightarrow MVSS}}} \quad (7)$$

It shows that the mass fraction of the vapor form of CsOH increase with increasing temperature inside the containment, and becomes dominant when the temperature exceeds 800 K. A similar trend can be observed in the fraction of Cs deposited in the scrubber as a function of the mass averaged temperature in the drywell.

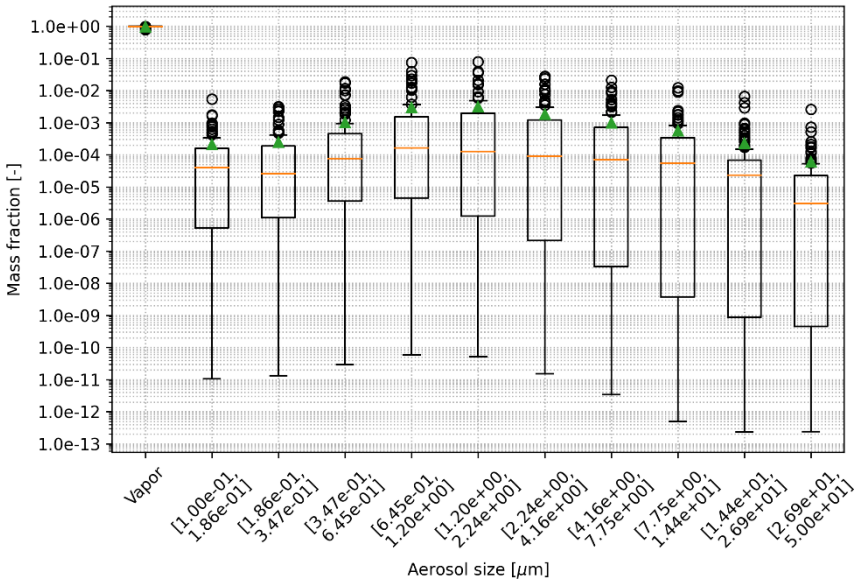

Figure 5-15. Size distribution of CsOH aerosols released from the containment to the MVSS in LOCA-IDEJ1 scenario.

This is also evident from Figure 5-15 (LOCA-IDEJ1) and 5-16 (LOCA-IDEJ0), which show that the major part of CsOH is released in vapor form in the LOCA-IDEJ1 scenario, and approximately ~15% in the LOCA-IDEJ0. It is also important to note that in the LOCA-IDEJ0 scenario, and the LOCA-IDEJ0-SRP and LOCA-IDEJ1-SRP scenarios, the major bulk

of aerosols released into the scrubber is composed of very fine aerosol particles (0.1-1 μm). Therefore, the scrubbing efficiency of the MVSS and its decontamination factor can on the lower end of the range of the MVSSDFA parameter considered in the analysis. However, this aspect is not considered in the present analysis, and the same decontamination factor is applied to all aerosol sizes.

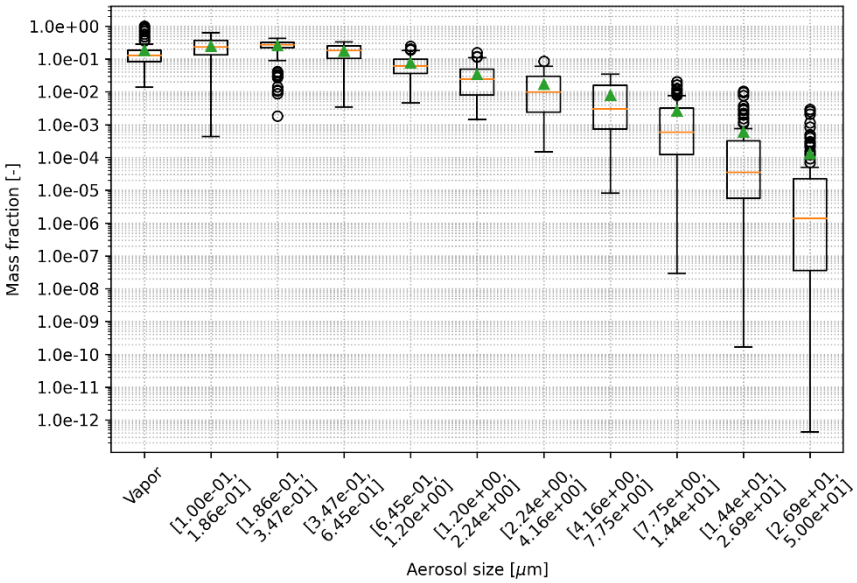

Figure 5-16. Size distribution of CsOH aerosols released from the containment to the MVSS in LOCA-IDEJ0 scenario.

Another important observation from Figure 5-17 and 5-18, is that, even though the fraction of the vapor form of CsOH is significantly higher in LOCA-IDEJ1-SPR than that in LOCA-IDEJ0-SPR, the major part of CsOH in LOCA-IDEJ0-SPR is released from the containment to the scrubber in the form of fine aerosol particles (0.1-0.2 μm), whereas in the case of LOCA-IDEJ1-SPR, the aerosol particles are distributed in a wider range between 0.1 and 10 μm. This difference can positively affect the scrubbing efficiency when using a more detailed filtering model in MELCOR, where the MVSS decontamination factor will depend on the aerosol size (in the MELCOR code, different values of decontamination factors can be assingned for every aerosol size section [6,7]).

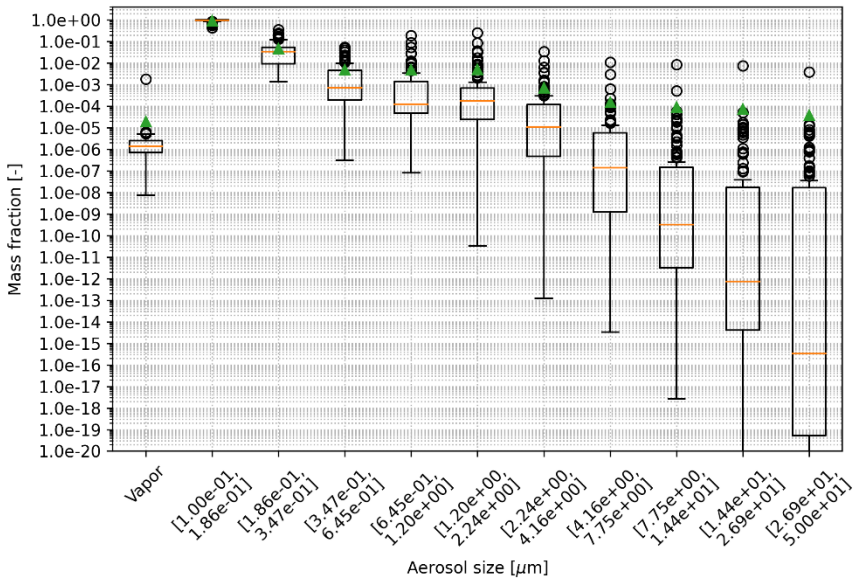

Figure 5-17. Size distribution of CsOH aerosols released from the containment to the MVSS in LOCA-IDEJ0-SPR scenario.

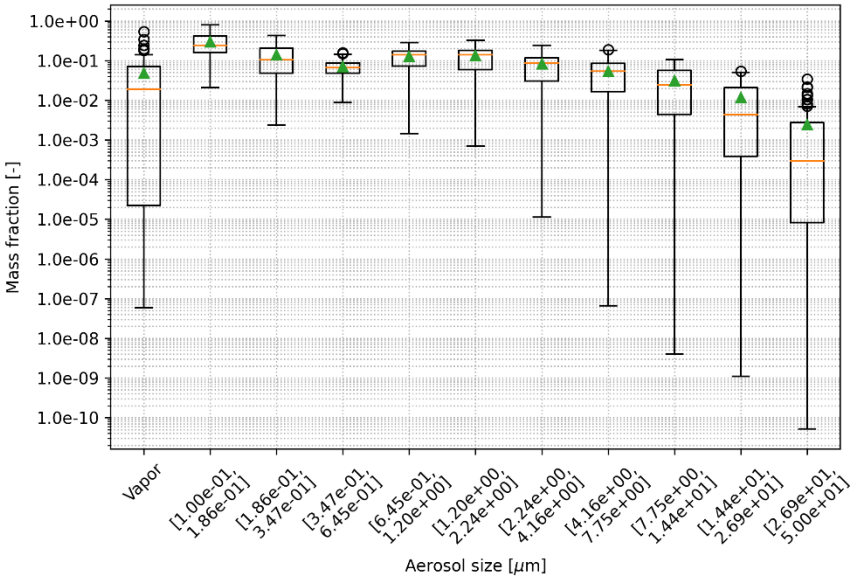

Figure 5-18. Size distribution of CsOH aerosols released from the containment to the MVSS in LOCA-IDEJ1-SPR scenario.

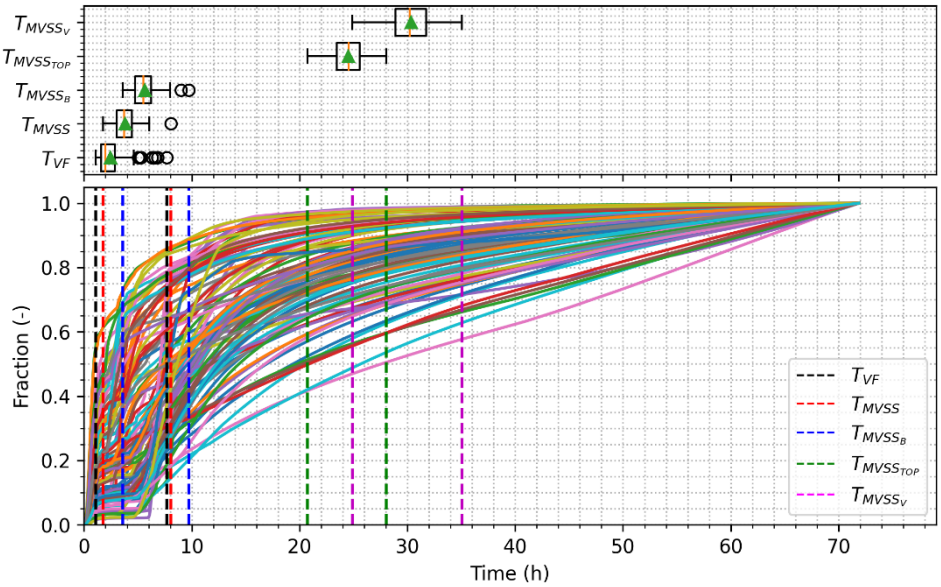

Figure 5-19. Fraction of the total Cs release to the environment [-] as a function of time [h] in LOCA-IDEJ0 scenario.

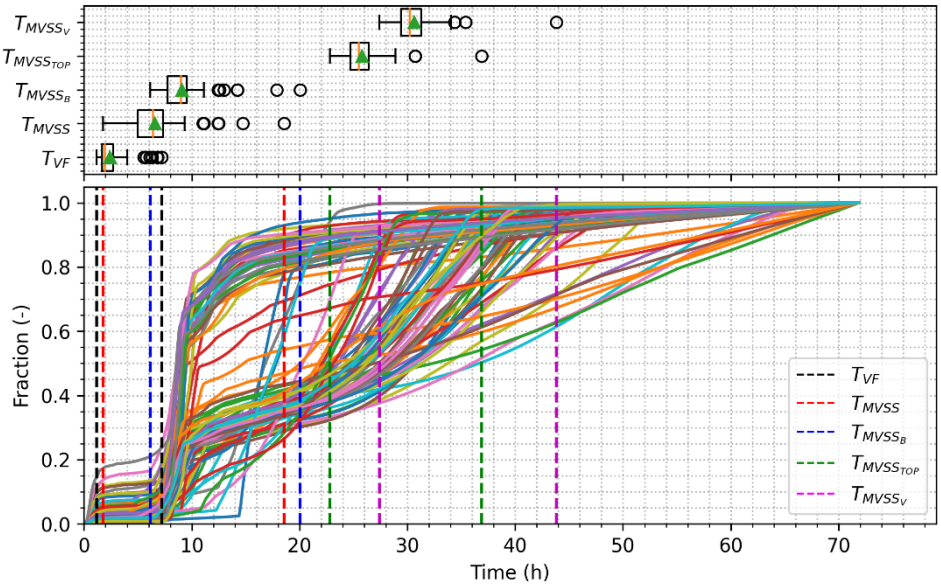

Figure 5-20. Fraction of the total Cs release to the environment [-] as a function of time [h] in LOCA-IDEJ1 scenario.

Figure 5-19 and Figure 5-22 illustrate the release rate of Cs to the environment in the form of the fraction of the total release for every simulated case for the accident scenarios considered in the analysis, accompanied by the timing of key events (dashed lines representing range and distributions are presented in box and whisker plots), such as T_{MVSS} – timing of MVSS activation, T_{MVSS_B} – time when the water pool in the MVSS start to boil, T_{VF} – timing of the vessel lower head failure and T_{SPR} – timing of activation of the independent spray system (in spray scenarios). The release rate in LOCA-IDEJ0 (Figure 5-19) follows quite a similar pattern in all simulated cases, where a significant fraction of Cs is released after the initiation of the MVSS release (within first 10-15 hours after the initiating event), gradually increasing and reaching 100% towards the end of the simulation (72 hour). The release rate in LOCA-IDEJ1 (Figure 5-22) follows two slightly different patterns. In the first it behaves similarly to the LOCA-IDEJ0 scenario, where the release occurs rather gradually over time, after MVSS activation. In the second pattern the release plateaus in the range 25-35% after approximately 10 hours after initiating event, and then starts to increase rapidly after 20-30 hours after initiating event, approaching 100% towards 30-50 hours after the initiating event.

Spraying inside the containment reduces the Cs source term released to the environment in both LOCA-IDEJ0-SPR and LOCA-IDEJ1-SPR scenarios. In the LOCA-IDEJ0-SPR scenario the major bulk of Cs is released within the first 5-10 hours after the initiating event, and the release plateaus afterwards. In the LOCA-IDEJ1-SPR scenario, we still observe a more protracted Cs release to the environment, with a significant fraction of Cs being released during several hours after the initiation of the MVSS release, stabilizing after 30-50 hours.

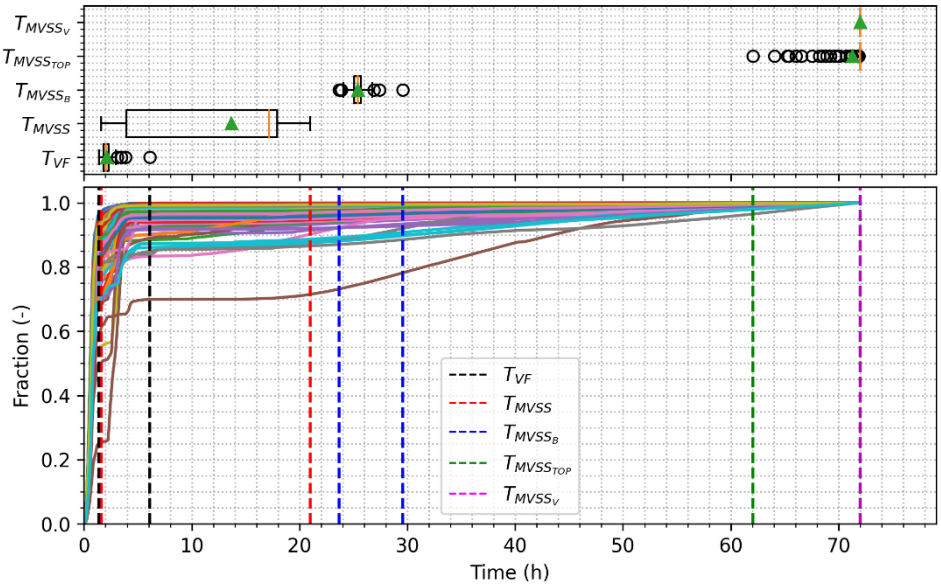

Figure 5-21. Fraction of the total Cs release to the environment [-] as a function of time [h] in LOCA-IDEJ0-SPR scenario.

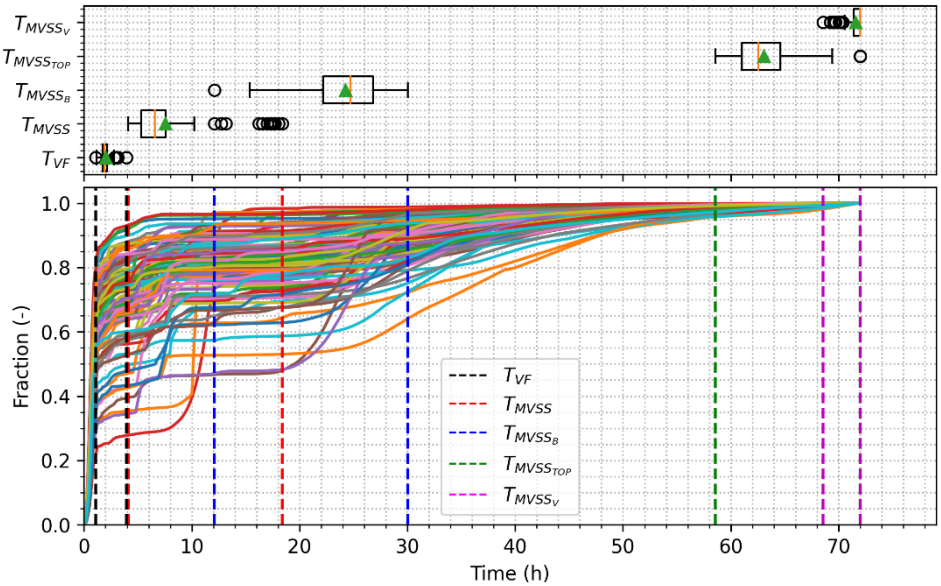

Figure 5-22. Fraction of the total Cs release to the environment [-] as a function of time [h] in LOCA-IDEJ1-SRP scenario.

Furthermore, Figures 5-19 to 5-22 show the timing (both the range shown in dashed lines and the distribution, illustrated in the box-and-whisker plot) when the water in the MVSS reaches saturation condition (T_{MVSS_B}); the water level in the scrubber drops below the venturi outlet, leading to the loss of pool scrubbing ($T_{MVSS_{TOP}}$); and the water level in the scrubber dropped below the elevation of the venturi throats, leading to the loss of venturi scrubbing (T_{MVSS_V}). It should be noted that these results are not conservative, as the decay heat from the fission products deposited in the simple filter model implemented in the MELCOR model of Nordic BWR is not transferred to the MVSS pool, leading to underestimation of the energy transferred to the pool and the pool heat-up and evaporation rate.

These results indicate that manual operator actions to maintain the water inventory in the MVSS in both mitigated and unmitigated scenarios need to be evaluated and implemented in

the models. Additionally, the MVSS model can be refined to account for fission product vapor condensation in the MVSS system pipes and venturi assembly. Aerosol scrubbing in the self-priming venturis can be implemented using an analytical model that takes into account aerosol size and pool properties (e.g., [51,52,53]), as well as the effect of pool scrubbing, using models such as SPARC90.

5.2.4. Discussion and Conclusions

The uncertainty analysis results considering the MELCOR code's epistemic modeling parameters and options, show that spraying in the containment with the independent spray system can significantly limit fission products release to the environment. In the accident scenarios with the independent spray system (LOCA-IDEJ0-SPR and LOCA-IDEJ1-SPR) the release of Cs to the environment is below the acceptable release threshold[2] regardless uncertainties in the MELCOR code modelling parameters. To compare, the fraction of Cs released to the environment in unmitigated scenarios (LOCA-IDEJ0 and LOCA-IDEJ1) exceeds the acceptable release threshold in 16% and 90% of the simulations performed, respectively.

Furthermore, the results of this analysis emphasize the importance of a more detailed modelling of the multi-venturi scrubbing system (MVSS). This includes modelling of the structures and components between the containment and the scrubber, and the multi-venturi manifold. This can be done in the form of control volumes and associated heat structures to account for cooling and condensation of gases released from the containment. Additionally, a more detailed modelling of the venturi scrubbing is necessary, where scrubbing efficiency accounts for the size of the aerosols.

Another crucial aspect that needs to be considered in the future analysis is the long-term behavior of the scrubber. This involves consideration the effects of scrubber water temperature and level, as well as the impact of decay heat from fission products deposited in the filter pool on the scrubbing efficiency of the MVSS. This may necessitate modelling of additional operator actions, such as scrubber inventory makeup, which are currently not considered in either the MELCOR model of Nordic BWR or in the PSA L2 for Nordic BWR.

5.3. MELCOR modelling of the Filtered Containment Venting System

The current MELCOR model of the Nordic BWR employ a simplified MVSS model that uses the simple filtering model in the MELCOR code with constant decontamination factors defined for aerosols (MVSSDFA) and vapors (MVSSDV). Furthermore, the current model does not take into account the pool properties and the size of aerosol particles released from the containment into the MVSS. Both of these factors can affect significantly the scrubbing efficiency of the MVSS, as illustrated in the results presented in Section 5.2.

The simplified filter model of the MVSS in the MELCOR model of the Nordic BWR employs:

- The decontamination factor for aerosol fission products - MVSSDFA = 500 (best estimate value). The uncertainty range is taken from 100 (conservative DF) to 1000 (optimistic DF)
- The decontamination factor for fission products vapors – MVSSDFV considered to be distributed in the range [10, 1000] according to a lognormal distribution, as specified in Table 5-3, in Section 5.2.1. The ranges and parameters of the probability distribution of the MVSSDFV are based on expert judgement, and not necessarily conservative.

To increase realism of the MELCOR code analysis results of the filtered containment venting scenarios in the Nordic BWR it was proposed to perform more detailed modelling of the MVSS.

The work was split into 2 separate parts:

- Uncertainty analysis using the SPARC-90 model in the MELCOR code to evaluate the effectiveness of pool scrubbing in the MVSS – Section 5.3.2.
- Implementation of the refined MVSS mode in the MELCOR model of the Nordic BWR – Section 5.3.3.

5.3.1. Accident scenario

Based on previous results [49,50] the scrubbing efficiency of the MVSS filter was identified as one of the major factors contributing to the uncertainty in the source term released to the environment and the exceedance frequency of the unacceptable release threshold in accident scenarios initiated by a LOCA that leads to filtered venting of the containment via the MVSS. Therefore, the present analysis will focus on evaluating the scrubbing efficiency of the MVSS in an accident initiated by a Loss of Coolant Accident (LOCA), with all active safety systems unavailable, such as Emergency Core Cooling Systems (high and low pressure ECCS) or containment sprays, which lead to filtered venting of the containment and release through the MVSS.

Furthermore, for every accident scenario, the MELCOR code simulations are performed for two options of the mode of debris ejection from the vessel – IDEJ0 and IDEJ1. In total 2 sets of calculations are considered in the analysis:

- LOCA-IDEJ0 – Accident initiated by a LOCA that leads to filtered containment venting via MVSS with IDEJ0.
- LOCA-IDEJ1 – Accident initiated by a LOCA that leads to filtered containment venting via MVSS with IDEJ1.

5.3.2. MELCOR Simulations using SPARC90 model

To evaluate the efficiency of pool scrubbing in the MVSS the original model of the Nordic BWR was modified as follows:

- Flow path FL-362 decontamination factors MVSSDFA (aerosols) and MVSSDFV (vapors) were set to 1 (see Figure 3-3).
- SPARC-90 model was enabled for the FL-362 with RN aerosol and vapor scrubbing for all RN classes.

The analysis was performed for 2 accident scenarios, denoted as:

- LOCA-IDEJ0-SPARC - Accident initiated by a LOCA that leads to filtered containment venting via MVSS with IDEJ0 and SPARC-90 model.
- LOCA-IDEJ1-SPARC - Accident initiated by a LOCA that leads to filtered containment venting via MVSS with IDEJ1 and SPARC-90 model.

For the uncertainty analysis, a sample size of 100 MELCOR code calculations was chosen for each accident scenario and IDEJ parameter combination (in total - 400 MELCOR code runs). This sample size is expected to yield adequate results based on the 95% tolerance/confidence levels for upper bounds and lower bounds (two sided), as discussed in section 4.1.2.

5.3.2.1. Results

The results of the analysis of the effectiveness of pool scrubbing in the MVSS, presented in Figures 5-23 to 5-37 are compared to the results obtained with the original model, that employ constant decontamination factors – LOCA-IDEJ1 and LOCA-IDEJ0, as discussed in Section 5.2.

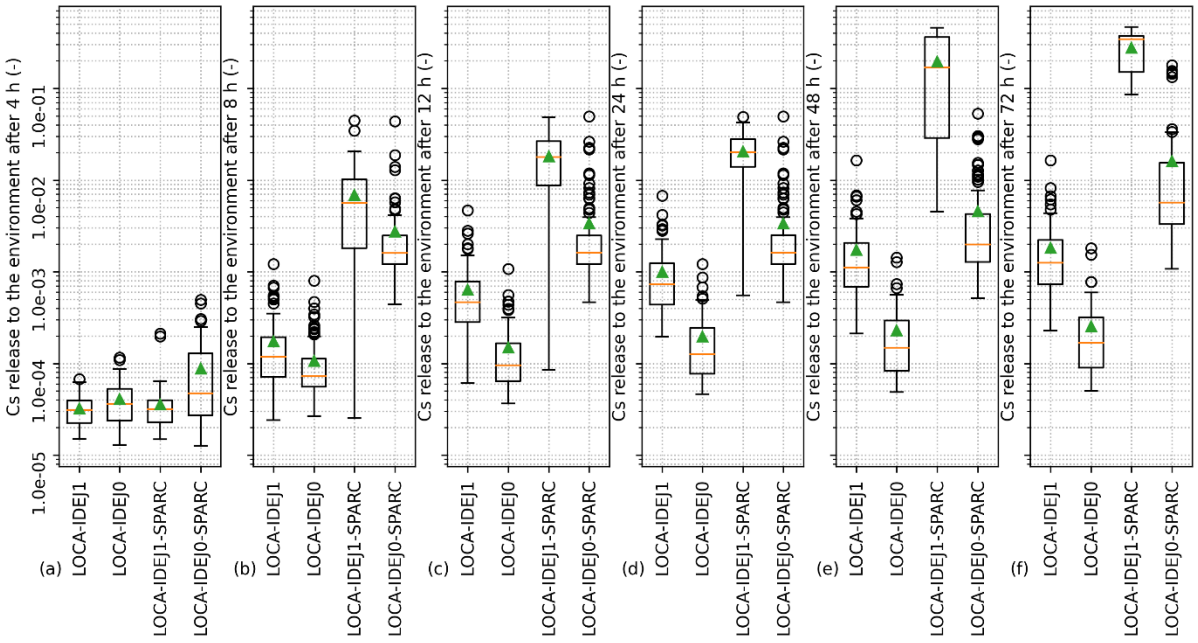

Figure 5-23. Fraction of the core inventory of Cs [-] released to the environment after (a) 4 hours; (b) 8 hours; (c) 12 hours; (d) 24 hours; (e) 48 hours; (f) 72 hours after initiating event.

Figure 5-23 show the fraction of the core inventory of Cs released to the environment 4, 8, 12, 24, 48 and 72 hours after initiating event. The difference between the SPARC-90 model and the constant decontamination factor model becomes significant already after 8 hours after the initiating event.

Figures 5-24 to 5-31 show the fractional distribution of Cs among different control volume groups considered in the MELCOR model of the Nordic BWR.

The groups are defined as follows:

- Cs_F/DB: the fraction of the core inventory of Cs that remains in the fuel or debris.
- Cs_RCS: the fraction of Cs in the reactor coolant system[6].
- Cs_DW: the fraction of Cs in the drywell[6].
- Cs_WW: the fraction of Cs in the wetwell[6].
- Cs_MVSS: the fraction of Cs deposited in the MVSS (both the simple filter and MVSS CVs) [6].
- Cs_ENV: the fraction of Cs released to the environment.
- Cs_ENV_DL: the fraction of Cs released to the environment via diffuse leakage from the containment.

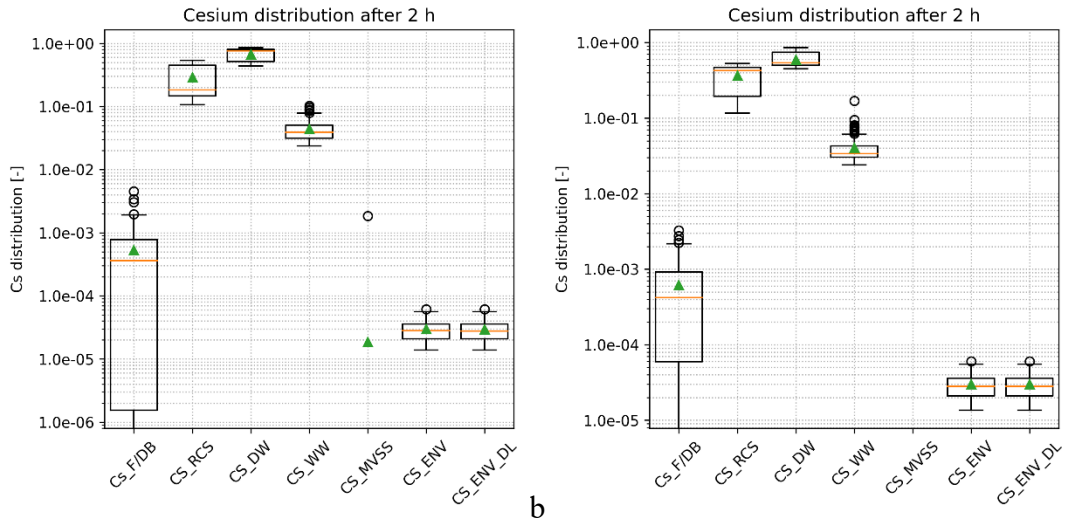

a b

Figure 5-24. Fractional distribution of Cs between different control volumes groups after 2 hours after initiating event; (a) LOCA-IDEJ1, (b) LOCA-IDEJ1-SPARC.

The results presented in Figures 5-24 to 5-31 show that the difference in the fraction of Cs released to the environment between the constant DF model and the SPARC90 model becomes significant after 8 hours after the initiating event. A similar trend can be observed for the fraction of Cs deposited in the MVSS. This difference can be explained by the relatively low release rate during the first 8 hours after the initiating event (see Figure 5-36 and Figure 5-37).

[6] Airborne and deposited in the pool and heat structures.

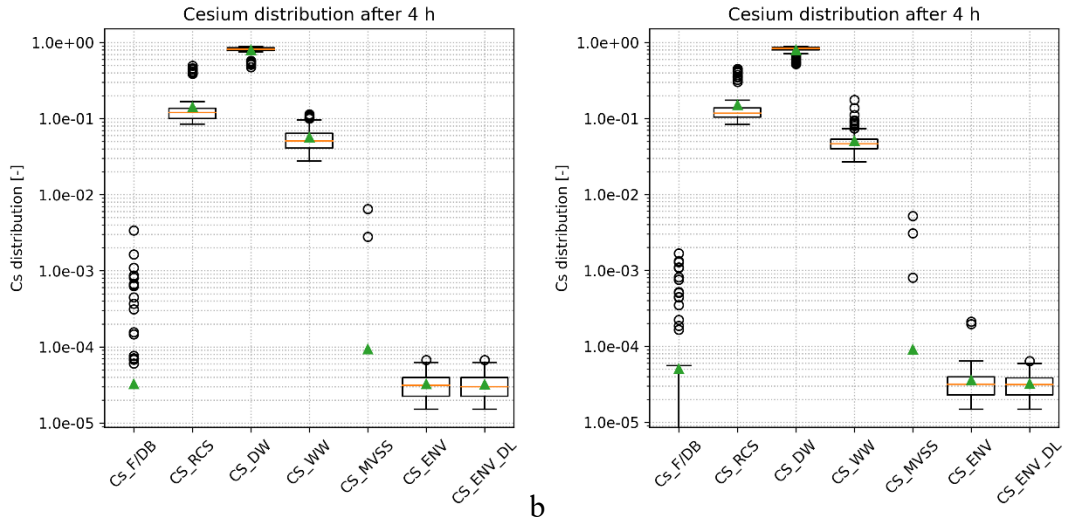

Figure 5-25. Fractional distribution of Cs between different control volumes groups after 4 hours after initiating event; (a) LOCA-IDEJ1, (b) LOCA-IDEJ1-SPARC.

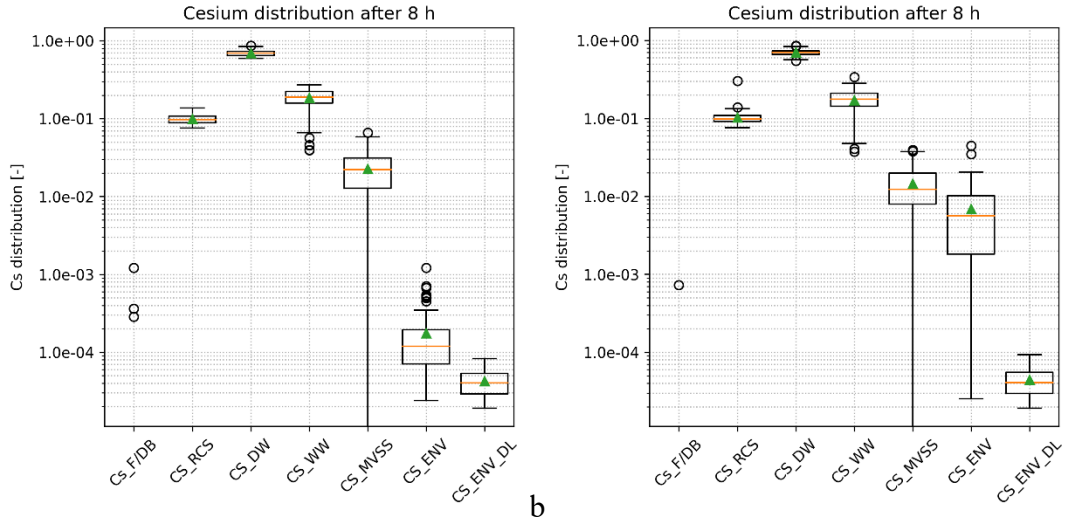

Figure 5-26. Fractional distribution of Cs between different control volumes groups after 8 hours after initiating event; (a) LOCA-IDEJ1, (b) LOCA-IDEJ1-SPARC.

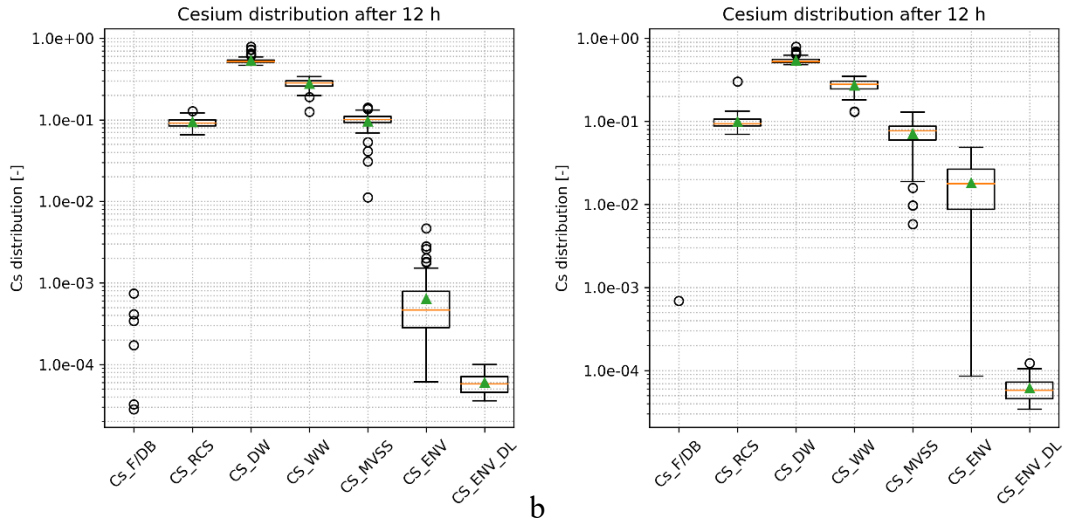

Figure 5-27. Fractional distribution of Cs between different control volumes groups after 12 hours after initiating event; (a) LOCA-IDEJ1, (b) LOCA-IDEJ1-SPARC.

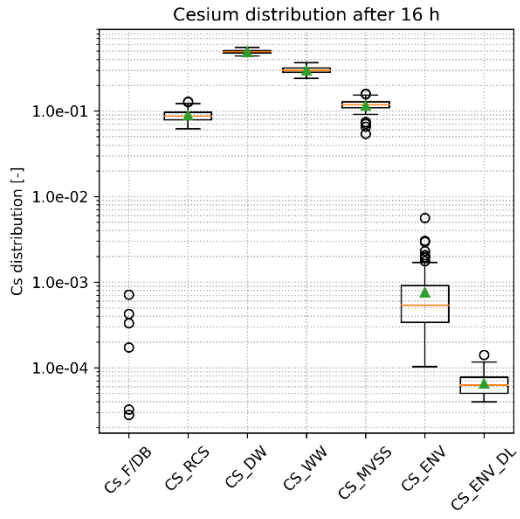

a

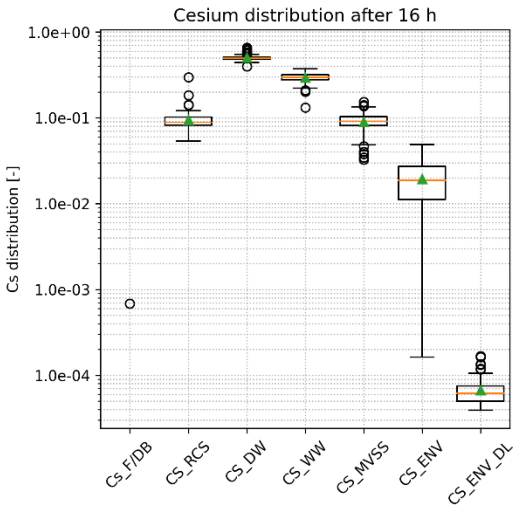

b

Figure 5-28. Fractional distribution of Cs between different control volumes groups after 16 hours after initiating event; (a) LOCA-IDEJ1, (b) LOCA-IDEJ1-SPARC.

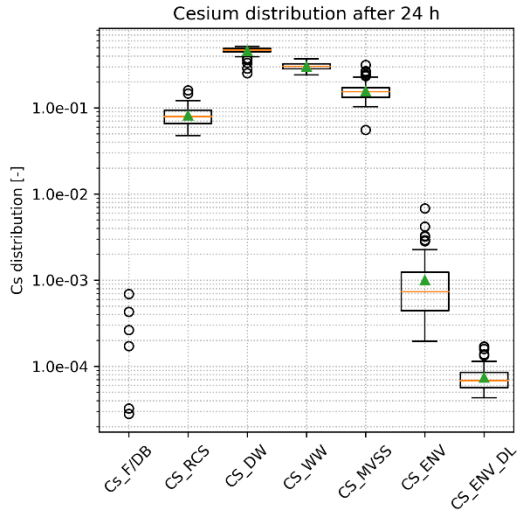

a

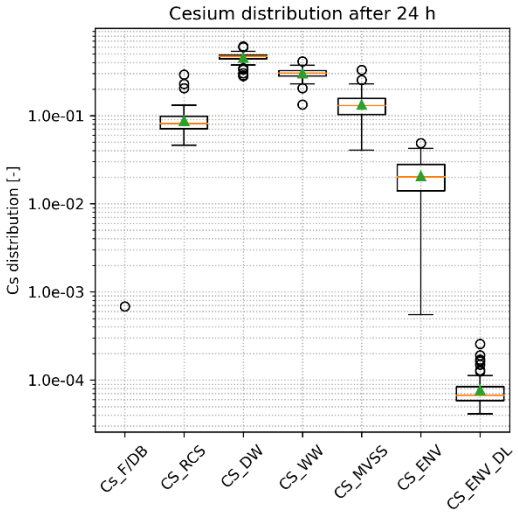

b

Figure 5-29. Fractional distribution of Cs between different control volumes groups after 24 hours after initiating event; (a) LOCA-IDEJ1, (b) LOCA-IDEJ1-SPARC.

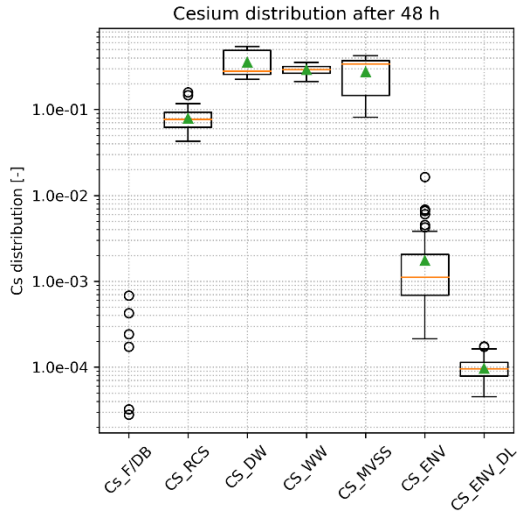

a

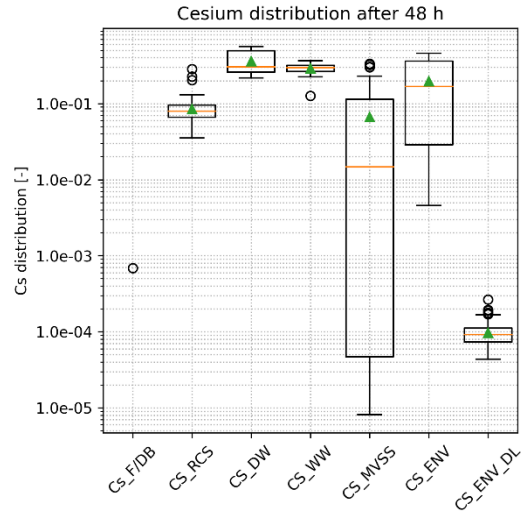

b

Figure 5-30. Fractional distribution of Cs between different control volumes groups after 48 hours after initiating event; (a) LOCA-IDEJ1, (b) LOCA-IDEJ1-SPARC.

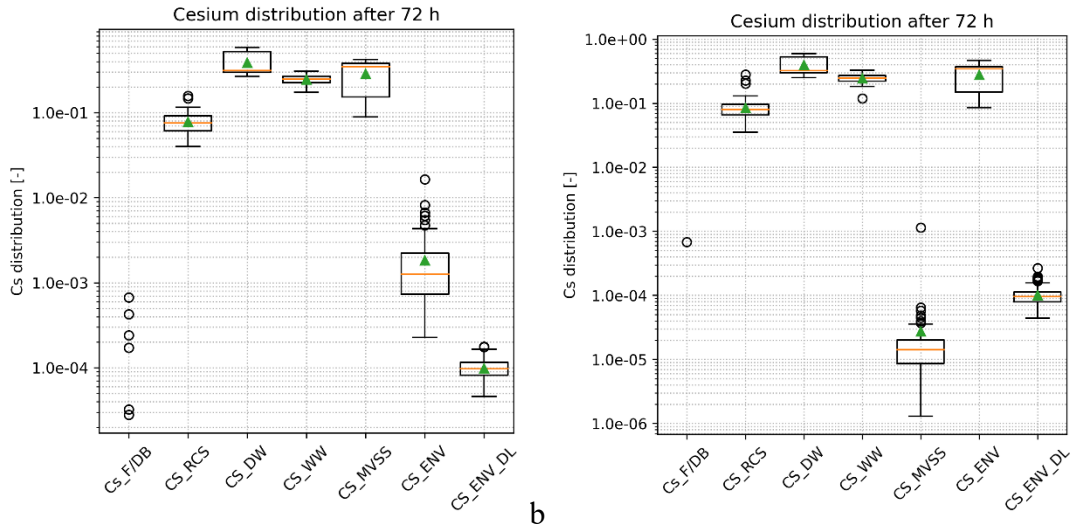

Figure 5-31. Fractional distribution of Cs between different control volumes groups after 72 hours after initiating event; (a) LOCA-IDEJ1, (b) LOCA-IDEJ1-SPARC.

Another important observation from the results presented in Figures 5-24 to 5-31 is that the fraction of Cs deposited in the MVSS starts to decrease 16 to 24 hours after the initiating event, which can be explained by the evaporation of water in the MVSS. After 72 hours, the fraction of Cs deposited in the MVSS drops below 1.E-4, which effectively means that all water in the MVSS scrubber has evaporated, and the Cs suspended in the pool has resuspended and been released into the atmosphere.

This behavior correlates with the evolution of the water level in the MVSS, illustrated in Figures 5-32 and 5-33. The water level drops below the venturi pipes' outlet height 15 to 20 hours after the initiating event, depending on the model of debris ejection and the filtering model being used. Venturi throats are expected to be uncovered within 35 hours after the initiating event, and the total evaporation of water in the MVSS is estimated to occur approximately 40 hours after the initiating event, depending on the mode of debris ejection (IDEJ) and the filtering model being used.

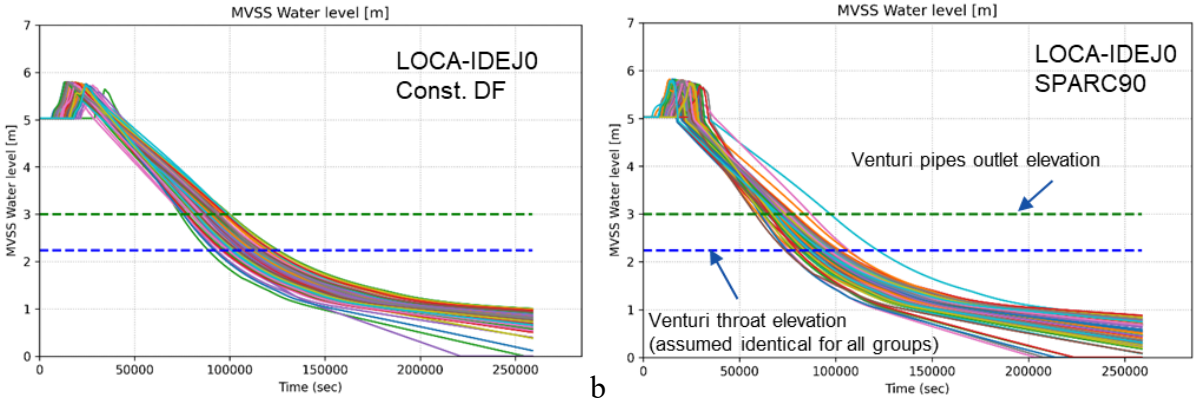

Figure 5-32. Evolution of water level in the MVSS in (a) LOCA-IDEJ0, (b) LOCA-IDEJ0-SPARC.

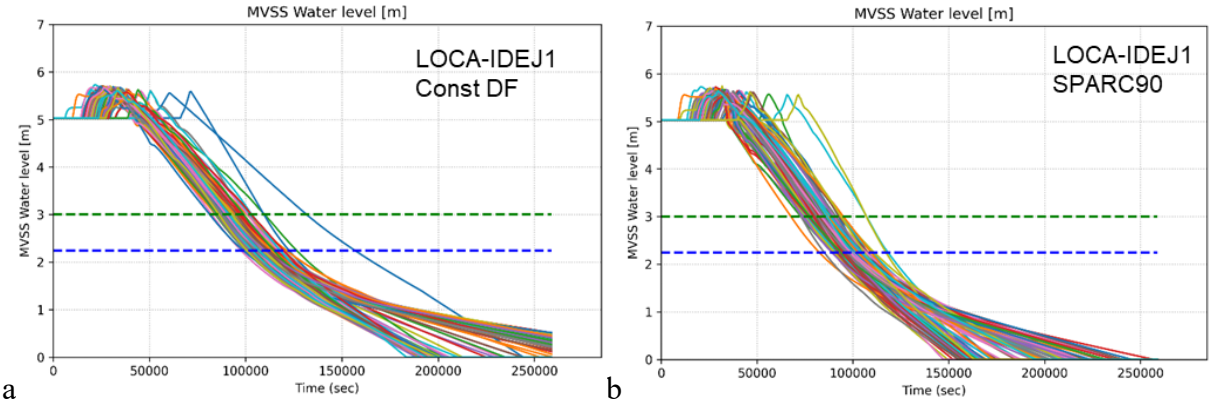

a b

Figure 5-33. Evolution of water level in the MVSS in (a) LOCA-IDEJ1, (b) LOCA-IDEJ1-SPARC.

Figures 5-34 to 5-37 illustrate the release rate of Cs to the environment in the form of the fraction of the total release for every simulated case for the accident scenarios considered in the analysis, accompanied by the timing of key events (dashed lines representing range and distributions are presented in box and whisker plots), such as T_{MVSS} – timing of MVSS activation, T_{MVSS_B} – time when the water pool in the MVSS start to boil, T_{VF} – timing of the vessel lower head failure and T_{SPR} – timing of activation of the independent spray system (in spray scenarios).

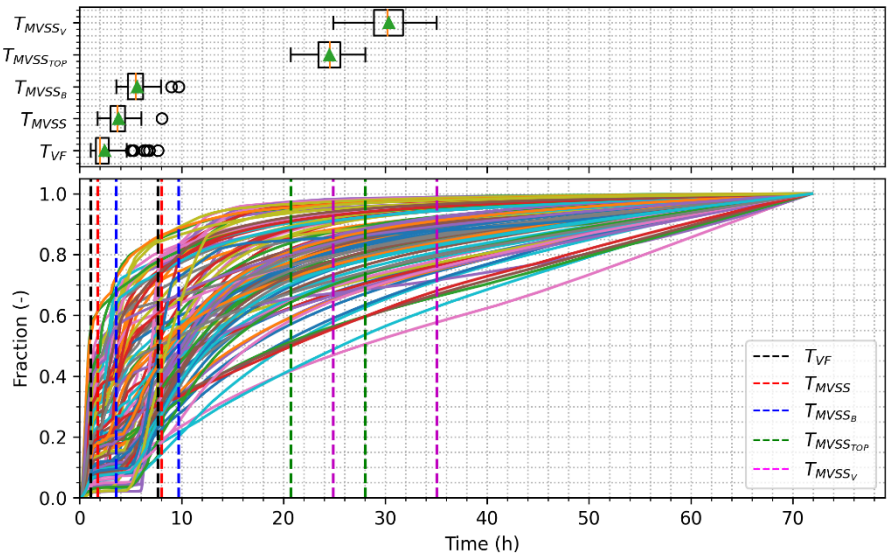

Figure 5-34. Fraction of the total Cs release to the environment [-] as a function of time [h] in LOCA-IDEJ0 scenario.

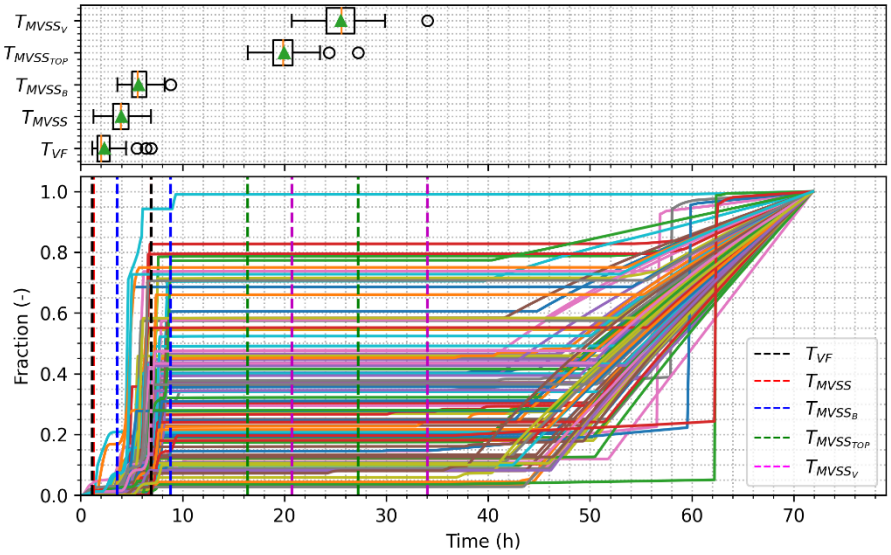

Figure 5-35. Fraction of total the Cs release to the environment [-] as a function of time [h] in LOCA-IDEJ0-SPARC scenario.

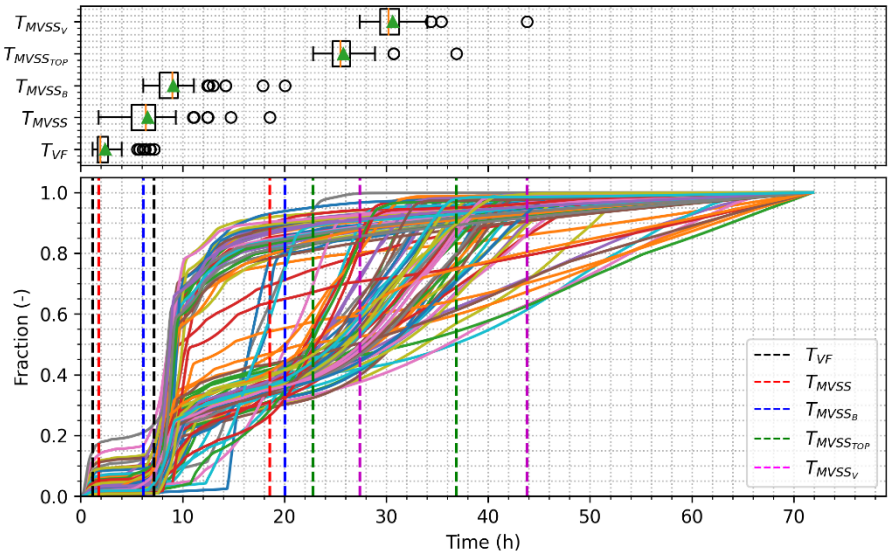

Figure 5-36. Fraction of the total Cs release to the environment [-] as a function of time [h] in LOCA-IDEJ1 scenario.

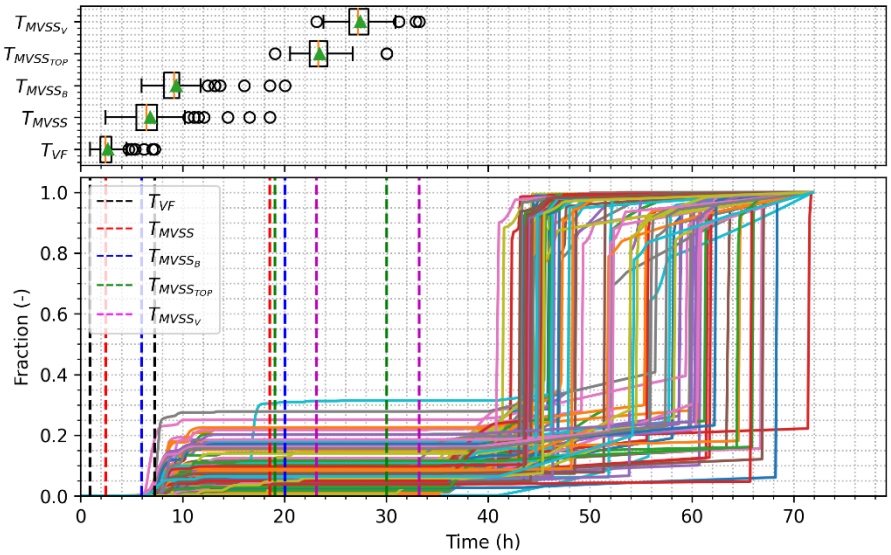

Figure 5-37. Fraction of the total Cs release to the environment [-] as a function of time [h] in LOCA-IDEJ1-SPARC scenario.

Figures 5-35 and 5-37 show the similar trend, as in Figures 5-24 to 5-31, where almost all Cs deposited in the MVSS has resuspended and released into the environment, 40-72 hours after the initiating event.

The current version of the MELCOR model of the Nordic BWR does not include manual operator actions to replenish the water inventory in the MVSS, as the constant DF model was employed. When using the SPARC-90 model, the filtering efficiency of the MVSS depends greatly on pool conditions, such as pool subcooling and water level. Since the current model does not account for any means to replenish the water inventory in the MVSS, the scrubbing efficiency of the pool will decrease over time due to elevated temperatures and water boil-off. Furthermore, since there are no heat structures modeled in the MVSS scrubber (such as MVSS concrete shell or liner), the aerosols suspended in the pool will be resuspended and released into the environment.

It is assumed in the MELCOR code, when the volume settles into itself (i.e. no settling surfaces (heat structures) or settling into the volume underneath is possible, when the pool disappears from any such volume the aerosols that were suspended in the liquid are resuspended in the largest section of the gas phase aerosols and allowed to settle where they want. Similarly, vapors that were held in the liquid phase are put into the gas phase [6,7].

To address this issue, it necessary to model manual operator actions to makeup water inventory in the MVSS and include additional heat structures into the MELCOR model, that represent the MVSS external and internal structures.

5.3.3. MELCOR Simulations using refined MVSS model

5.3.3.1. Refined model of the MVSS

The MELCOR model of the Nordic BWR (see section 3.2.1) employs the simple filter model for the Multi-Venturi Scrubbing System (MVSS). In the current implementation, the MVSS consists of two control volumes: CV800, representing the scrubber, and CV801, representing the moist separator. The scrubber volume CV800 is connected to the drywell via flow path FL362, where the simple filtering model is applied. This model assumes two constant decontamination factors (DFs) for aerosol and vapor forms of fission products released from the drywell.

The filtering efficiency of the scrubber does not depend on the size of the aerosols released from the containment or the pool properties in the scrubber (such as subcooling, water level, etc.). Additionally, the decay heat produced by the fission products deposited in the filter is not added to the pool, meaning that the pool properties are not affected by the fission products (amount and decay heat produced) deposited in the filter. This can lead to non-conservative results.

The efficiency of venturi scrubbing depends significantly on the size of aerosols. Thus, applying larger values of DF to the entire release, while disregarding pool properties and aerosol characteristics, can lead to overestimation of the scrubbing efficiency of the MVSS, and underestimation of the environmental release and potential consequences to the public that the release may entail. Furthermore, the scrubbing efficiency of fission product vapors depends on processes such as vapor condensation, aerosol formation, and growth. Modeling these complex processes with the simple filter model, along with the other factors mentioned, can result in overly optimistic results.

To overcome this issue, the modelling of the MVSS in the MELCOR model of Nordic BWR was refined, to include the components and structures inside the MVSS.

In the new model (Figure 5-38) the MVSS inlet line is represented by CV801, which is connected to the drywell via FL36200. The pipes that represent the header pipes and branches are represented by CV802. The venturing riser pipes are represented by CV812 and CV813, representing the MVSS tubes in the group 1-3 (348 tubes) and the tubes in the group 4 (516 tube), respectively. The total amount of tubes is 864. The dimensions of the pipes and associated control volumes and flow paths were defined based on the data provided by SSM and engineering judgments/assumptions. This grouping is motivated by the numerical efficiency of the MELCOR code (small CVs may result in large pressure/temperature changes and numerical issues in the code).

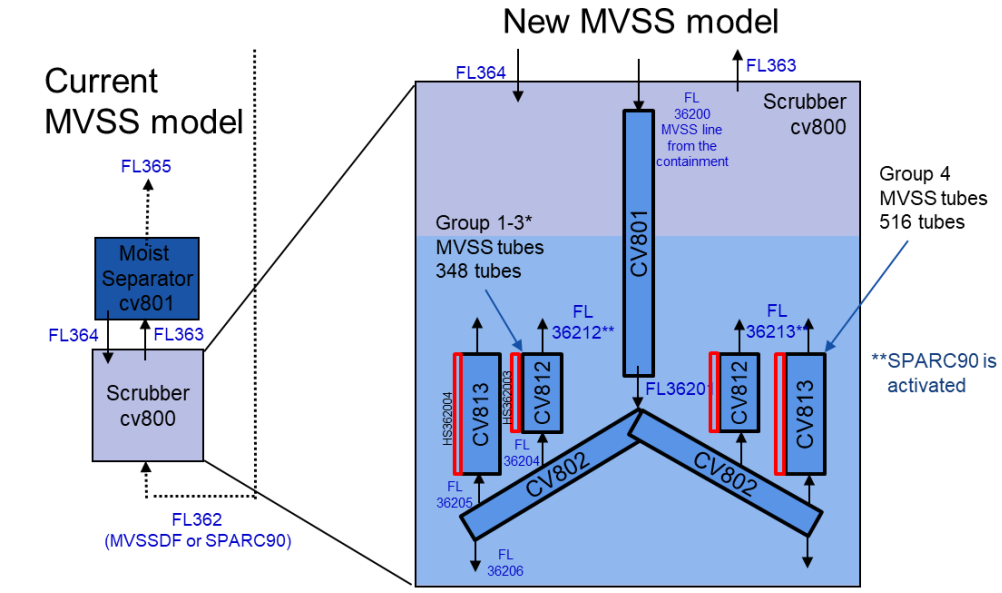

Gr1 = 24; Gr2 = 108; Gr3 = 240

.

Figure 5-38. Refined nodalization of the MVSS in the MELCOR model of Nordic BWR

For the flow paths that connects the MVSS pipes outlets with the pool (FL-36212 and FL-36213), the SPARC-90 model is applied, assuming the that the number of vents in the flow path is equal to the number of riser pipes in the venturi manifold. Furthermore, the heat structures representing the riser pipes of the venturi groups are modeled to simulate heat transfer between the gas mixture flowing through the venturi manifold and the pool, as illustrated in Figure 5-38.

The control volume CV802 at the bottom of the volume is connected to CV800, by FL36206 – that represents the drainage pipes of the venturi manifold. In the default option, the flow is allowed in the reverse direction only.

Note that the refined modelling does not include venturi scrubbing as modeling of self-priming venturi scrubbing explicitly in the MELCOR code is deemed impossible. Therefore, venturi scrubbing should be implemented in the form of an analytical model. The implementation of a such model would require a comprehensive literature review on aerosol scrubbing in self-priming venturi nozzles, selection and implementation of a suitable model in the MELCOR model of the Nordic BWR. This will be performed in further development of the MVSS model.

The new MVSS filter model was integrated into the MELCOR model of Nordic BWR.

5.3.3.2. Results

A set of MELCOR simulations was performed for the accident scenario initiated by a LOCA that leads to filtered venting of the containment. The simulations considered both options for the mode of debris ejection from the vessel (IDEJ).

Simulations were performed for 24 hours after the initiating event, as the design criteria for the MVSS is that no manual actions are required within the first 24 hours after the initiating event.

Table 5-5. MELCOR code simulations with refined MVSS model.

Case ID	Description	Cs release fraction [-]
C1-IDEJ0 C1-IDEJ1	Base case, as per the model description in Section 5.3.3.1. No modelling of venturi scrubbing.	1.99E-04 4.41E-04
C2-IDEJ0 C2-IDEJ1	Sensitivity case to C1. No HS for the riser pipes.	2.19E-04 3.90E-03
C3-IDEJ0 C3-IDEJ1	Sensitivity case to C1. FL36206 (drain line) – flow in both directions.	1.79E-04 7.70E-04
C4-IDEJ0 C4-IDEJ1	Sensitivity case to C1. Turbulent deposition on pipe bends and venturi is switched on.	4.57E-04 1.64E-04
C5-IDEJ0 C5-IDEJ1	Sensitivity case to C3. FL36206 (drain line) – flow in both directions.	8.84E-03 2.96E-03

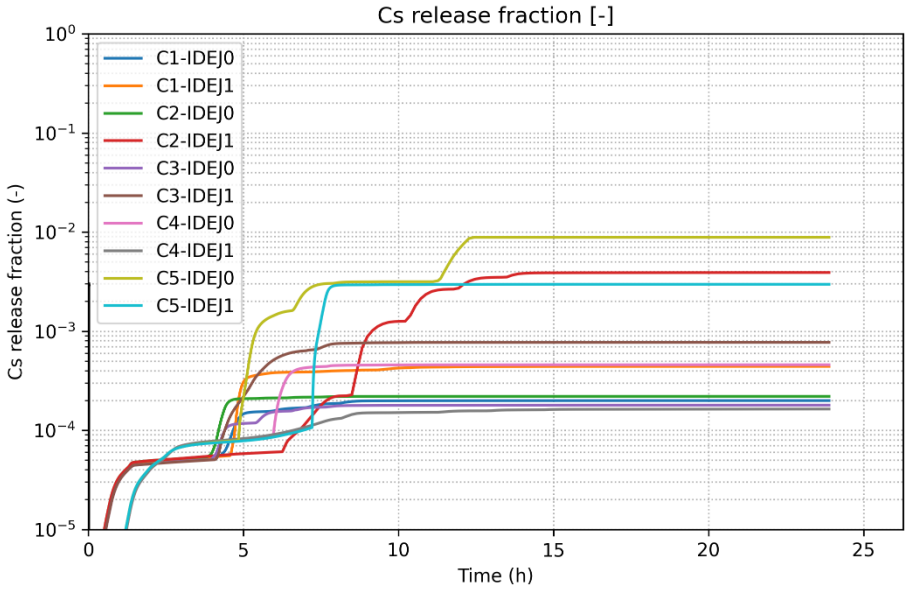

Figure 5-39. Fraction of the core inventory of Cs released to the environment [-] as a function of time [h].

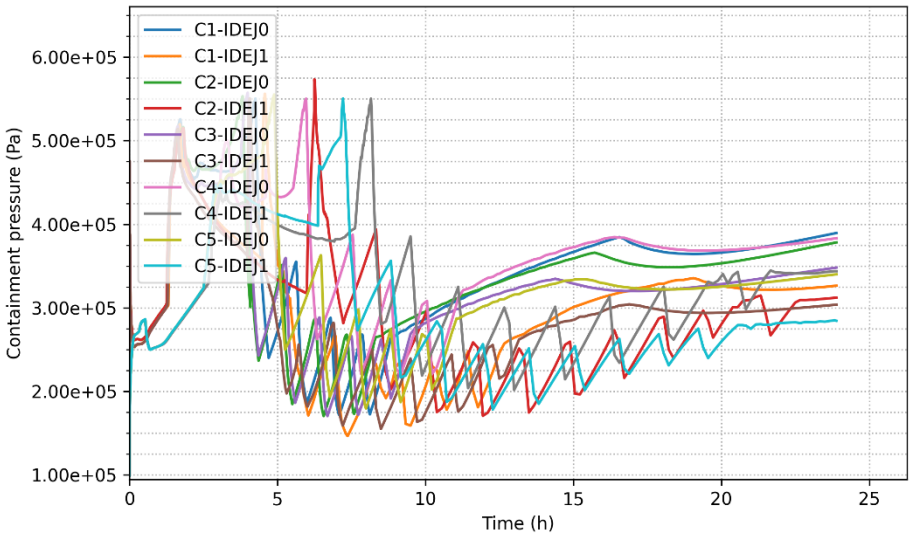

Figure 5-40. Containment (UDW) pressure [Pa] as a function of time [h].

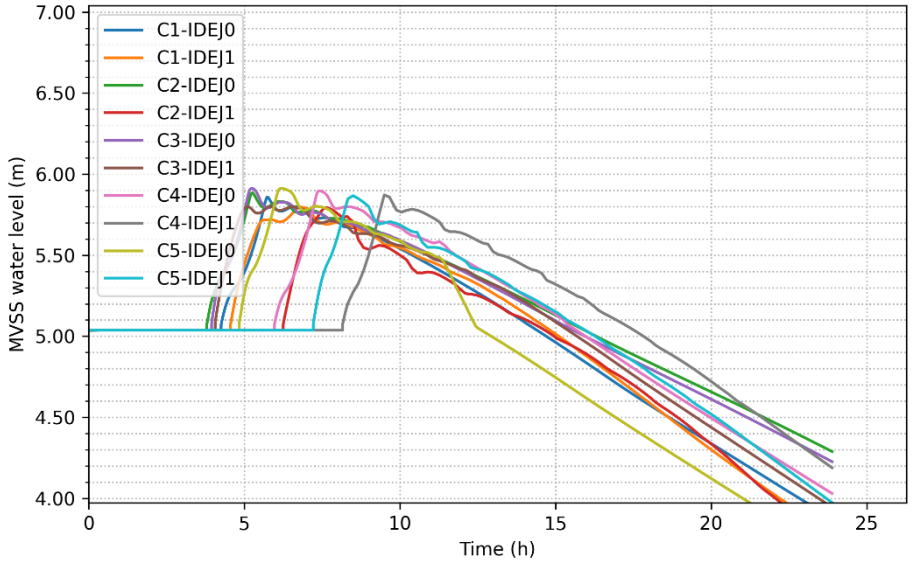

Figure 5-41. MVSS water level [m] as a function of time [h].

The results presented in Table 5-5 are preliminary and do not consider various sources of uncertainty that can affect the accident progression and the source term released to the environment.

Based on the preliminary results, the modeling of heat structures representing the MVSS internal parts, and, in the future, the entire flow path from the containment to the MVSS, is important to correctly predict the behavior of the fission product vapors and aerosols released from the containment into the scrubber, and, thus, the scrubbing efficiency of the MVSS (i.e., Venturi scrubbing of aerosols and pool scrubbing).

The preliminary results indicate that the effect of turbulent deposition on the surfaces in the MVSS is relatively small and within the numeric uncertainty of the code. This, however, needs to be addressed further by performing sensitivity and uncertainty analyses.

Finally, as mentioned in 5.3.3.1, the refined MVSS model does not include self-priming venturi scrubbing, making the results overly conservative. Implementation of analytical models for venturi scrubbing will be considered in the future development of the MELCOR model for the Nordic BWR.

5.3.4. Discussion and Conclusions

The results of the analysis show that the pool scrubbing is effective during the first hours after the initiation of the MVSS release. With pool heat up and water boiloff in the scrubber, the scrubbing efficiency of the pool decrease significantly. Furthermore, the results indicate that that the water level in the scrubber can drop below the venturi manifold riser pipes outlet ~20 hours after the initiating event, which means that the manual actions to makeup the water inventory in the scrubber needs to be initiated within this time frame.

The preliminary results using the refined MVSS model show that accurate modelling of heat structures and the entire flow path from the containment to the MVSS is essential for predicting fission product behaviour and scrubbing efficiency of the MVSS. Turbulent deposition effects in the MVSS are minor but further sensitivity and uncertainty analyses are necessary to quantify the importance of this retention mechanism. Finally, the results indicate importance of the self-priming venturi scrubbing, which was not included in the current model and will be addressed in future MELCOR model developments for the Nordic BWR.

5.4. Effect of Steam Explosion on the Source Term

Extensive sensitivity and uncertainty analysis including the effect of release path in case of containment failure due to ex-vessel phenomena.

During the earlier phases of the project KTH performed sensitivity and uncertainty analysis considering containment failure due to a steam explosion (SE) occurring at RPV failure, leading to opening of flow paths to the environment, ENV_CNT_FAIL and DIFF_LEAK (FL359 and FL360 respectively) from the upper dry well (UDW). Here an assumption was made that air lock door in the UDW failed due to SE. However, there is a possibility of failure of containment hatch door in the lower dry well (LDW) [15,16], leading to an additional pathway for the release of fission products to the containment. The simulations for SE in different accident scenarios (LOCA and SBO) are in progress. Figure 5-42 shows the mass of melt ejected and its mass flow rate (derived from mass ejected during consecutive time steps) for the best estimate case for each of accident scenarios. Here, the containment was assumed to be intact on RPV failure to effectively analyse SE probabilities.

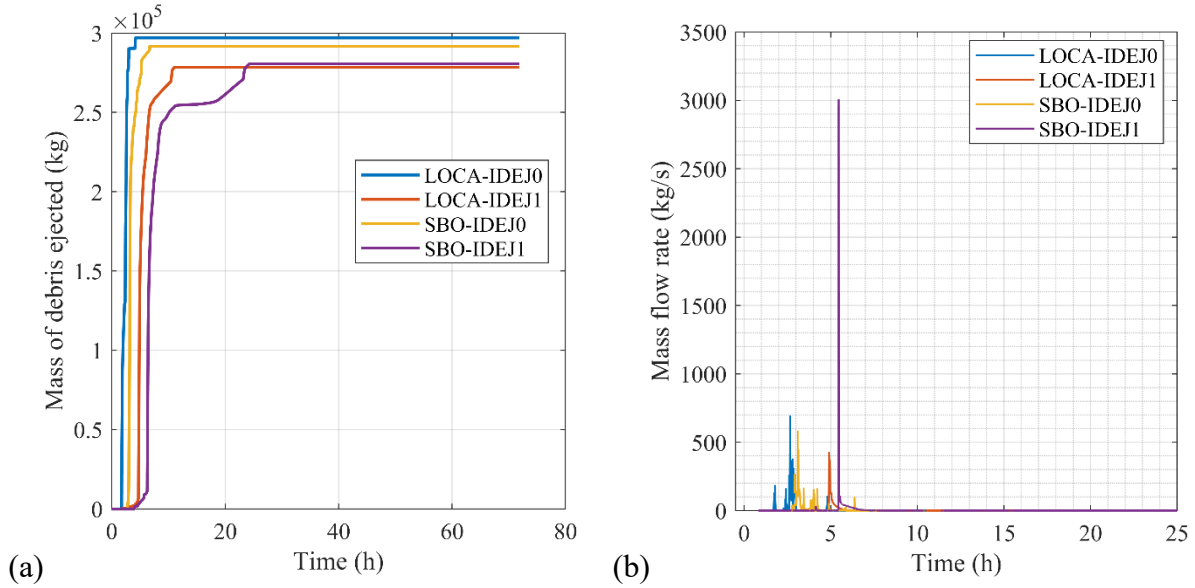

Figure 5-42. (a) Mass of melt ejected from the core upon RPV failure to the cavity; and (b) Mass flow rate of the melt.

During the first 1-24h of the accidents when the mass flow rate of melt can peak, SE premixing calculations are run for every 100s in TEXAS-V [59], and for each premixing case 2000 SE calculations are run. Subsequently, a database of probabilities of SE at these time intervals is developed and source term can be calculated considering containment hatch door failure when the probability crosses a threshold (0.5). TEXAS-V calculations and postprocessing of results is ongoing. The results will be presented in a later publication.

5.4.1. Basemat Melt-through in the Cavity

In addition to loss of containment integrity due to SE, basemat of the containment in O3 is riddled with instrumentation steel tube penetrations and large drainage pipe, where non-coolable debris bed may lead to melting of penetration protection and cavity rupture [60]. The reactor building below the containment is protected through physical separation. There are 4 subdivisions for safety equipment, pumps, valves, fire cell, heat exchangers for each of the emergency core cooling system trains [61]. Basemat penetration failure can have unintended consequences for the source term, with potential for hydrogen explosions.

5.4.1.1. MELCOR Model Modifications

In order to study the effect of basemat melt-through the NBWR MELCOR model was upgraded with an additional control volume (CV) representing the reactor building below the containment (CV211), flow paths (FLs) between the newly added CV and the cavity (FL210 – leakage to the reactor building through the hatch door, FL215 – rupture of the cavity), and modified FLs between cavity and the environment (FL359 and FL360). Heat structures were also added to represent the walls (cylindrical) and the floor (rectangular) of the reactor building. Figure 5-43 shows the MELCOR model of the modifications. Volume of the CV211 is considered to be a cylinder of diameter equivalent to that of WW (27.08m). The containment hatch door is about 4.3m in height and 6m in width. The flow path to the environment FL359 is assumed to be a partial opening of the hatch door of $1m^2$.

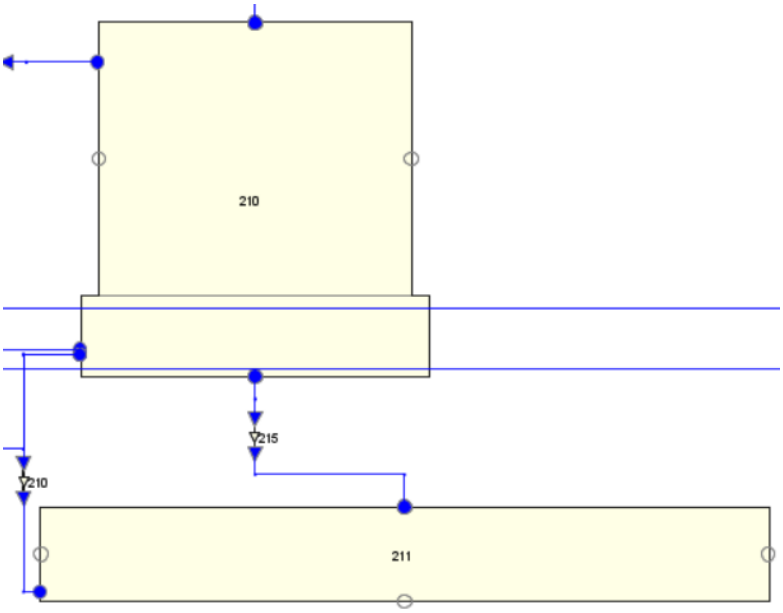

Figure 5-43. MELCOR nodalisation of the modifications for the reactor building.

The added CV is associated with a second CAV. MELCOR can have additional CAV, where melt can flow from one to the other based on certain cavity rupture conditions [6,7], axial rupture, radial rupture and rupture based on control functions (CFs). However, overflow from cavities is unidirectional. Cavity ruptures axially with breach of basemat and radially with breach of outer walls. CF can also control when the breach happens and the elevation of the breach. CAV_SP card can be used also to model the spreading of the melt in the cavity. The radius of the melt spread can be fed via a tabular function (TF), or via a CF, or an external datafile or internally calculate inside MELCOR. Here it is assumed that both axial and radial ruptures lead to melt being transferred into the reactor building CV below the containment.

5.4.1.2. Parametric Study of the Modified MELCOR Model

The thermo-physical parameters and chemical composition of the atmosphere were varied as given in Table 5-6 below. Case 001 – 040 were run for the first 10000s of LOCA-IDEJ0 scenario with varying parameters. Case 041 – 055 were run for full 72h of the accident progression. Figure 5-44 shows the pressure in the cavity for these cases. There are minor variations due to changing thermo-physical properties of the CV and HS.

CV_T – Initial temperature of CV211, CV_P Initial pressure of CV211, N2O2 – Atmospheric composition, CAV_HIT_BB – Cavity height, HS_W/F_HTC – Wall/Floor HS characteristic length, HS_W/F_len – Wall/Floor HS length, HS_WF_IC – Wall/Floor HS initial conditions, TLHF – Time of lower head failure, TCR – Time of cavity rupture.

Table 5-6. Cavity Parametric Study Parameters.

	comments	status	CV_T	CV_P	N2_O2	CAV_HIT_BE	HS_W_HTC	HS_W_len	HS_WF_IC	HS_F_HTC	HS_F_len	TLHF	TCR
Case_001		good	323	95000	N2	3.5/2	3.5	3.5	SS	13.54	13.54	6030.7	
Case_002	same as 1	bad	293										
Case_003	same as 2	bad	293	1.00E+05									
Case_004	same as 3	bad	293	1.00E+05	N2O2								
Case_005		good	323	1.00E+05	N2O2							5640.1	
Case_006	updated HS	bad	323	1.00E+05	N2O2					13.55	13.55		
Case_007	updated CV, HS	good	323	1.00E+05	N2O2					13.54	13.54	6796.7	
Case_008	updated CAV	good				5.0/2	5	5				5851.3	
Case_009	same as 8	bad	323	95000									
Case_010	revert CAV, updated CV	good	293	1.00E+05		3.5/2	3.5	3.5				6572.1	
Case_011	update CAV	good				3.5/1						6572.1	
Case_012	no LDW CV in WW HS	good										5335.1	
Case_013	revert case 12 WW	bad	323	95000									
Case_014	CAV only N2	bad			N2								
Case_015		good	293	1.00E+05								6419.6	
Case_016	same as 15, update HS	good								3.5	1	5648.5	
Case_017	update CAV	bad	323	1.00E+05	N2O2	3.5/2				3.5	2		
Case_018	revert CAV	bad	293			3.5/1				3.5	1		
Case_019		good			N2							5348.5	
Case_020	update HSIC	good							293			5348.5	
Case_021	same as 20	good								20	1	6070.1	
Case_022		bad			N2O2					3.5	1		
Case_023		good	323	1.00E+05	N2				323	20	1	6334.7	
Case_024		good			N2O2							5981.3	
Case_039		good					3.5	3.5		0.5/3.5	24/27.08	6171.1	
Case_040		good								13.54/27.08	27.08/23.99	6384.8	140896/140745
Case_042		good	323	1.00E+05	N2O2	3.5/1	3.5	3.5	SS	27.08	27.08	6631.9	147697
Case_043	CAV_SP 0.0	good										6631.9	103622
Case_044	CAV_SP -1.0	good										6631.9	103622
Case_045	CAV_SP 0.05	good										6631.9	122515
Case_046	CAV_SP 0.10	good										6631.9	89499.7
Case_047	CAV_SP 0.25	good										6631.9	125121
Case_048	CAV_SP 0.50	good										6631.9	127000
Case_052	CAV_SP 1.525	good										6631.9	19507.4
Case_053	CAV_SP 3.05	good										6631.9	44750.3
Case_054	CAV_SP 4.575	good										6631.9	98599.7
Case_055	CAV_SP 6.1	good										6022.8	160478

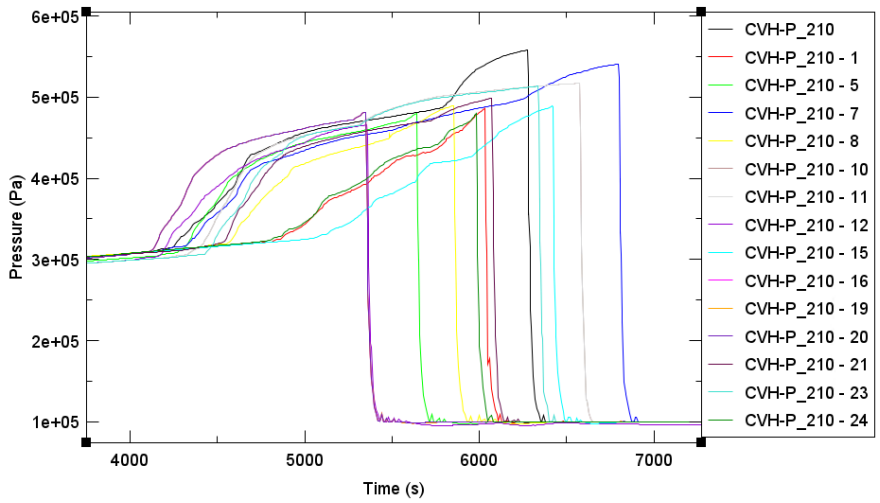

Figure 5-44. Pressure in the cavity.

As seen in Case 001/002, and Case 023/024, addition of O2 in the CV of the reactor building reduces the TLHF. Case 042 with realistic values for the characteristic lengths of the HS, and physical dimensions successfully ran with TLHF of 1.842h in comparison to 1.735h of the unmodified LOCA-IDEJ0 case. Case 043 was run with MELCOR internally calculating the melt spread. While in the default case melt would instantaneously spread across the complete width of the cavity, this spread is analytically calculated assuming a cylindrical melt debris where spreading is driven by gravitational and opposed by viscous forces. When CAV_SP is 0 MELCOR calculates the viscosity based on Ramacciotti model for melt component and oxide components. Sensitivity coefficient SC2303 controls the influence of viscosity term and the stopping logic for the spread. In the study default values are used.

Additionally, with CAV_SP as 0, an initial radius should be specified by the user. Negative number (Case 044) assumes initial radius based on COR-ABRCH area, zero implies the code calculates initial radius and positive numbers imply the specified initial radius of melt. Figure 5-45 shows the radius of the melt debris in the cavity. Case 045 – 048 are those where MELCOR calculates the radius with specified initial radius, and Case 052 – 055 are those where a CF was used to parametrically specify radius of the melt (constant throughout the accident sequence). Water level in the cavity for these cases are shown in Figure 5-46. Mass of molten material in the cavity and the mass of melt transferred to the second cavity CV are shown in Figure 5-47.

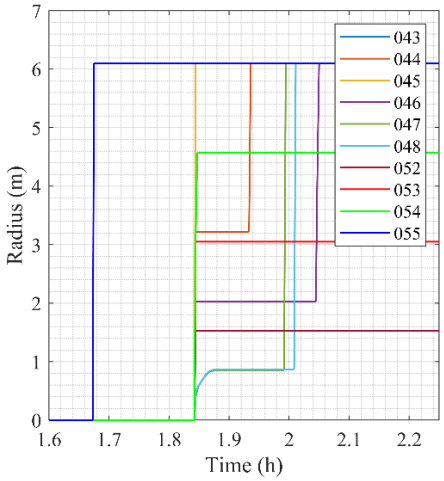

Figure 5-45. Time dependent melt debris radius for the cavity.

Even though CAV_SP is used with a specified initial radius MELCOR spreads the melt to the entire width of the cavity within ~0.3h. Case 055 is seen leading to a quicker LHF, but this is due to numerical effect of having different maximum time steps in calculation, as opposed to Case 052 – 054. It has to be noted that maximum time step, in some cases, plays a greater influence than physical phenomenon when using MELCOR.

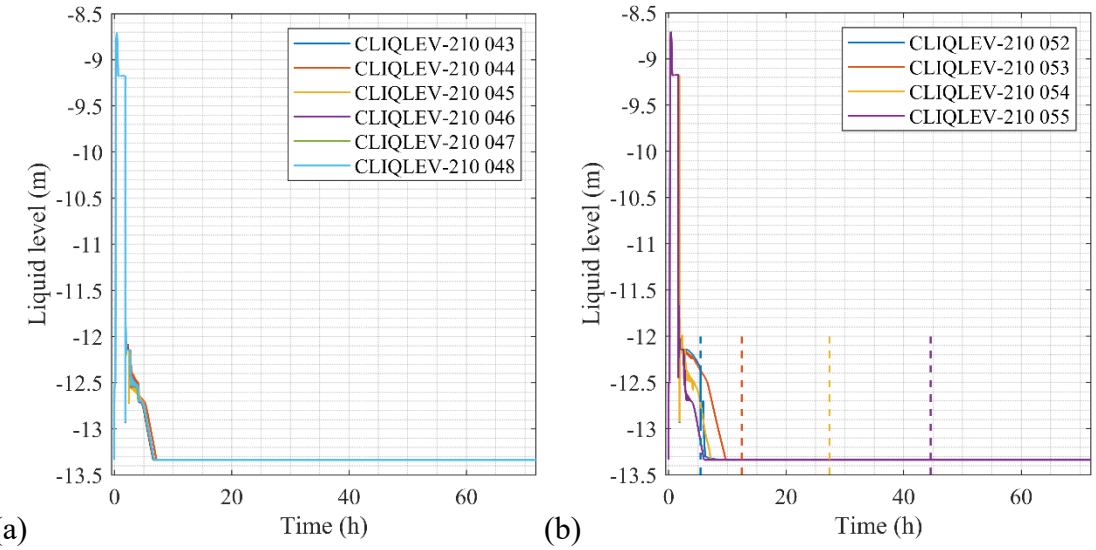

Figure 5-46. Collapsed liquid water level in the cavity. (Dashed lines in (b) represent the time when cavity ruptures).

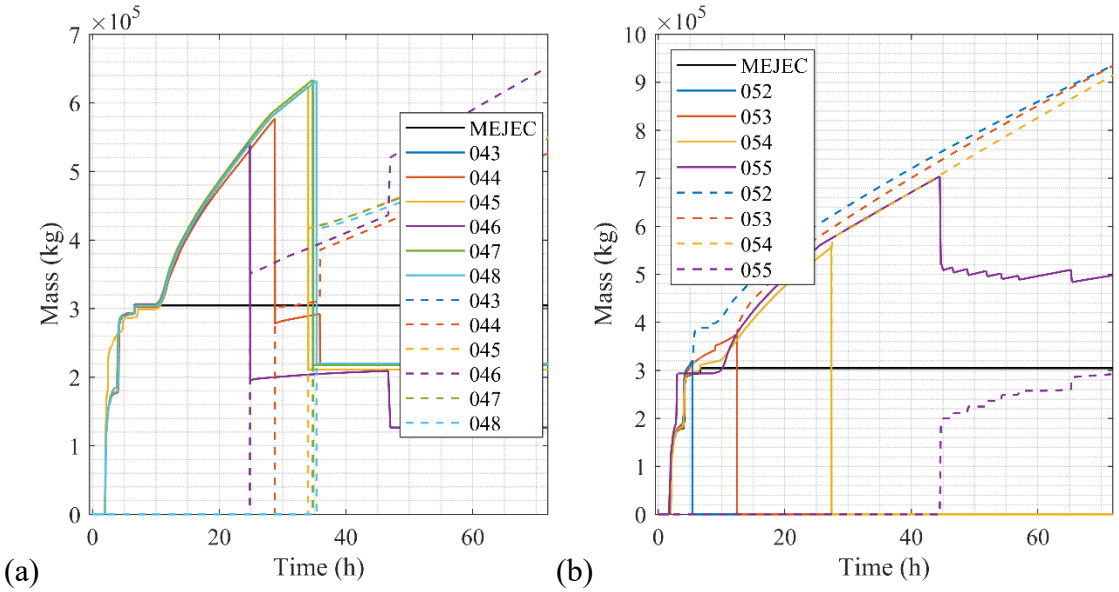

Figure 5-47. Molten mass of material in cavity and the reactor building. (Black line represents the total mass of melt ejected from the core, and the dashed lines show the mass of melt in the reactor building CV that is transferred from the cavity).

In Case 052, Figure 5-46 (b) even before all the water has either escaped through the hatch door or evaporated, the cavity basemat has failed, and some water flows into the reactor building. In this case the debris bed is uncoolable and MCCI starts even when part of melt is submerged. For other cases (Case 043 - 048) Figure 5-46 (a), MCCI starts only after water has escaped out of the cavity. This is due to the fact that a smaller radius implies a smaller area for heat exchange with the coolant, and so higher propensity for degrading the basemat concrete. This is also seen in Case 053 – 055, Figure 5-47 (b). The time for cavity rupture in Case 043 – 048 falls between ~25-35h after start of transient. Whereas it happens as early as ~5h in Case 052, and ~12.5h, ~27.5h and ~45h in Case 053 – 055 respectively.

Cesium and iodine release fractions for these cases are shown in Figure 5-48 and Figure 5-49 below. Hydrogen generated (during core degradation and melt coolant concrete interactions in the 2 cavity CVs) for the cases are shown in Figure 5-50 below.

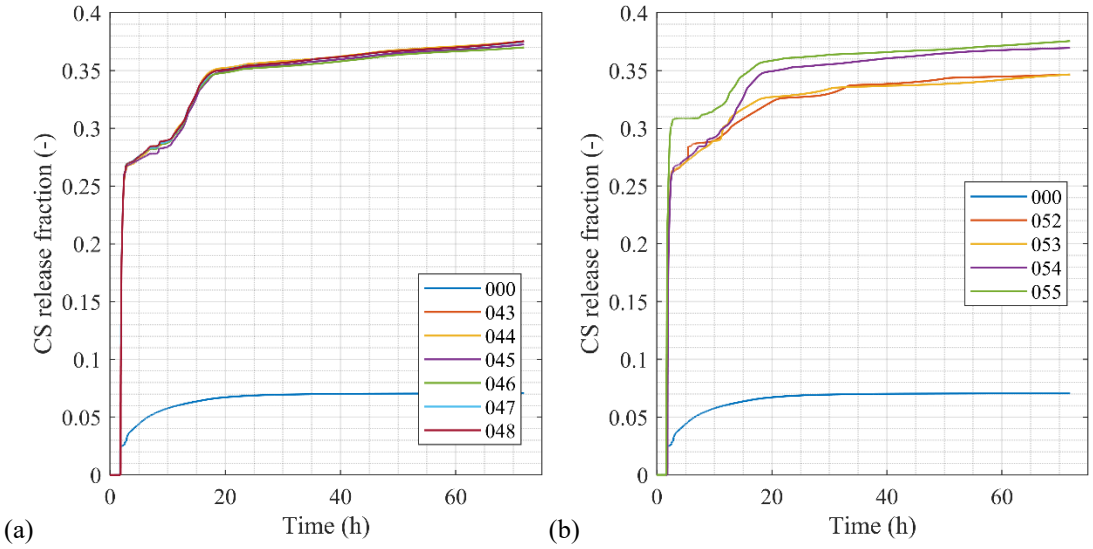

Figure 5-48. Cesium release fractions for (a) Case 043 – 048 and (b) 052 - 055. (000 is the best estimate case for LOCA-IDEJ0 without any MELCOR model modifications).

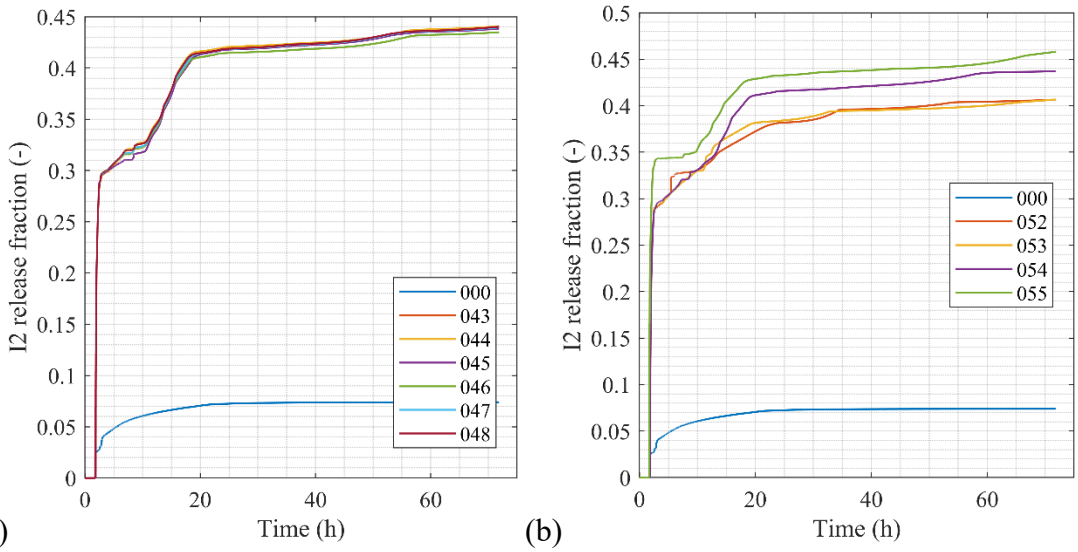

Figure 5-49. Iodine release fractions for (a) Case 043 – 048 and (b) 052 - 055. (000 is the best estimate case for LOCA-IDEJ0 without any MELCOR model modifications).

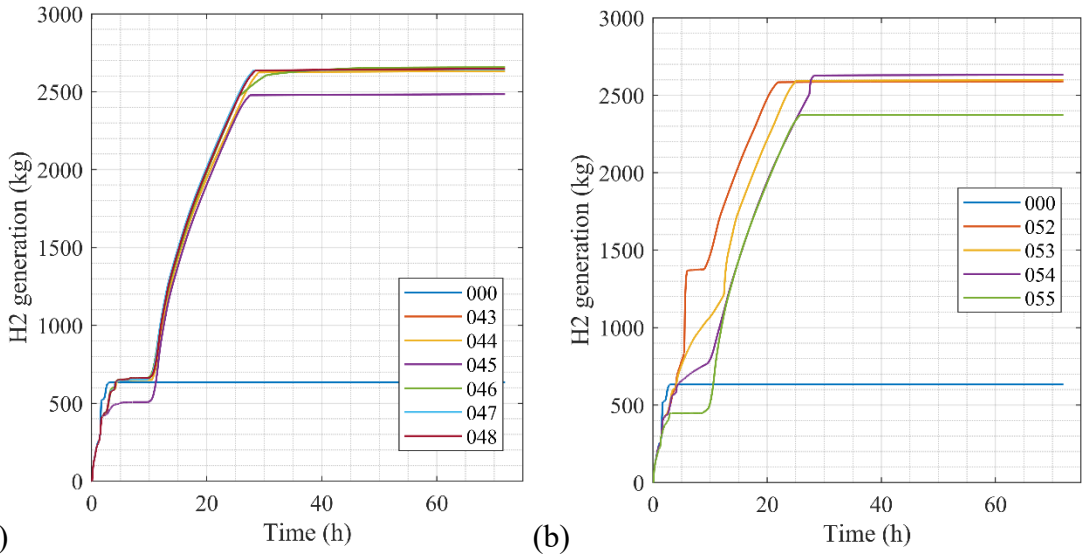

Figure 5-50. Hydrogen generation for (a) Case 043 – 048 and (b) 052 - 055. (000 is the best estimate case for LOCA-IDEJ0 without any MELCOR model modifications).

CS and I2 releases in these cases are at least 5 times greater than the best estimate scenario. Firstly, in LOCA the steam is discharged through the blowdown pipes into the WW and most of the FPs are retained. When the LDW is flooded, and subsequently containment fails, FP contaminated water escapes to the environment. Water from WW keeps flowing into the cavity trying to cool the melt, and FP gets suspended into the atmosphere and flows into the environment. MCCI releases large amounts of gases (CO_2, CO, H_2O and H_2) which can carry the FP aerosols to the environment. From Figure 5-50 we see roughly 6 times more hydrogen generated from the core and MCCI in the two cavity CVs when compared to the best estimate scenario.

5.5. Studies of the Uncertainties related to the Containment Spray System

VTT studied the uncertainties related to the containment spray system using MELCOR and SNAP program.

In the first two phases of the project, VTT modelled a station black out (SBO) scenario for a Finnish BWR. Since a complete loss of electricity was assumed, the containment spray system was also expected to be offline. In hopes of utilizing the results from the previous phases (result comparisons, timestep adjustments for stability), the same model is applied to this work with the assumption that at some point during the accident, enough power is regained to run the containment spraying system. This is, of course, a bit unconventional approach as spray systems are usually being relied on during a LOCA event and not SBO.

In the VTT's MELCOR model of the Finnish BWR, the containment spraying system consists of drywell and wetwell sprays that source their water from the wetwell. The system is triggered by low water level in RPV, high upper drywell pressure or temperature, fast pressure or temperature rise in the upper drywell, or high vapor temperature in the lower drywell. In order to study the effect of the timing of activation of the spray system, the trigger was switched to manual. The sprays were assumed to start after the vessel breach and melt ejection, and an adjustable time delay was set to the trigger.

5.5.1. Selection of input parameters and figures of merit

In the previous phases of the project, VTT studied cesium release to the environment and the opening times of the filtered containment venting. Since the spraying system is assumed to influence the aerosol scrubbing, the figures of merit have been updated to include the release of iodine to the environment. The spray system could be assumed to be affecting the containment pressure as well, but since the FCV is assumed to start at the same time with melt ejection, causing an instant pressure relief, monitoring e.g. maximum pressure seemed pointless. Moreover, the input parameters chosen for the analyses were assumed to be affecting mostly the post breach phenomena, so in theory there was no need to monitor the FCV opening times. However, during the calculations, it was noticed that seemingly unrelated parameters seemed to affect the in-vessel phenomena and vessel breach/FCV opening times, so it was retained as a FOM.

One of the most important parameters was the delay between the vessel breach and the start of the spray system, named here as SPRDELAY. From the results of the previous analyses, it could be seen that without the containment spray system, the majority of the Cesium release occurs within the first 3 000 seconds after the breach, so this was chosen as the upper boundary. As most of the release happens towards the beginning of this sequence, the PDF was set to loguniform for SPRDELAY.

The other input parameters were chosen from the list provided in the Phase 1 of the STATUS project. The focus was on the parameters that were thought to be affecting the post breach phenomena, especially the spray system. The parameters, their upper and lower boundaries and PDFs can be found in Table 5-7 below.

Table 5-7. Input parameters chosen for the sensitivity and uncertainty analysis.

Parameter	Lower boundary	Upper boundary	Default	PDF	PDF justification
SC710611	5.00E-08	7.625E-07	1.00E-06	Loguniform	
SC710621	2.50E-07	8.125E-07	1.00E-06	Uniform	
SC710641	2.41E+05	3.46E+05	3.81E+05	Uniform	
CHI	1.50	3.00	1	Beta: a = 1.0, b = 1.5, min = 1.0, max = 5.0	[62]*
GAMMA	1.50	3.00	1	Beta: a = 1.0, b = 1.5, min = 1.0, max = 5.0	[62]*
STICK	0.50	1	1	Beta biased to 1 (p=2.5, q=1)	[62]*
RHONOM	870	4500	1000	Triangular	[64]*
SC7111I1	4.235	5.729	4.982	Uniform	
SC7111I2	467.5	632.5	550	Uniform	
SC7111CS1	3.075	4.160	3.617	Uniform	
SC7111CS2	82.45	111.55	97	Uniform	
SC7170CS	3.36	4.54	3.95	Uniform	
SC7170CSI3	0.37	0.51	0.44	Uniform	
SC7170CSI4	1.91	2.59	2.25	Uniform	
DECAYH[7]	0.96	1.04	1	Uniform	
DIAMO[8]	0.0001	0.002	0.001	Loguniform	
SPRDELAY	1.00	3000.00	0	Loguniform	
SC715010	1.50	3.00	1	Uniform	
SC715111	2.9325	3.9675	1.79182	Uniform	
SC71521	5.00E-03	8.00E-03	7.00E-03	Uniform	
SC71531	6.690	9.057	7.876	Uniform	
SC71551	1.52300	2.06060	1.79182	Uniform	
SC71555	0.99681	1.30980	1.13893	Uniform	
SC71542	2.56E-03	3.46E-03	3.0110E-03	Uniform	
SC71568	-2.67E-03	-1.97E-03	-2.3210E-03	Uniform	

[7] DECAYH is missing from the Morris analysis.

[8] Due to a coding error, DIAMO is not considered in the uncertainty analysis

5.5.2. Sensitivity analysis

Two methods for sensitivity analysis were used in this work: sensitivity correlations calculated by DAKOTA/SNAP and Morris method. The former is the only method found in SNAP by default, and the latter was included using a Python job stream and SALib package.

5.5.2.1. Morris method

A simple Morris analysis was performed to test out the newly implemented code and its combability with SNAP. No detailed quantitative analyses were performed afterwards, so the method is only used to give a rough estimate about the relative influence of the different parameters.

A total of 24 parameters were assessed with the number of elementary effects being 10. This resulted into 250 model evaluations. A Python stream was set up with the SALib library to sample and run the cases in SNAP, and to perform a simple Morris analysis. Ten or so crashed cases were fixed and run manually afterwards.

The following figures illustrate the Morris indices in the case of cesium and iodine release, and FCV opening time.

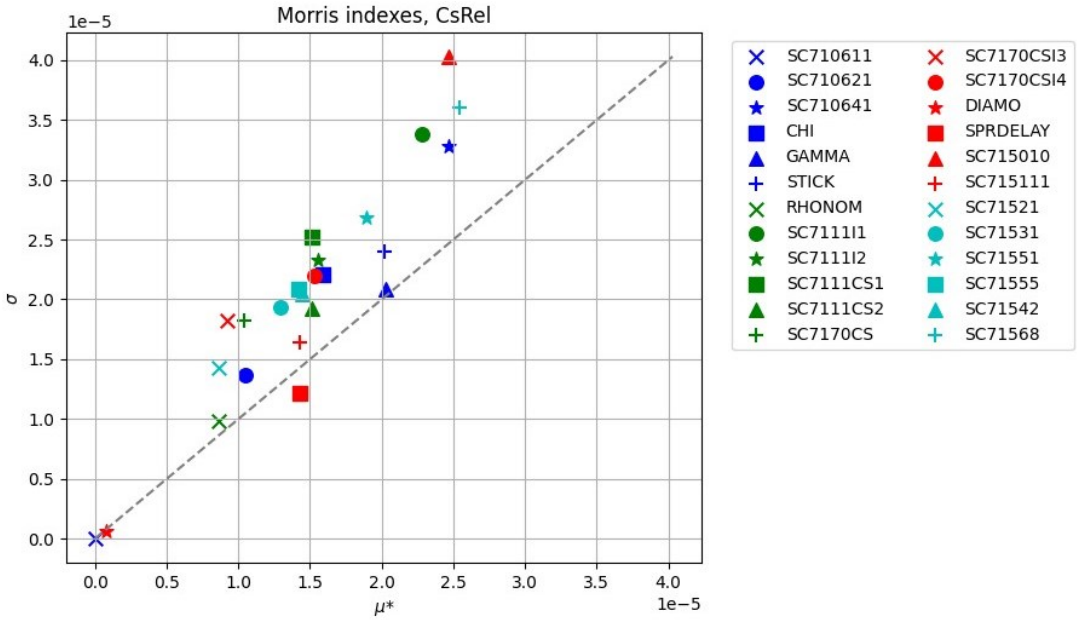

Figure 5-51. Morris indices for Cs release.

The above figure shows, that according to the Morris analysis, the most influential parameters for Cs release include some spray and pool scrubbing parameters such as SC715010, SC71568, and SC71551. SPRDELAY seems to have some influence but less than most. Interestingly, iodine vapor diffusivity parameters seem to affect Cs release as well.

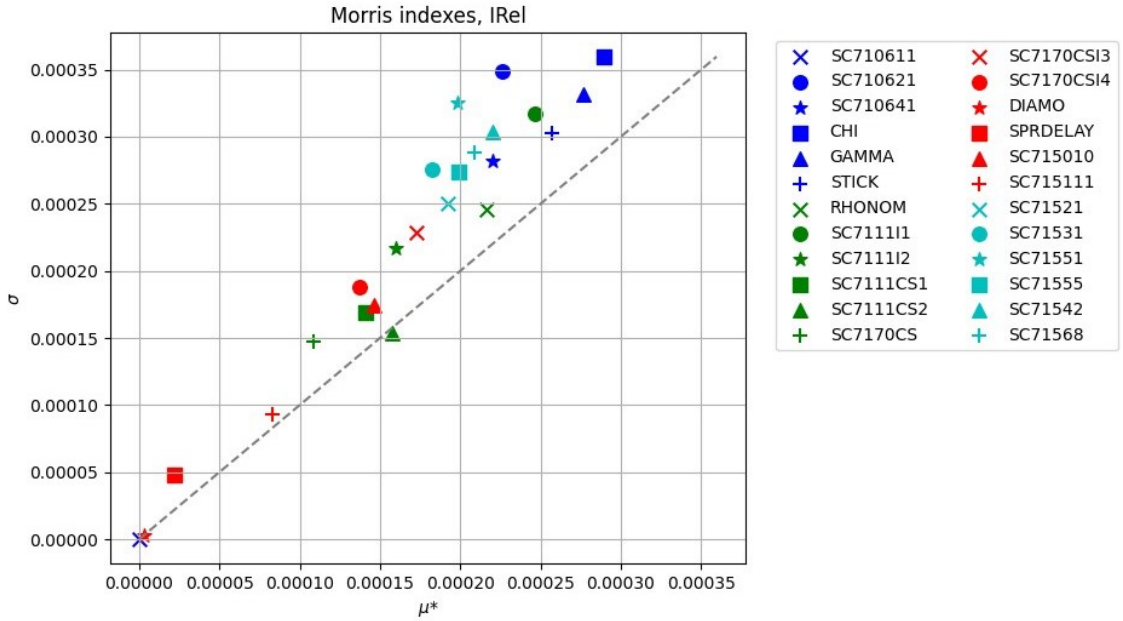

Figure 5-52. Morris indices for iodine release.

For iodine, the analysis would suggest that the most influential parameters are the ones describing FP release from fuel, aerosol dynamics and pool scrubbing. The least influential parameters are SC710611, DIAMO, SPRDELAY, and SC715111. Cs solubility and diffusivity parameters are also quite low on the graph, which is understandable. The low ranking of DIAMO and SPRDELAY are also worth noting.

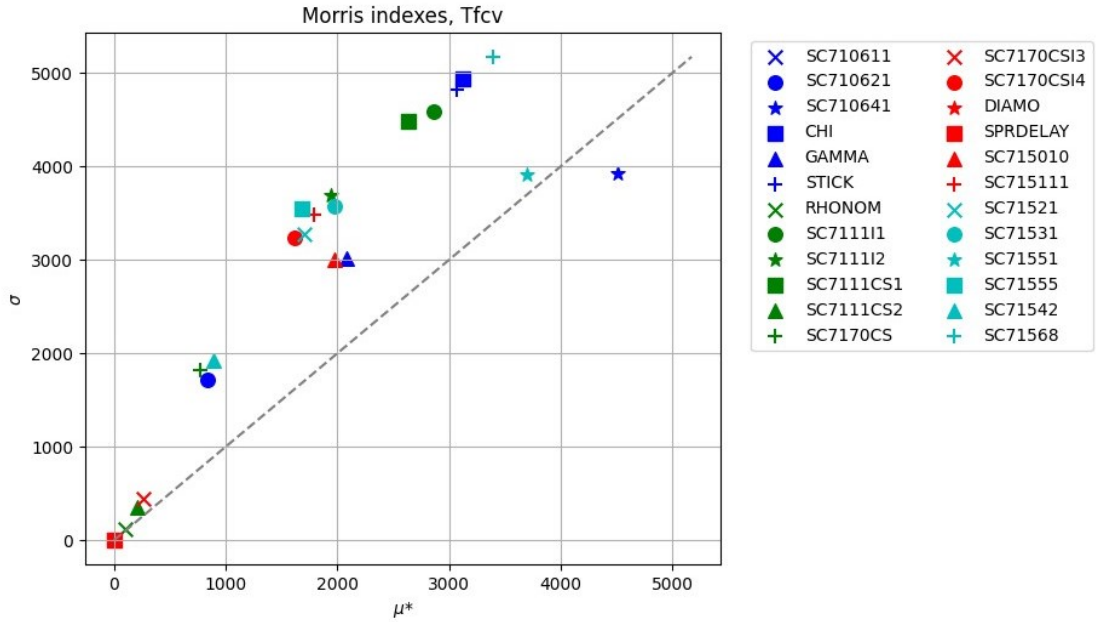

Figure 5-53. Morris indices for FCV opening times.

With FCV starting time, there seem to be slightly more nonlinearity than in the previous figures. The analysis would also suggest that the most influential parameters include parameters related to e.g. aerosol dynamics and pool scrubbing, which doesn't seem quite right. Without further analyses one can't be sure, but it is very possible that the dependencies shown in the plot are just coincidental and they might have been affected by numerical noise or by the data outliers shown next.

FOMs from all the Morris model evaluations are shown in Figure 5-54. In the plot for FCV opening times, one can see that in 55 cases the values get significantly higher than normal. The exact reason for these outliers was not discovered as their occurrence seemed completely random. A single change in a parameter was able to cause an outlier in the FCV opening time, whereas the next change in the next parameter usually returned the value back to the previous level. Further studies showed that the vessel breach occurred around the "correct" time, but despite the adjustments done to COR package sensitivity coefficients, the melt was not ejected until 4 000 – 5 000 seconds later.

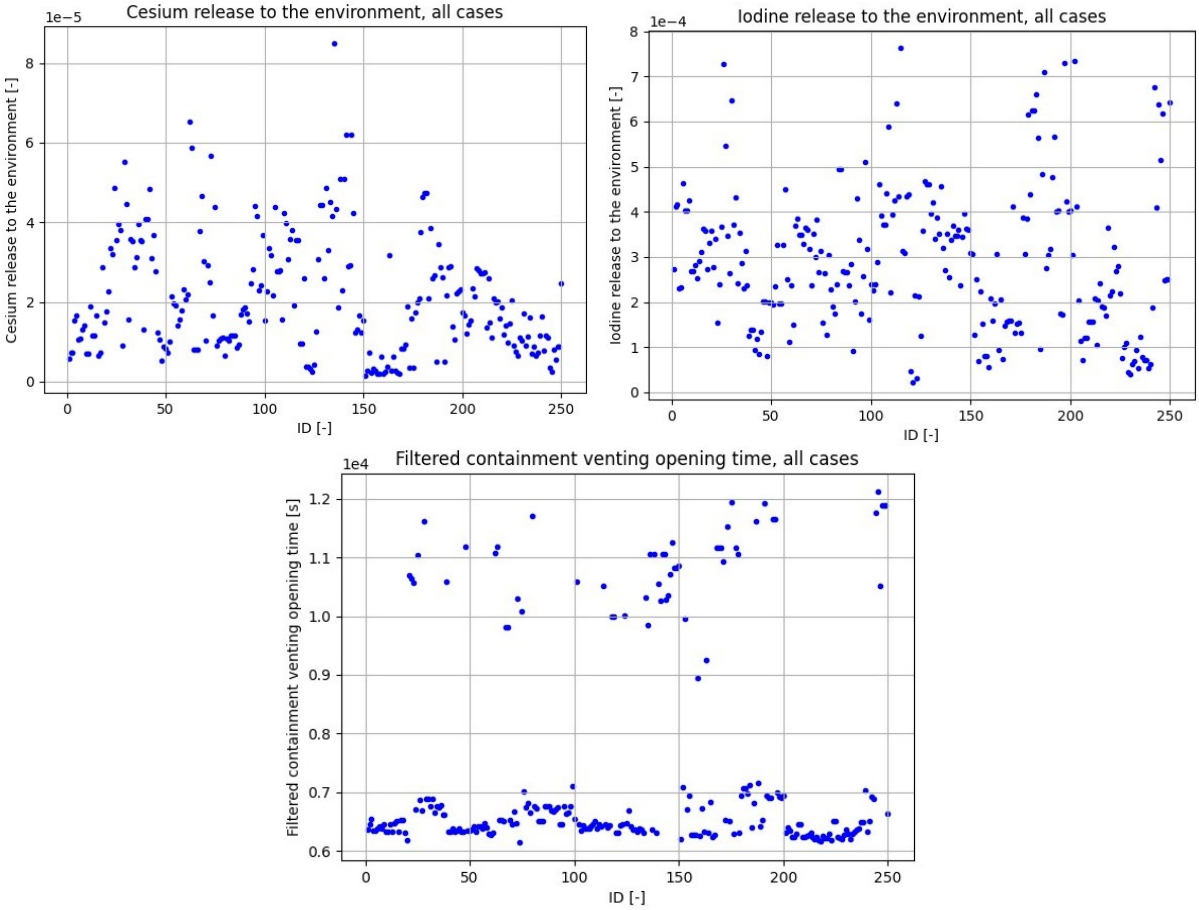

Figure 5-54. Cesium and iodine release, and FCV starting time in all cases.

Since the outlier changes in the FCV opening time output are rather large and random, it is possible that they case bias in the results by falsely increasing the observed influence of a noninfluential parameters.

5.5.2.2. Sensitivity correlation coefficients

Sensitivity correlation coefficients were obtained form the python-directed uncertainty run on SNAP. Monte Carlo was used in sampling the parameters. Due to a programming error DIAMO was not properly sampled and applied to the models, so only 24 input parameters were assessed instead of 25. The total number of the model evaluations was 153, of which 3 needed to be resampled. Each case was run for 36 000 seconds. The following figures show the most influential parameters for each FOM.

GAMMA (Aerosol agglomeration shape factor) and SPRDELAY seem to be the most influential parameters in this case, whereas in the Morris analysis neither was nowhere near the top.

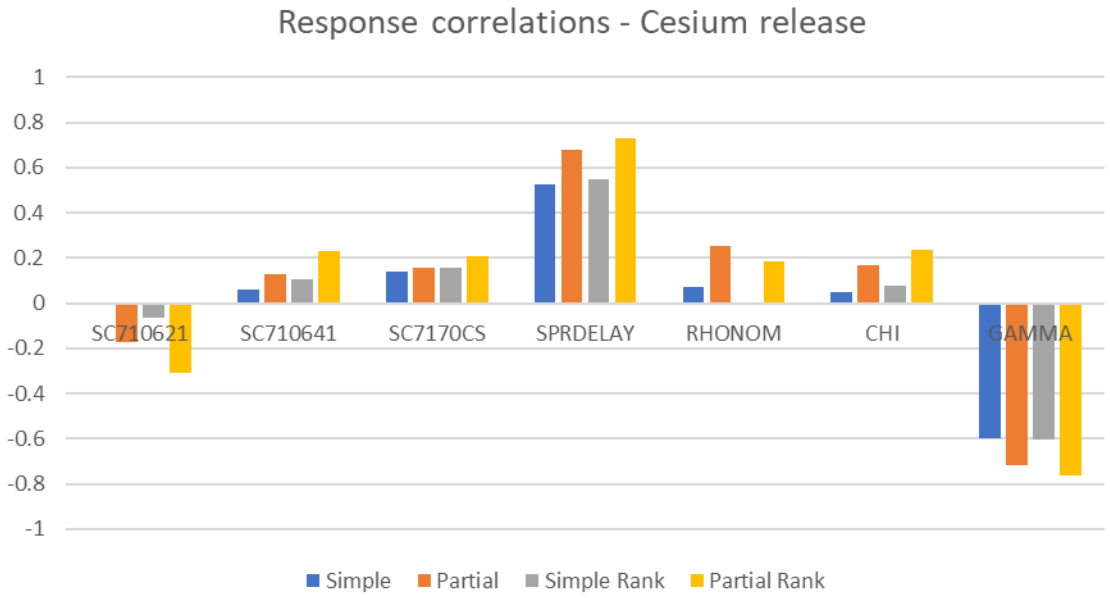

Figure 5-55. Cesium release: the most influential parameters + SPRDELAY according to the response correlations.

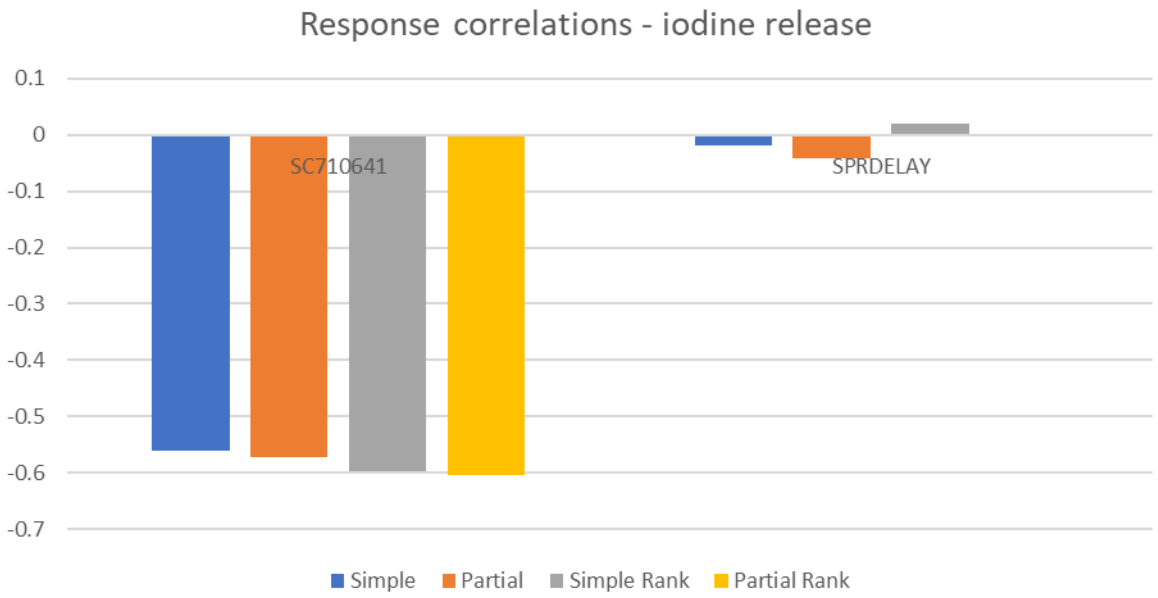

Figure 5-56. Iodine release: the most influential parameters + SPRDELAY according to the response correlations.

According to these results, iodine release is affected mostly by SC710641 (Activation energy), and the scrubbing effects of spray seem to be nonexistent. However, the lack of effect of SPRDELAY and other spray parameters on the iodine release might be caused by the upper limit of the SPRDELAY. As Figure 5-57 shows, the majority of the iodine release occurs much later in the simulation, in most cases between 17 000 and 20 000 seconds, i.e. 11 000 – 14 000 seconds post breach. Since the spray start delay is limited to the first 3 000 seconds post breach, the majority of the iodine release occurs when the sprays are already operational, and therefore we don't get to observe the effect of the spray delay on the increasing iodine concentrations. To properly assess how the spray starting time affects the iodine release, the cases should be rerun with an increased SPRDELAY.

Morris sensitivity analysis highlighted SC710641 as an influential parameter, among many others that weren't deemed influential by the correlation coefficients.

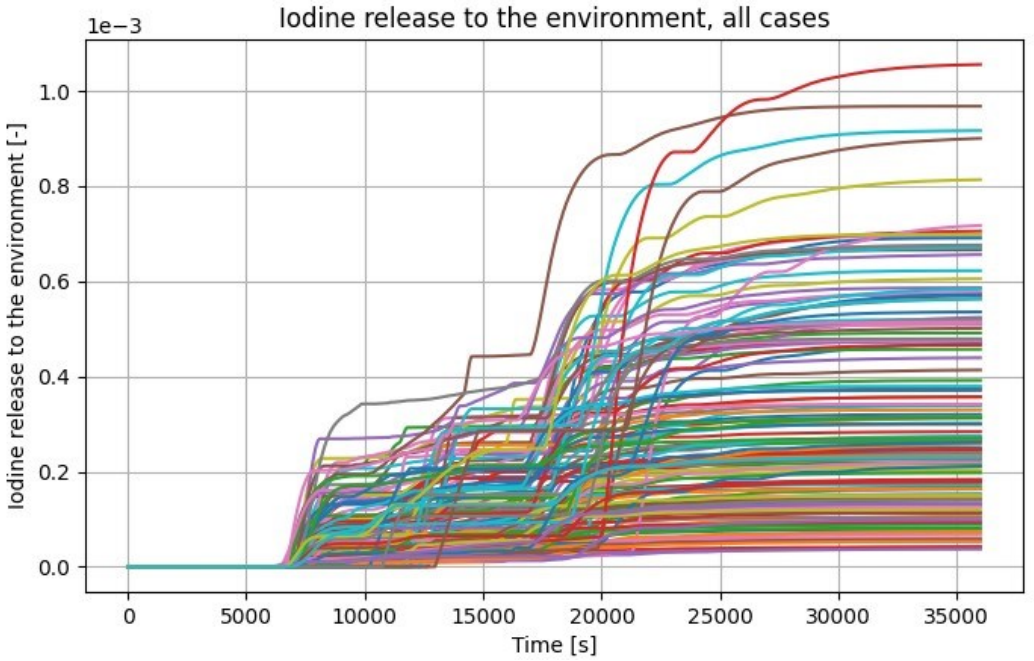

Figure 5-57. Iodine release to the environment, all cases.

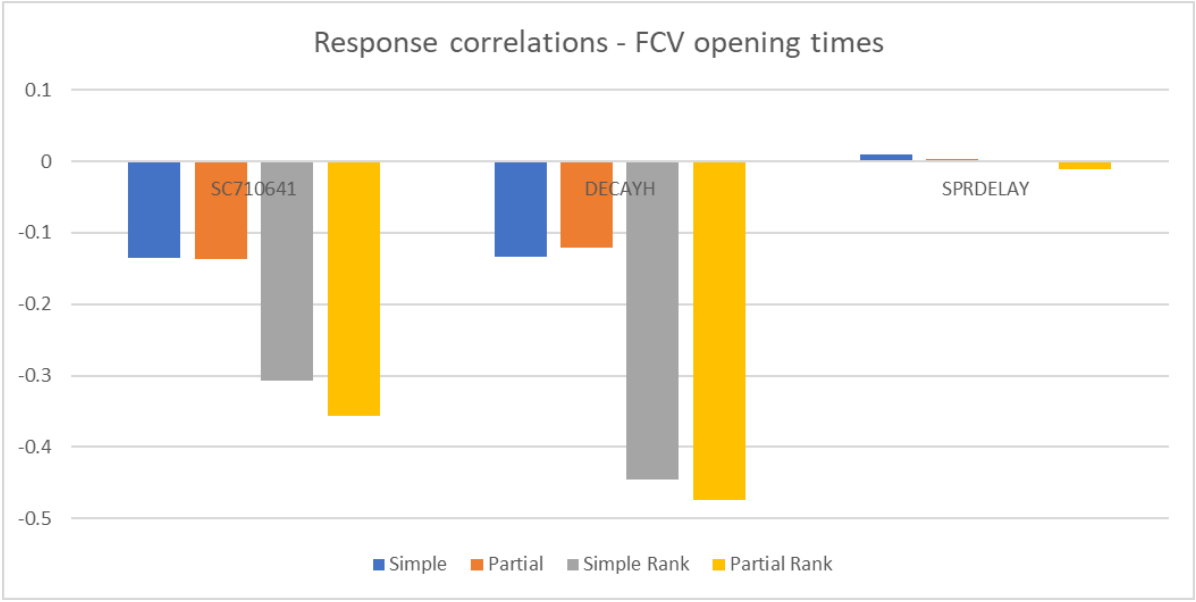

Figure 5-58. FCV opening times: the most influential parameters + SPRDELAY according to the response correlations.

It would seem that FCV opening time was mostly influenced by SC710641 (Activation energy) and DECAYH (decay heat). The former was ranked rather high in the Morris analysis, whereas DECAYH was not considered at all in the simulations. As expected, SPRDELAY does not have a real effect on FCV opening time.

5.5.3. Uncertainty analysis

Uncertainty analysis was performed simultaneously with the sensitivity analysis on SNAP. A total of 24 parameters were varied at the same time in 153 calculation rounds. Sampling was done in SNAP using Monte Carlo method.

The following figures illustrate the probability density functions for cesium release, iodine release and FCV opening times.

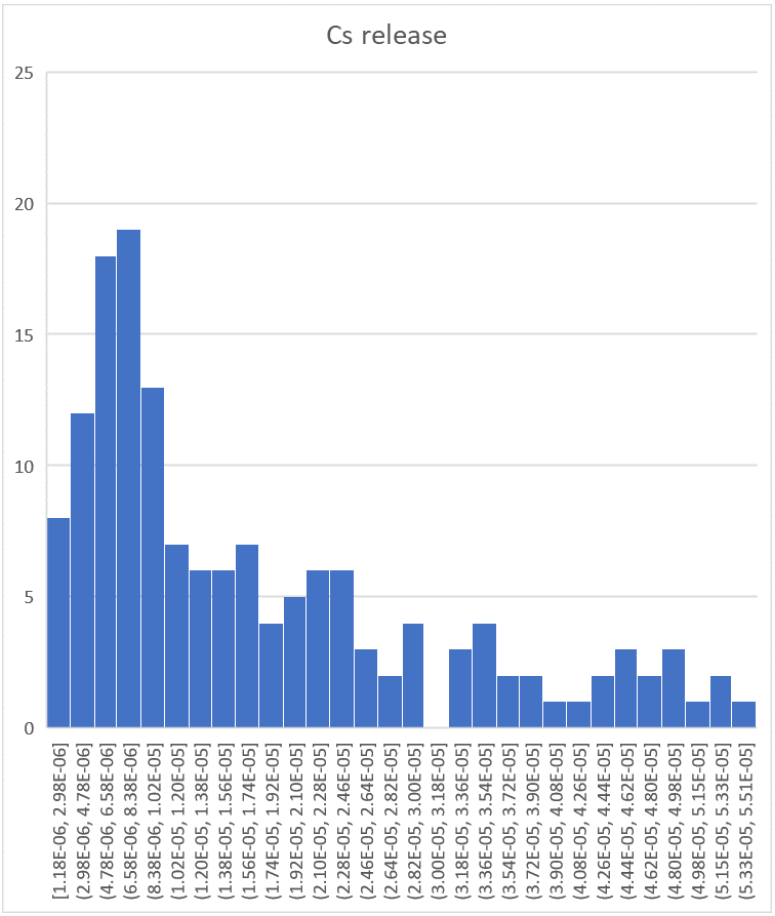

Figure 5-59. Cesium release: probability density function. Histogram limited to 30 bins.

The distribution of cesium release seems to be very close to lognormal distribution. Majority of the releases are on the smaller side, whereas the larger releases are sparser.

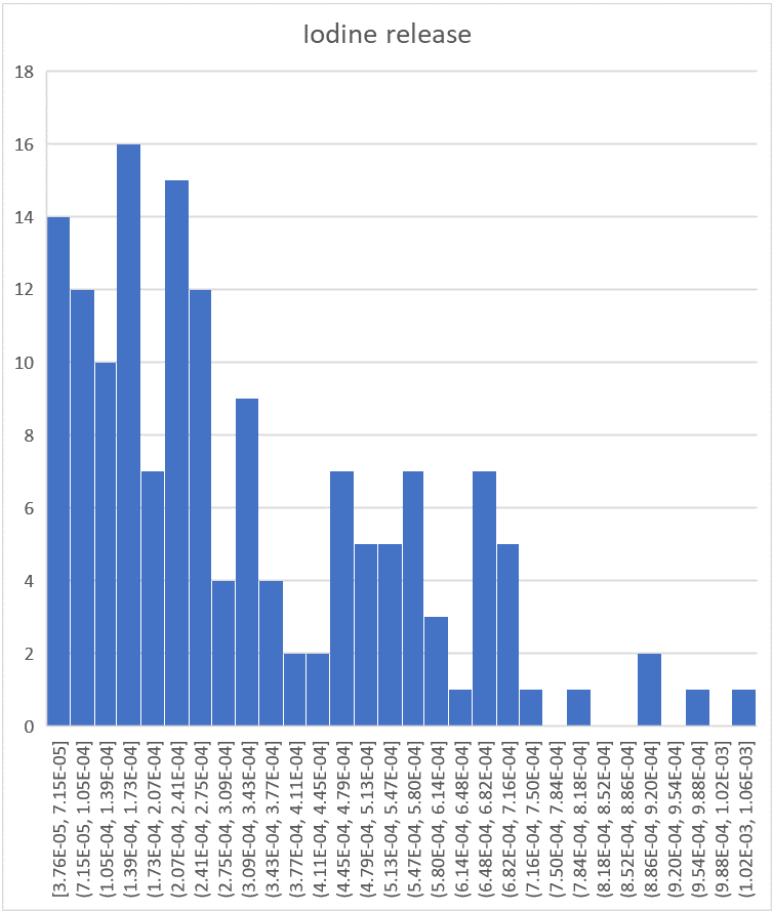

Figure 5-60. Iodine release: probability density function. Histogram limited to 30 bins.

With iodine, the probability density function does not have as clear shape. It can be observed that in most cases the iodine release is rather low, although, it is very likely that the shape is caused by the previously mentioned insufficient range for SPRDELAY.

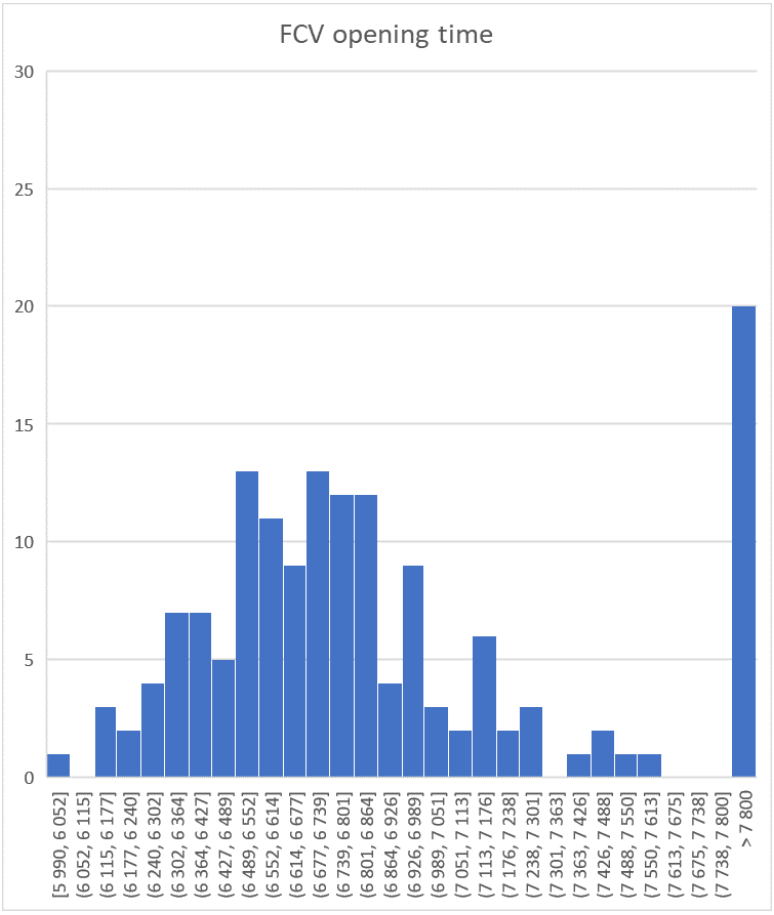

Figure 5-61. FCV opening time: probability density function. Histogram limited to 30 bins

If the outliers were ignored, it could be stated that the PDF for FCV opening time has quite clear normal distribution.

In Table 5-8 some key values are listed and compared to the case without the spray system. It can be seen that overall, the usage of the sprays lowers both the cesium and iodine releases. As for FCV opening time, there are only small differences, which is completely expected since spray system should not affect the vessel breach and FCV start. It should be also noted that outliers appear in both cases.

Table 5-8. Some key values of each FOM compared to another uncertainty run without the sprays. Green cells indicate lower values.

	CsRel		IRel		t_FCV	
	SPRAY OFF	SPRAY ON	SPRAY OFF	SPRAY ON	SPRAY OFF	SPRAY ON
min	1.5084E-06	1.1805E-06	4.6811E-05	3.7600E-05	5990.0	5990.0
max	1.7552E-04	5.5147E-05	1.0546E-03	1.0554E-03	12800.2	12970.1
avg	3.5048E-05	1.6933E-05	3.7604E-04	3.1877E-04	7483.1	7307.3
median	2.4173E-05	1.1492E-05	3.4185E-04	2.4952E-04	6740.0	6750.0
5 %	7.5167E-06	2.8078E-06	9.0542E-05	5.5701E-05	6230.0	6270.0
10 %	9.0224E-06	4.1974E-06	1.0592E-04	7.3934E-05	6350.0	6345.0
90 %	6.8557E-05	4.0255E-05	7.4698E-04	6.7036E-04	11400.0	10581.1
95 %	1.0070E-04	4.6397E-05	8.0521E-04	6.9597E-04	11880.2	11600.0

6. Discussion and conclusions

In this project several tasks related to the assessment of the source term uncertainty in the Nordic BWR-type reactor have been addressed. The main conclusions from these tasks are summarized further in this section.

The analysis show that the structures, systems and components located outside the containment can significantly reduce the conservatism in the source terms in the case of a containment bypass (for the scenarios in the RC3 release category [23]). The results indicate that further reducing the uncertainty in the release path geometry, the effect of components and structures (such as turbine internals and turbine building internals), and systems (such as the turbine building ventilation system) may lead to even greater reduction of the conservativism in the analysis.

For the RC4 release category (containment failure due to containment phenomena) additional pathways for the release of FP were analyzed during RC4A (LOCA-IDEJ0) scenario. The failure of containment hatch doors significantly affects the release pathways for FP, increasing the quantity of their release into the environment. The study further explores the consequences of basemat melt-through in the cavity, a critical concern given the presence of instrumentation steel tube penetrations and large drainage pipes. The potential for non-coolable debris beds to compromise the integrity of the basemat poses significant risks, including the possibility of hydrogen explosions. Cesium and iodine release fractions underscore the severe implications of cavity rupture and melt spread. The release fractions for cesium and iodine are significantly higher in the modified scenarios compared to the best estimate case, primarily due to the interaction of steam and fission products with containment breach pathways. The retention of fission products in water and their subsequent suspension in the atmosphere during containment failure highlight the complex dynamics of source term release in severe accident scenarios.

The source term analysis for the RC7 release category (filtered release through the filtered containment venting system (MVSS)) was further refined to cover the accident progression during the 72 hours after the initiating event, and additional analysis of the effect of mitigative actions performed by the operator.

The uncertainty analysis results considering the MELCOR code's epistemic modeling parameters and options, show that spraying in the containment with the independent spray system can significantly limit fission products release to the environment. In the accident scenarios with the independent spray system (LOCA-IDEJ0-SPR and LOCA-IDEJ1-SPR) the release of Cs to the environment is below the acceptable release threshold[2] regardless uncertainties in the MELCOR code modelling parameters. To compare, the fraction of Cs released to the environment in unmitigated scenarios (LOCA-IDEJ0 and LOCA-IDEJ1) exceeds the acceptable release threshold in 16% and 90% of the simulations performed, respectively.

Furthermore, the results of this analysis emphasize the importance of a more detailed modelling of the multi-venturi scrubbing system (MVSS). This includes modelling of the structures and components between the containment and the scrubber, and the multi-venturi manifold. This can be done in the form of control volumes and associated heat structures to account for cooling and condensation of gases released from the containment. Additionally, a more detailed modelling of the venturi scrubbing is necessary, where scrubbing efficiency accounts for the size of the aerosols.

Another crucial aspect that needs to be considered in the future analysis is the long-term behavior of the scrubber. This involves consideration the effects of scrubber water

temperature and level, as well as the impact of decay heat from fission products deposited in the filter pool on the scrubbing efficiency of the MVSS. This may necessitate modelling of additional operator actions, such as scrubber inventory makeup, which are currently not considered in either the MELCOR model of Nordic BWR or in the PSA L2 for Nordic BWR.

Finally, considering the unresolved questions regarding the performance of the filtered containment venting system (MVSS - Multi-Venturi Scrubbing System) identified in both earlier phases of the project and the results presented in this report, the modelling of the MVSS has been refined. This includes more detailed modelling of the structural components of the MVSS and marks the first step towards a more realistic modelling of the MVSS and its performance under different severe accident conditions.

The results of the analysis show that the pool scrubbing is effective during the first hours after the initiation of the MVSS release. With pool heat up and water boiloff in the scrubber, the scrubbing efficiency of the pool decrease significantly. Furthermore, the results indicate that that the water level in the scrubber can drop below the venturi manifold riser pipes outlet ~20 hours after the initiating event, which means that the manual actions to makeup the water inventory in the scrubber needs to be initiated within this time frame.

The preliminary results using the refined MVSS model show that accurate modelling of heat structures and the entire flow path from the containment to the MVSS is essential for predicting fission product behaviour and scrubbing efficiency of the MVSS. Turbulent deposition effects in the MVSS are minor but further sensitivity and uncertainty analyses are necessary to quantify the importance of this retention mechanism. Finally, the results indicate importance of the self-priming venturi scrubbing, which was not included in the current model and will be addressed in future MELCOR model developments for the Nordic BWR.

VTT studied the effects and uncertainties of spray systems in a Finnish BWR. The work was continued from the previous phases of the project using the same models and newly implemented python job streams for sensitivity and uncertainty analyses. Two types of sensitivity analyses were used: a simple Morris method was employed to study the relative influence of the input parameters, and SNAP/DAKOTAs sensitivity correlation coefficients were used to try to quantify the sensitivity of the model for the different parameters.

The Morris method seemed to work with SNAP without major issues. The results varied – some made more sense than others. In the case of the cesium release, the most influential parameters seemed to be SC7111I1, SC715010, SC71568, and SC71551. For iodine release, most of the parameters are located quite close to each other, and there is not much difference in their relative influence. With FCV opening time the more influential parameters seemed to include parameters that should not affect the vessel breach and FCV start in any way. The most likely reason for the odd parameters was determined to be the significantly larger FCV start time outliers that could potentially cause the overestimating of the influence of noninfluential parameters. It is also possible that the parameters were affected by numerical noise produced by the COR package. SPRDELAY i.e. the delay between the vessel breach and the start of the spray system and DIAMO i.e. spray droplet diameter did not seem to have significant influence on any of the FOMs, even though these were initially thought to be the most influential ones.

Because no further analyses such as ANOVA were made with the Morris dataset, one can’t really determine absolute influence of different parameters on the output. Instead, only relative influence was studied. In the future, a step analyzing variance could be added to the script.

Sensitivity correlation coefficients were calculated by DAKOTA during the uncertainty step. For cesium release the most influential parameters seemed to be SPRDELAY and GAMMA, i.e. aerosol agglomeration shape factor. In the Morris analysis neither of these parameters stood out as more influential than the others. For iodine release, the most influential parameter seemed to be SC710641, i.e. activation energy, which was ranked rather high in the Morris analysis as well. However, at this point it was noticed that the selection of the upper limit for SPRDELAY was too low for iodine release, and as the result sprays became fully operational before the iodine concentration started increase properly. Therefore, changes in SPRDELAY or spray parameters affected iodine release only little. For FCV opening time, the most influential parameters were SC710641 and DECAYH, which is as expected – spray or aerosol parameters should not affect FCV opening time.

Uncertainty analysis was performed using a newly implemented python job stream. For cesium release, the results formed a quite clear log normal shaped probability density function. The shape of iodine PDF was not as clear due to the too low maximum value for SPRDELAY. As the sprays are fully operational in the beginning of the iodine release, the release was lower in every MELCOR run, resulting to a logarithmic looking shape for the PDF. As for FCV opening time, if the outliers were ignored, the shape of the PDF was very close to a normal distribution. As the spray parameters shouldn't affect the FCV opening times, the variation is most likely caused by numerical noise and the few in-vessel parameters.

Overall, the containment spraying system seemed to decrease the cesium and iodine releases compared to a case with no sprays. Even though the FCV opening time was thought to be influenced by something on the spray system, a comparison with the non-spray case shows that the spray system does not affect the start of the FCV. Outliers appear in both cases as well.

7. Outlook

The findings presented in this report, together with those from previous phases of the project [25,50], have identified several research points that can be addressed in greater detail in the future. These efforts aim to reduce excessive conservatism in the results and provide a more detailed definition of release categories for containment bypass sequences (RC3) or containment failure sequences (RC4). Additionally, there is a need to increase confidence in the results and refine the definition of release categories for filtered containment venting sequences (RC7). Uncertainty analysis has shown that the acceptable release threshold may be exceeded depending on the accident scenario and modeling uncertainties in the MELCOR code.

Some of these issues will be addressed in the next phase of the project.

In particular, to gain better understanding of the driving phenomena behind Cs and I2 remobilization after 20-24 hours in the accident scenarios initiated by a transient, it is proposed to perform detailed analysis of the results obtained within the second and third phases of the project, in order to identify the main sources of Cs/I2 remobilization (i.e. fission products deposited in the condensation pool, lower drywell, upper drywell, or RPV/RCS volumes and associated heat structures), and to identify thermal hydraulic parameters that affect Cs and I2 remobilization (such as pool temperature vs. pressure (boiling), temperatures of heat structures (in case of Cs/I2 remobilization from the heat structures surfaces)); and to perform separate effect analysis with MELCOR code, by disabling/enabling different MELCOR code models that can affect fission products behavior in the containment ; and identification of the most influential MELCOR code parameters. Based on these findings, identify and evaluate possible mitigative actions that can limit Cs and I2 remobilization, such as late containment spray with independent spray system, water filling of the containment, as well as possible effect of timing of these mitigative actions on the code response (including uncertainty quantification).

The effect of early manual containment depressurization via MVSS on the melt release conditions (corium properties, containment pressure, water pool temperature) will be performed using MELCOR code. The results of this analysis will be used to evaluate the effect of ex-vessel steam explosion loads on the containment using standalone codes and models developed by KTH. Based on the results, in scenarios with partial loss of leak tightness of the containment, due to ex-vessel phenomena, the release to the environment will be evaluated using MELCOR code.

Finally, accident scenarios initiated by a LOCA that lead to filtered containment venting can exceed the acceptable release threshold (in terms of the fraction of the core inventory of Cs released to the environment), depending on the combinations of uncertain parameters and selected modeling options in the MELCOR code. Furthermore, spray in the containment, which is currently not considered in the Level 2 Probabilistic Safety Assessment (PSA) of Nordic BWR for accident sequences leading to filtered containment venting, could also influence the classification of release categories. Both of these factors may impact the classification of release categories in the Level 2 PSA and overall frequency of unacceptable release to the environment. Therefore, it is proposed to evaluate the impact of the MELCOR analysis results on the frequency of unacceptable releases in the Level 2 PSA for Nordic BWR.

Acknowledgements

NKS conveys its gratitude to all organizations and persons who by means of financial support or contributions in kind have made the work presented in this report possible.

The work performed by VG was performed with additional support from the Swedish Radiation Protection Authority (SSM).

Disclaimer

The views expressed in this document remain the responsibility of the author(s) and do not necessarily reflect those of NKS. In particular, neither NKS nor any other organization or body supporting NKS activities can be held responsible for the material presented in this report.

References

[1] Preparedness and Response for a Nuclear or Radiological Emergency, INTERNATIONAL ATOMIC ENERGY AGENCY, 2015

[2] Actions to Protect the Public in an Emergency due to Severe Conditions at a Light Water Reactor, INTERNATIONAL ATOMIC ENERGY AGENCY, 2013

[3] Störningshandboken – BWR, SKI Rapport 03:02, 2003

[4] Nilsson L., Development of an Input Model to MELCOR 1.8.5 for Oskarshamn 3 BWR, SKI Report 2007:05, May 2006.

[5] Strandberg, M., Hydrogen Fire Risk in BWR Simulations with MELCOR. Research Report VTT-R-00669-17, 2017.

[6] L.L. Humphries, B.A. Beeny, F. Gelbard, T. Haskin, D.L. Louie, J. Phillips, R.C. Schmidt, MELCOR Computer Code Manuals Vol. 2: Reference Manual Version 2.2.18019, SAND2021-0241 O, 2021.

[7] L.L. Humphries, B.A. Beeny, F. Gelbard, D.L. Louie, J. Phillips, MELCOR Computer Code Manuals Vol. 1: Primer and Users' Guide Version 2.2.19018, SAND2021-0252 O, 2021.

[8] A. Saltelli, S. Tarantola, F. Campolongo and M. Ratto, "Sensitivity Analysis in Practice. A Guide to assessing scientific models". John Wiley & Sons Ltd, The Atrium, Southern Gate, Chichester, West Sussex PO19 8SQ, England. 2004.

[9] F. Campolongo, J. Cariboni, A. Saltelli, An effective screening design for sensitivity analysis of large models, Environmental Modelling & Software, Volume 22, Issue 10, 2007, Pages 1509-1518, ISSN 1364-8152. 2007.

[10] Adams, B.M., et al., Dakota, A Multilevel Parallel Object-Oriented Framework for Design Optimization, Parameter Estimation, Uncertainty Quantification, and Sensitivity Analysis: Version 6.0 Reference Manual. 2014, Sandia National Laboratories. (2014).

[11] Troy C. Haskin, The MELCOR Plot File Format, SAND2018-9566, 2018.

[12] Bertrand Ioos, Paul Lemaitre, A review on global sensitivity analysis methods.

[13] S. Galushin, D. Grishchenko, P. Kudinov, "Implementation of Framework for Assessment of Severe Accident Management Effectiveness in Nordic BWR", Reliability Engineering & System Safety, Vol 203, Article 107049, https://doi.org/10.1016/j.ress.2020.107049, November 2020

[14] Jon C. Helton, Jay D. Johnson , William L. Oberkampf & Cédric J. Sallaberry Representation of analysis results involving aleatory and epistemic uncertainty, International Journal of General Systems, 39:6, 605-646, (2010)

[15] Grishchenko D., Basso S., Kudinov P., "Development of a surrogate model for analysis of ex-vessel steam explosion in Nordic type BWRs," Nuclear Engineering and Design, Volume 310, Pages 311-327, 2016

[16] Dmitry Grishchenko, Sergey Galushin, Pavel Kudinov, “Failure Domain Analysis and Uncertainty Quantification using Surrogate Models for Steam Explosion in a Nordic type BWR”, Nuclear Engineering and Design, Volume 343, Pages 63-75, 2019.

[17] Galushin and P. Kudinov “Uncertainty Analysis of Vessel Failure Mode and Melt Release in Station Blackout Scenario in Nordic BWR Using MELCOR Code.” 18th International Topical Meeting on Nuclear Reactor Thermal Hydraulics (NURETH-18), no. Portland, OR, USA, August 18-22, (2019).

[18] S. Galushin S., Kudinov P., “Sensitivity Analysis of the Vessel Lower Head Failure in Nordic BWR using MELCOR Code”, Probabilistic Safety Assessment and Management PSAM 14, September 2018, Los Angeles, CA. (2018).

[19] N. W. Porter, Wilks' Formula Applied to Computational Tools: A Practical Discussion and Verification, SAND2019-1901J

[20] T. G. Theofanous, “On Proper Formulation of Safety Goals and Assessment of Safety Margins for Rare and High-Consequence Hazards,” Reliability Engineering and System Safety, 54, pp.243-257, (1996).

[21] SARNET Technical Report, In-Vessel Core Degradation in Water-Cooled Reactor Severe Accidents, State-of-the-Art Report Update, (CoreSOAR), 1996-2018, SARNET Report No. SARNET-CoreSOAR-D3, 2018.

[22] Galushin, S., and P. Kudinov. “Sensitivity and Uncertainty Analysis of the Vessel Lower Head Failure Mode and Melt Release Conditions in Nordic BWR Using MELCOR Code.” Annals of Nuclear Energy, Volume 135, 2020, ISSN 0306-4549.

[23] Sergey Galushin, Anders Riber Marklund, Dmitry Grishchenko, Pavel Kudinov, Tuomo Sevón, Sara Ojalehto, Ilona Lindholm, Patrick Isaksson, Elisabeth Tengborn, Naeem Ul-Syed, Source Term And Timing Uncertainty in Severe Accidents (NKS-STATUS), NKS-461, 978-87-7893-554-0, 01 Jul 2022.

[24] S. Galushin, P Kudinov “Uncertainty Analysis of Vessel Failure Mode and Melt Release in Station Blackout Scenario in Nordic BWR Using MELCOR Code.” 18th International Topical Meeting on Nuclear Reactor Thermal Hydraulics (NURETH-18), Portland, OR, USA, August 18-22, (2019).

[25] Sergey Galushin, Pavel Kudinov, Sensitivity and uncertainty analysis of the vessel lower head failure mode and melt release conditions in Nordic BWR using MELCOR code, Annals of Nuclear Energy, Volume 135, 2020

[26] Rafael Bocanegra, Luis E. Herranz, CIEMAT’s outcomes from the PHEBUS-FPT1 uncertainty analysis in the framework of the EU-MUSA project, The 10th European Review Meeting on Severe Accident Research (ERMSAR2022), Karlsruhe, Germany, May 16-19, 2022

[27] Darnowski, P.; Mazgaj, P.; Włostowski, M. Uncertainty and Sensitivity Analysis of the In-Vessel Hydrogen Generation for Gen-III PWR and Phebus FPT-1 with MELCOR 2.2. Energies 2021, 14, 4884

[28] Rafael Bocanegra, Luis Enrique Herranz, The importance of characterizing input uncertainties in severe accident analyses. The effect on pool scrubbing modeling in a Fukushima Unit 1 sequence, Sociedad Nuclear Española, Reunion Virtual, 2020.

[29] Fukushima Daiichi Unit 1 Accident Progression Uncertainty Analysis and Implications for Decommissioning of Fukushima Reactors – Volume I, SAND2016-0232,Sandia National Laboratories

[30] Lucas I. Albright, Nathan Andrews, Larry L. Humphries, David L. Luxat, Tatjana Jevremovic, Material Interactions in Severe Accidents – Benchmarking the MELCOR V2.2 Eutectics Model for a BWR-3 Mark-I Station, Nuclear Engineering and Design Volume 383, November 2021, 111398 Blackout: Part II – Uncertainty Analysis.

[31] F. Mascari, M. Massone, G. Agnello, M. Angelucci, S. Paci, M. D'Onorio, F. Giannetti, Comparison of PHEBUS FPT1 uncertainty applications using MELCOR 2.2 with three different methodologies The 13th Meeting of the "European MELCOR and MACCS User Group" 27th –29th April 2022

[32] T.K.S. Liang, L,Y, Chou, Z. Zhang, H.Y. Hsueh, and M. Lee. "Development and application of a deterministic-realistic hybrid methodology for LOCA licensing analysis," Nuclear Engineering and Design, 241 (5), pp. 1857-1863, (2011).

[33] I.M. Chakravarti, R.G. Laha, and J. Roy. "Handbook of Methods of Applied Statistics, Volume I," John Wiley and Sons, pp. 392-394, (1967).

[34] T.W. Anderson, and D.A. Darling. "Asymptotic theory of certain "goodness-of-fit" criteria based on stochastic processes," Annals of Mathematical Statistics, 23 (2), pp. 193-212, (1952).

[35] A. Buse. "The Likelihood Ratio, Wald, and Lagrange Multiplier Tests: An Expository Note," The American Statistician, 36 (3-1), pp. 153-157, (1982).

[36] B. Efron, and R.J. Tibshirani. An Introduction to the Bootstrap. Chapman and Hall/CRC, (1994).

[37] Applied Programming Technology, Inc., "Symbolic Nuclear Analysis Package (SNAP): User's Manual, Version 3.1.9," Bloomsburg, 2021.

[38] B. M. Adams, W. J. Bohnhoff, K. R. Dalbey and Et.al., "Dakota, A Multilevel Parallel Object-Oriented Framework for Design Optimization, Parameter Estimation, Uncertainty Quantification, and Sensitivity Analysis: Version 6.16 User's Manual," Sandia National Laboratories, Albuquerque,, 2022

[39] A. Saltelli and P. Annoni, "How to avoid a perfunctory sensitivity analysis," *Environmental Modelling & Software,* vol. 25, no. 12, pp. 1508-1517, 2010,

[40] Pavel Kudinov, Sergey Galushin, Dmitry Grishchenko, Sergey Yakush, Yvonne Adolfsson, Lisa Ranlöf, Ola Bäckström, Anders Enerholm, Scenarios and Phenomena Affecting Risk of Containment Failure and Release Characteristics, NKS-395, ISBN 978-87-7893-483-3, 2017.

[41] Weimin Ma, Walter Villanueva, Sevostian Bechta, Qiang Guo, Andrei Komlev, Mohsen Hoseyni, Peng Yu, Anna Korpinen, Veikko Taivassalo, Tero Tyrväinen, Ilkka Karanta, Anders Riber Marklund, Sergey Galushin, Ola Bäckström, Scenarios and Phenomena Affecting Risk of Containment Failure and Release Characteristics, NKS-428, ISBN 978-87-7893-518-2, 2019.

[42] Sergey Galushin, Anders Riber Marklund, Dmitry Grishchenko, Pavel Kudinov, Tuomo Sevón, Sara Ojalehto, Ilona Lindholm, Patrick Isaksson, Elisabeth Tengborn, Naeem Ul-Syed, Source Term And Timing Uncertainty in Severe Accidents, NKS-461, 2022.

[43] Sergey Galushin, Anders Riber Marklund, Anders Olsson, Ola Bäckström, Dmitry Grishchenko, Pavel Kudinov, Treatment of Phenomenological Uncertainties in Level 2 PSA for Nordic BWR Using Risk Oriented Accident Analysis Methodology, Probabilistic Safety Assessment and Management PSAM 16, Honolulu, Hawaii, June 26-July 1, 2022.

[44] John N. Ridgely, Assessment of BWR Main Steam Line Release Consequences, PRAB-02-01, NRC, 2002.

[45] Browns Ferry Nuclear Plant (BFN), Units 1, 2, and 3 - Supplement to Proposed Technical Specification Change to Revise the Leakage Rate Through MSIVs (TS-485), Enclosure 1 TS-485 S1, Alternative Leakage Treatment (ALT) Pathway – U.S. NRC.

[46] Artur Szymański Sławomir Dykas, Evaluation Of Leakage Through Labyrinth Seals With Analytical Models, Scientific Bulletin of the Centre of Informatics - Tricity Academic Supercomputer & network, Volume 23, Issue 1, 2019

[47] Mark Anderson, Advanced Supercritical Carbon Dioxide Brayton Cycle Development, FINAL REPORT Advanced Supercritical Carbon Dioxide Brayton Cycle Development (NEUP project 12-3318)

[48] J-E. Holmberg, M. Knochenhauer, Probabilistic Safety Goals, Phase 1 – Status and Experiences in Sweden and Finland, NKS-153, ISBN 978-87-7893-216-7, (2007)

[49] Sergey Galushin, Govatsa Acharya, Dmitry Grishchenko, Pavel Kudinov, Source Term Uncertainty Analysis of Filtered Containment Venting Scenarios in Nordic BWR, The 11th European Review Meeting on Severe Accident Research (ERMSAR2024), Stockholm, Sweden, May 13-16, (2024)

[50] Sergey Galushin, Govatsa Acharya, Dmitry Grishchenko, Pavel Kudinov, Sara Ojalehto, Tuomo Sevón, Ilona Lindholm, Patrick Isaksson, Elisabeth Tengborn, Naeem Ul-Syed, Source Term and Timing Uncertainty in Severe accidents NKS-STATUS Phase 2 report, NKS-475, July (2023)

[51] C. Berna, A. Escrivá, J.L. Muñoz-Cobo, L.E. Herranz, Enhancement of the SPARC90 code to pool scrubbing events under jet injection regime, Nuclear Engineering and Design, Volume 300, (2016)

[52] Luis E. Herranz, Claudia Lopez, Jaime Penalva, Investigation on jet scrubbing in nuclear reactor accidents: From experimental data to an empirical correlation, Progress in Nuclear Energy, Volume 107, (2018)

[53] Taizo Kanai, Masahiro Furuya, Takahiro Arai, Yoshihisa Nishi, Development of an aerosol decontamination factor evaluation method using an aerosol spectrometer, Nuclear Engineering and Design, Volume 303, (2016)

[54] S. Johst, T. Steinrötter, Optimization of the MELCOR Input Deck of Oskarshamn-3 NPP for Source Term Analyses with MELCOR 2.2, GRS – V – SSM2019 – BWR (2019)

[55] Taizo Kanai, Masahiro Furuya, Takahiro Arai, Yoshihisa Nishi, Development of an aerosol decontamination factor evaluation method using an aerosol spectrometer, Nuclear Engineering and Design, Volume 303, (2016)

[56] C. Berna, A. Escrivá, J.L. Muñoz-Cobo, L.E. Herranz, Enhancement of the SPARC90 code to pool scrubbing events under jet injection regime, Nuclear Engineering and Design, Volume 300, (2016)

[57] Luis E. Herranz, Claudia Lopez, Jaime Penalva, Investigation on jet scrubbing in nuclear reactor accidents: From experimental data to an empirical correlation, Progress in Nuclear Energy, Volume 107, (2018)

[58] A. Saltelli and P. Annoni, "How to avoid a perfunctory sensitivity analysis," *Environmental Modelling & Software,* vol. 25, no. 12, pp. 1508-1517, 2010. DOI: https://doi.org/10.1016/j.envsoft.2010.04.012.

[59] Corradini, M.L., et al., Users' manual for Texas-V: One dimensional transient fluid model for fuel-coolant interaction analysis. 2002, University of Wisconsin-Madison: Madison WI 53706.

[60] T. Okkonen, T. N. Dinh, V. A. Bui, and B. R. Sehgal. Quantification of the Ex-vessel Severe Accident Risks for the Swedish Boiling Water Reactors. Scoping Study Performed for the APRI Project, SKI Report 95:76, July 1995.

[61] Aniello Amendola. Advanced Seminar on Common Cause Failure Analysis in Probabilistic Safety Assessment. Proceedings of the ISPRA Course held at the Joint Research Centre, Ispra, Italy, 16–19 November 1987. https://doi.org/10.1007/978-94-017-0629-2

[62] F. Mascari et al., "PHEBUS FPT1 Uncertainty Application With The MELCOR 2.2 Code," The 19th International Topical Meeting on Nuclear Reactor Thermal Hydraulics (NURETH-19), Brussels, Belgium, March 6 - 11, 2022.

[63] R. O. Gauntt, T. Radel, D. A. Kalinich, and M. Salay, "Analysis of Main Steam Isolation Valve Leakage in Design Basis Accidents Using MELCOR 1.8.6 and RADTRAD, SAND2008-6601," 2008.

[64] R. Bocanegra and L. E. Herranz, "CIEMAT's outcomes from the PHEBUS-FPT1 uncertainty analysis in the framework of the EU-MUSA project," *The 10th European Review Meeting on Severe Accident Research (ERMSAR2022) Log Number: 324 Akademiehotel, Karlsruhe, Germany, May 16-19*, 2022.

Bibliographic Data Sheet **NKS-487**

Title	Source Term and Timing Uncertainty in Severe accidents NKS-STATUS Phase 3 report
Author(s)	Sergey Galushin[1], Govatsa Acharya[2], Dmitry Grischenko[2], Pavel Kudinov[2] Sara Ojalehto[3], Tuomo Sevón[3], Ilona Lindholm[3] Patrick Isaksson[4] Naeem Ul-Syed[5]
Affiliation(s)	[1] Vysus Sweden AB [2] KTH Royal Institute of Technology [3] VTT Technical Research Centre of Finland Ltd [4] SSM Swedish Radiation Safety Authority [5] DSA Norwegian Radiation and Nuclear Safety Authority
ISBN	978-87-7893-583-0
Date	June 2024
Project	NKS-R / STATUS - NKS-R(23)133/2
No. of pages	85
No. of tables	10
No. of illustrations	68
No. of references	64

Abstract
max. 2000 characters

The overall goal of the project is to generate a body of knowledge regarding the uncertainty in the magnitude of fission products release in the case of a potential severe accident in Nordic nuclear power plants. The work aims to provide insights into the effect of various types of uncertainty on the source term predictions. The results of the work will be useful both for probabilistic and deterministic safety assessments as well as for emergency response applications.
The third phase of the project focused on the assessment of the source term uncertainty in Nordic BWR-type reactors, in cases of containment bypass, containment failure, and filtered release scenarios.
In the case of containment bypass scenarios, the results showed that structures, systems, and components outside containment can reduce conservatism in source term analysis. Further refinement of the level of detail in modeling release paths and system effects could enhance the accuracy of the source term analysis results.
Analysis of release pathways for fission products in the case of containment failure, especially through failed containment

hatch doors can lead to significant changes in the source term. Critical concerns include basemat melt-through and non-coolable debris beds.
The analysis of the effect of the independent spray system on the source term released to the environment in filtered containment venting scenarios showed significant reduction in the Cs release compared to that in the unmitigated scenarios. The analysis includes quantification of uncertainties related to the MELCOR code's epistemic modeling parameters and options, and their effects on the timing and magnitude of the source term. Furthermore, for the Finnish BWR the Morris method and SNAP/DAKOTA analyses highlighted the relative influence of parameters, with some unexpected influential parameters likely due to numerical noise. Containment spraying effectively reduced Cs and I releases, although it did not affect FCV opening times.
The analysis of the effectiveness of pool scrubbing in the Multi-Venturi Scrubbing System and the refined modelling of the MVSS showed how the efficiency of pool scrubbing changes during different stages of severe accident progression. It also showed the impact of MVSS structures on the behavior of fission products in the scrubber and the source term released to the environment.

Key words: Severe accident, uncertainty quantification, MELCOR, Nordic BWR, fission products, source term

Available on request from the NKS Secretariat, P.O.Box 49, DK-4000 Roskilde, Denmark.
Phone (+45) 4677 4041, e-mail nks@nks.org, www.nks.org